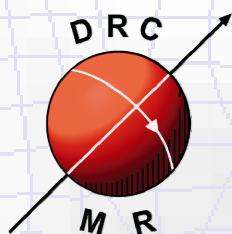


MRI in Severe Traumatic Brain Injury

Micro- and Macrostructural Changes

PhD thesis

Annette Sidaros, MD



Annette Sidaros

MRI in Severe Traumatic Brain Injury

Micro- and Macrostructural Changes

PhD Thesis

Faculty of Health Sciences
University of Copenhagen, Denmark

&

Danish Research Centre for Magnetic Resonance
Copenhagen University Hospital, Hvidovre, Denmark

&

Brain Injury Unit, Department of Neurorehabilitation
Copenhagen University Hospital, Hvidovre, Denmark

Submitted: December 2008

PREFACE

This thesis is submitted as part of the requirements for obtaining the PhD degree in Medicine at the Faculty of Health Sciences, University of Copenhagen. The work founding this thesis was carried out at the Copenhagen University Hospital, Hvidovre, at two departments: the Danish Research Centre for Magnetic Resonance (DRCMR) and the Brain Injury Unit, Department of Neurorehabilitation.

I prepared this project while working as a junior registrar at the Dept. of Neurorehabilitation 2002-2003. From August 2003 I was employed as a research assistant at DRCMR, initiating a pilot study and subsequently the PhD project, which was concluded in December 2008, interrupted by maternity leave.

This project was supervised by Professor Olaf B. Paulson, MD, DMSc (DRCMR), Aase W. Engberg, MD, DMSc, MScEng (Dept. of Neurorehabilitation), Egill Rostrup, MD, DMSc, MSc (DRCMR, subsequently Dept. of Clinical Physiology, Glostrup Hospital), Professor Terry L. Jernigan, PhD (DRCMR and University of California San Diego) and Palle Petersen, MD, DMSc (Dept. of Neurology, Rigshospitalet).

Note: My surname changed June 2006 from Nielsen to Sidaros.

Acknowledgements

First I wish to thank the patients participating in this study, and their relatives, for showing benevolence and strength to contribute to research despite their enormously stressful situation. I wish them all the best for the future.

For financial support I wish to thank Ludvig and Sara Elsass Foundation that supported this project generously throughout the study period. Grants were also received from the Danish Medical Society, the Brain Injury Resource Centre, the Danish Medical Research Council,

NeuroScience PharmaBiotec, Poul Lundbeck's Foundation, Hvidovre Hospital, and the Research Fund of the Copenhagen Hospitals Corporation.

This study could not have been possible without the collaboration of a number of people. Special thanks are directed to my supervisors for their encouragement and all the inspiring discussions we had throughout the time of the project. I am profoundly grateful to Aase W. Engberg, who founded the original idea of this project, served as my source of inspiration and provided theoretical and moral guidance with a rare and catching enthusiasm. I also wish to express my special gratitude to Olaf B. Paulson for encouraging and supporting this collaborative project from the very beginning. I am particularly thankful to the "tech's" of this project, Matthew G. Liptrot, Arnold Skimminge and Karam Sidaros, without whom I would never have made it through the MRI data analysis. Also Lars Hanson and Poul Ring spent several hours teaching me my way through the endless world of Linux. Statistical help was kindly provided by Kristoffer H. Madsen and Klaus Larsen, and for technical advice and interesting discussions I also want to thank Tim Dyrby and William Baaré. Special thanks go to Sussi Larsen and Margrethe Herring for devoting time and effort to the MRI acquisition and description, and to Hanns Reich for kindly offering his experienced anaesthesiological assistance. I am grateful to Henrik K. Mathiesen for sharing with me his experience and some normative data. For the skilled clinical rating I wish to acknowledge all staff at the Brain Injury Unit, with special thanks to Annette Nordenbo for continuous encouragement. I am indebted to Ole S. Jørgensen (Lab. Of Neuropsychiatry, Rigshospitalet), who educated me scientifically during my years as a medical student, encouraged me to enter the field of neuroimaging, supported the initiation of this project, and carried out the genetic analyses in his lab.

To all my colleagues and friends at DRMR: thank you for creating such a friendly, enthusiastic and inspiring environment, and for lots of memorable moments. Finally I want to thank my family and friends for their great support, patience and understanding, and not the least Adam for smiling and giggling during both ups and downs. My deepest thanks go to my beloved husband - for everything, but in particular, for letting "magnetism" lead to marriage and contribution to the youngest generation.



Annette Sidaros

Copenhagen, December 2008

SUMMARY

The principal aim of the present PhD project was to study quantitatively the long-term micro- and macrostructural brain changes in survivors from severe traumatic brain injury (TBI).

A total of 31 patients admitted for early rehabilitation following severe TBI were included and underwent magnetic resonance imaging (MRI), including Diffusion Tensor Imaging (DTI), at mean 8 weeks post-injury. Follow-up MRI at mean 12 months post-injury was acquired in 25 of the patients. For comparison, healthy matched controls were scanned twice with a similar time interval. Clinical rating during rehabilitation and at 1-year follow-up was performed by experienced staff.

Two papers make up the basis of this thesis. Paper I considers the DTI results. This MRI modality was chosen in order to evaluate diffusional changes in brain tissue, potentially useful for characterising the extent of microscopic white matter injury, as well as for tracking microstructural changes during recovery. Using a region-of-interest approach, four white matter regions were studied with additional regions in grey matter and CSF. At the initial scan, patients had abnormal fractional anisotropy (FA) in all white matter regions, which in the cerebral peduncle correlated with 1-year outcome, suggesting that DTI may have prognostic value. At follow-up, FA had partly normalised in some white matter regions, but deviated even more from normal values in other regions. Although these longitudinal findings warrant cautious interpretation, they might indicate microstructural reorganization.

Paper II describes a study on the macrostructural brain changes during recovery. Global and regional brain volume changes between the two scan time points were investigated using voxel-wise analyses. Despite remarkable clinical improvement in most patients, they all exhibited continued brain volume loss during the scan interval. Global volume change correlated with clinical injury severity, functional status at both scans, and with 1-year outcome. The areas which underwent the most change were structures particularly susceptible to traumatic axonal injury and consequent Wallerian degeneration, indicating that the long-term atrophy is attributable to consequences of axonal injury.

Together, these MRI analyses complemented each other in the quantitative assessment of structural brain changes following severe TBI. Applied in the late subacute/early chronic phase of TBI, DTI may capture biological severity at the microstructural level and provide prognostic information. Serial application of the MRI techniques applied in this study enables the monitoring of the extent and distribution of micro- and macrostructural changes during TBI rehabilitation.

DANSK RESUMÉ

Det primære formål med aktuelle ph.d.-projekt var kvantitativt at undersøge mikro- og makrostrukturelle ændringer i hjernen hos patienter med svær traumatisk hjerneskade (TBI).

I alt 31 patienter indlagt til tidlig rehabilitering efter svær TBI blev inkluderet og skannet med magnetisk resonans (MR), inklusiv diffusions-tensor-billeddannelse (DTI), omkring 8 uger efter traumet. Opfølgende MR blev foretaget hos 25 af patienterne ca. 12 måneder efter traumet. Til sammenligning blev raske kontrolpersoner MR-skannet to gange med et tilsvarende tidsinterval. Klinisk 'rating' under rehabilitering og ved 1 års opfølgning blev foretaget af erfarent personale.

To publikationer danner basis for nærværende afhandling. Artikel I omhandler DTI-resultaterne. Denne MR-modalitet blev valgt med henblik på at måle diffusionsforandringer i hjernevævet, potentielt anvendeligt til at karakterisere graden af mikroskopisk hvid substans-skade, og til at følge mikrostrukturelle ændringer over tid. Fire regioner i hvid substans blev analyseret, foruden regioner i grå substans og CSF. Ved første skanning var den fraktionelle anisotropi (FA) abnorm i alle hvid substans-regioner, og svarende til pedunculi cerebri var der korrelation med 'outcome' 1 år efter skaden, tydende på en mulig prognostisk værdi af DTI. Ved opfølgende skanning var FA delvis normaliseret i nogle hvid substans-regioner, men blevet yderligere abnorm i andre regioner. Om end disse longitudinelle fund må fortolkes med betydeligt forbehold, kunne de muligvis indikere mikrostrukturel reorganisering.

Artikel II beskriver en undersøgelse af makrostrukturelle ændringer i hjernen efter svær TBI. Globale og regionale volumenændringer mellem de to skanningstidspunkter blev kvantificeret vha. voxel-vis analyse. På trods af bemærkelsesværdig klinisk bedring hos størstedelen af patienterne i denne periode, udviste de alle fortsat hjernevolumentab i skanningsintervallet. Global volumenændring korrelerede med klinisk sværhed af traumet, funktionel status på skanningstidspunkterne, og med 'outcome' 1 år efter skaden. De regioner som udviste størst volumentab var strukturer som er særlig udsatte for traumatisk aksonal skade og resulterende

Wallersk degeneration, hvilket kunne indikere at den progressive atrofi betinges af konsekvenserne af aksonal skade.

Tilsammen komplementerede disse MR-analyser hinanden i kvantificeringen af strukturelle ændringer i hjernen efter svær TBI. Anvendt i den sene subakutte/tidlig kroniske fase af TBI, kan DTI sandsynligvis afspejle biologisk sværhedsgrad på det mikrostrukturelle niveau samt muligvis bibringe prognostisk information. Seriel anvendelse af MR-teknikkerne anvendt i dette studie muliggør monitorering af omfang og lokalisation af mikro- og makrostrukturelle ændringer under TBI rehabilitering.

CONTENTS

Preface	i
Summary	iii
Dansk Resumé	v
Abbreviations	ix
1 Introduction	1
1.1 Objectives	2
1.2 Overview	2
2 Traumatic Brain Injury (TBI)	5
2.1 Definition and Severity	5
2.2 Causes and Consequences	6
2.3 Neuropathology	7
2.4 The Recovery Process	10
2.5 Predictors of Outcome	11
3 Magnetic Resonance Imaging (MRI)	13
3.1 Basic Principles	13
3.2 Diffusion Imaging	14
3.3 Morphometry	17
4 MRI of TBI	21
4.1 Practical and Ethical Issues	21
4.2 Conventional MRI	22
4.3 Diffusion Imaging	23
4.4 Morphometry	25
4.5 Motivation for the Present Studies	26
5 Methods and Results	29
5.1 Design and Subjects	29

5.2	Clinical Assessments	32
5.3	MRI Acquisition	32
5.4	MRI Data Processing	34
5.5	Results, Paper I (Diffusion Study)	35
5.6	Results, Paper II (Morphometry Study)	37
5.7	Supplemental Results.....	40
6	Discussion	43
6.1	Interpretation of Results.....	43
6.2	MRI Methodological Limitations.....	47
6.3	Limitations of Clinical Ratings	49
7	Conclusions	51
7.1	Conclusions	51
7.2	Perspectives	52
7.3	Future Directions.....	52
	References	55

Appendices

- A1 Paper I: Diffusion tensor imaging during recovery from severe traumatic brain injury and relation to clinical outcome: a longitudinal study.
- A2 Paper II: Long-term global and regional brain volume changes following severe traumatic brain injury: a longitudinal study with clinical correlates.
- A3 Supplemental short review in Danish: [Magnetic resonance imaging in severe traumatic brain injury].
- A4 Clinical rating scales

ABBREVIATIONS

ADC = apparent diffusion coefficient
APOE = apolipoprotein E
BPV = brain parenchymal volume
%BVC = percent brain volume change
CP = cerebral peduncle
CSF = cerebrospinal fluid
CSO = centrum semiovale
CT = computerized tomography
DTI = diffusion tensor imaging
DWI = diffusion-weighted imaging
EPI = echo-planar imaging
FA = fractional anisotropy
FDR = false discovery rate
FIM = functional independence measure
FLAIR = fluid-attenuated inversion recovery
GCS = Glasgow coma scale
GOS = Glasgow outcome scale
GOS-E = extended Glasgow outcome scale
MD = mean diffusivity
MR = magnetic resonance
MRI = magnetic resonance imaging
PCC = posterior aspect of corpus callosum
PLIC = posterior limb of internal capsule
PTA = post-traumatic amnesia
ROI(s) = region(s) of interest
SIENA(X) = structural image evaluation, using normalisation, of atrophy
TAI = traumatic axonal injury
TBI = traumatic brain injury
TBM = tensor-based morphometry
VBM = voxel-based morphometry

CHAPTER 1

INTRODUCTION

Traumatic brain injury (TBI) is among the most frequent causes of death and morbidity for the population younger than 45 years in the Western countries (MacKenzie, 2000). Most severe and fatal TBI's are caused by traffic accidents, while falls account for the second largest number of such incidents. In patients who survive the acute phase of severe TBI, long-term clinical outcome is highly variable, ranging from nearly complete recovery of function to persistent vegetative state or death. Individual outcome depends upon multiple factors, making prediction of outcome an extremely difficult and complex task.

One of the key problems hindering outcome prediction is that characterization of the individual brain injury, in particular the microscopic white matter injury, is limited using conventional diagnostic tools. The tremendous development within the field of neuroimaging during the last three decades has greatly impacted on the acute management of head injury, and has also brought us a large step forward towards characterization of injury *in vivo*. However, we are still not able to capture the true biological severity of TBI using standard imaging techniques such as computerized tomography (CT) or conventional magnetic resonance imaging (MRI), presumably due to their limited sensitivity to microscopic white matter injury.

Although clinical recovery and final outcome vary remarkably, the vast majority of patients who have sustained and survived even a severe TBI do recover to some extent, and many continue to show functional improvement years after injury (Sbordone et al, 1995). However, during rehabilitation it is a common observation, on repeated CT or MRI, that the brain undergoes widespread atrophy concurrently with the clinical improvement. Whether this atrophy has clinical relevance in terms of outcome is poorly understood, and knowledge regarding the distribution of volume loss and the underlying mechanisms is limited.

The basis of the present PhD thesis is a project designed as a prospective longitudinal study of adult patients with non-penetrating severe TBI. In addition to conventional MRI acquired at two time points, a relatively recent MRI technique, Diffusion Tensor Imaging (DTI), was applied, as

this method allows for the quantitative measurement of the directionality of tissue water diffusion *in vivo*, which is thought to reflect tissue micro-architecture. For quantitative evaluation of macrostructural changes over time, recent techniques suited for longitudinal studies (Structural Image Evaluation, using Normalisation, of Atrophy, SIENA; and Tensor Based Morphometry, TBM) were chosen. These methods are thought to be more robust than traditional morphometric approaches for the analysis of structurally highly heterogeneous brains.

The present thesis is based on the following papers, which are given as appendices:

- I *Annette Sidaros et al. Diffusion tensor imaging during recovery from severe traumatic brain injury and relation to clinical outcome: a longitudinal study. Brain 2008; 131 (Pt 2): 559-72.*
- II *Annette Sidaros et al. Long-term global and regional brain volume changes following severe traumatic brain injury: a longitudinal study with clinical correlates. NeuroImage 2009, 44 (1): 1-8.*

For Danish readers, a supplemental short review (invited) is provided:

- III *Annette Sidaros & Margrethe Herning. Magnetisk resonans-skanning ved svær traumatisk hjerneskade. Ugeskr Laeger 2007; 169 (3): 214-6.*

1.1 Objectives

The overall objective of this PhD project was to study quantitatively the long-term micro- and macrostructural brain changes during recovery in patients with severe TBI.

In the post-acute phase, the main objective was to characterize injury at the microstructural level, attempting to measure biological severity of traumatic white matter injury with the prospect of improving prediction of long-term functional outcome.

With the longitudinal MRI data, the objective was to study micro- and macrostructural changes during recovery, comparing early (~8 weeks post-injury) and late (~12 months post-injury) MRI quantities, and relating findings to clinical status and outcome.

1.2 Overview

Chapter 1 is a general introduction and lists the objectives of this work.

The Chapters 2, 3 and 4 provide some background for the studies constituting this thesis. **Chapter 2** is a brief introduction to TBI, and in **Chapter 3** the basic principles of the applied MRI techniques are described. **Chapter 4** considers application of MRI in TBI patients and comprises some practical and ethical considerations, a summary of previous studies relevant for the present project, and finally the motivation and hypotheses for this work.

Chapter 5 describes the methods used in the present studies and summarises the results presented in Papers I and II. Some additional unpublished results are also provided. Interpretation of the results and limitations of the studies are discussed in **Chapter 6**. Finally, **Chapter 7** lists some overall conclusions and perspectives of this work, and comments on future directions for related research.

CHAPTER 2

TRAUMATIC BRAIN INJURY (TBI)

In this chapter severe TBI is defined, and a brief introduction is given to its causes and clinical consequences. Following, some of the most common lesion types in TBI are considered, with special attention on traumatic (diffuse) axonal injury. A short introduction is then given to clinical recovery following TBI and to the current knowledge of the underlying neurobiology. The chapter concludes with an overview of prognostic indicators.

2.1 Definition and Severity

TBI refers to brain damage resulting from head injury, but there is no consensus on a more exact definition. Head injury or head trauma implies an external mechanical force to the craniofacial region, but a clear definition of brain injury is less straightforward. While it is intuitive to associate brain injury with damage to brain tissue, this is not always readily detectable *in vivo* by the current diagnostic techniques in routine clinical use. Newer advanced imaging methods, such as those which are the focus of the present thesis, may provide new possibilities in the future.

Currently, the most widely accepted definition of TBI is that posed in 1995 by the Centers for Disease Control and Prevention (CDC; Thurman et al, 1995). Corresponding to codes in the International Classification of Diseases (ICD diagnoses), CDC defines TBI as:

“Craniocerebral trauma, specifically, an occurrence of injury to the head (arising from blunt or penetrating trauma, or from acceleration/deceleration forces) that is associated with any of these symptoms attributable to the injury: decreased level of consciousness, amnesia, other neurologic or neuropsychologic abnormalities, skull fracture, diagnosed intracranial lesions, or death.”

This definition includes skull fracture without indications of neurological injury *per se*. This is due to the fact that the CDC definition was developed as a tool for public health surveillance, not clinical practice.

Traditionally, the severity of TBI is graded into mild, moderate and severe, based on the initial score on the Glasgow Coma Scale (GCS; see Appendix 4; Teasdale and Jennett, 1974); more specifically, the lowest post-resuscitation GCS score measured within the first 24 hours post-trauma and prior to the initiation of paralytics or sedatives. According to this severity grading, GCS 13-15 corresponds to mild TBI, GCS 9-12 to moderate TBI and GCS 3-8 to severe TBI. At later stages post-injury it is more relevant, in terms of long-term outcome, to grade severity according to the duration of post-traumatic amnesia (PTA; evaluated e.g. by the Galveston orientation and amnesia test; see Appendix 4; Levin et al, 1979). However, the duration of PTA bears the disadvantage of being a prospective measure and so is not useful in the acute stage. A PTA of more than 4 weeks is sometimes referred to as very severe TBI (Engberg et al, 2006).

Note that the present work regards exclusively adult patients with closed (non-penetrating) severe TBI, according to the grading based on initial GCS (i.e. GCS 3-8). Paediatric TBI and penetrating TBI will not be considered further in this thesis, and other studies of mild/moderate TBI will only be considered if of particular interest.

2.2 Causes and Consequences

Mechanisms of closed TBI include 1) direct impact (the head being struck or the head striking an object), and 2) acceleration-deceleration-rotation of the brain within the skull. Both mechanisms can be involved, but the latter mechanism is a constant feature of high-velocity injuries. Of hospitalized closed TBI the most common cause is traffic-related injury, usually motor vehicle accidents. Falls constitute the second most common cause, but within certain age groups (children and elderly) the frequency of falls typically exceeds that of traffic-related injury. Less common causes are assaults, sport-related injuries and suicide attempts (Engberg, 1995; Thurman et al, 2006).

Decreased level of consciousness is the most conspicuous feature characterizing survivors of severe TBI in the acute phase. Following the initial phase of coma, most enter a vegetative state with spontaneous eye opening and sleep/wake cycles while still unconscious. The minority of patients which stall in the vegetative state, not showing any evidence of consciousness within one year of the injury, are said to have entered a 'persistent' vegetative state.

The majority of patients who fully recover consciousness may have temporary or persistent impairment of cognitive, physical and/or psychosocial functions which vary considerably in nature and severity. Most common long-term sequelae of TBI are cognitive and behavioural/emotional changes leading to reduced social and occupational adaptability (e.g. Van Zomeren et al, 1984). Typical cognitive problems are mental slowness, memory impairment and impairment of executive functioning; emotional/behavioural consequences can include depression, anxiety, impulsivity, agitation, among others. Examples of common physical consequences are spasticity, dyscoordination, seizures, and fatigue.

Final outcome in severe TBI thus ranges from almost complete recovery of function to persistent vegetative state or death. In some of the following sections, the basis of this extreme variability of outcome will be dealt with. The inherent heterogeneity of TBI lies primarily in the numerous different lesions which can arise from head trauma, and their various location and severity. Therefore, an introduction to the neuropathology of TBI will be given in the section below.

2.3 Neuropathology

A number of different lesion types can occur with TBI, and very often different lesion types coexist. Lesions caused by head trauma can be divided into *primary* injuries, occurring at the moment of trauma and caused directly by mechanical forces; and *secondary* injuries, occurring after the moment of trauma as a consequence of the primary brain injury or systemic factors. Further, brain injuries can be divided into *diffuse* and *focal* injuries. Focal injuries are localized, whereas diffuse-type injuries affect larger regions of the brain usually involving both cerebral hemispheres. As mentioned below, some lesions categorized as diffuse are probably more correctly described as multifocal. Within these categories a number of lesion types are described in the pathological literature (e.g. Graham & Gennarelli, 1997). The following description is confined to some of the most common *parenchymal* lesions. For a complete review of the neuropathology of TBI, see e.g. (Graham & Gennarelli, 1997).

Traumatic Axonal Injury

A primary 'diffuse' lesion type that requires special attention is traumatic axonal injury (TAI), also known as diffuse axonal injury (DAI). In this thesis I will be using the term TAI instead of the more widely used DAI, since the distribution of this lesion type is actually multifocal rather than diffuse (Meythaler et al, 2001), and because some terminological confusion has been associated with the term DAI, which is sometimes used for non-traumatic injuries as well (Geddes et al, 2000). Note however, that in Paper I (Appendix 1) the term DAI is used instead of TAI.

TAI was first described by the neuropathologist Sabina J. Strich in 1956 (Strich, 1956) who investigated the relation between head trauma and dementia, and proposed that these lesions play an integral role in the eventual development of dementia due to head trauma.

TAI refers to microscopic white matter injury induced by sudden acceleration-deceleration and/or rotational forces, causing shearing of the axons. The resulting cell injury is characterized by axonal stretching, disruption and eventual separation of fibres. TAI occurs in the majority of patients with severe TBI, and is a constant feature in high-velocity traffic accidents. Lower levels of impact energy (including falls or violent assaults) may also sometimes produce TAI (Graham & Gennarelli, 1997).

The predominant sites of TAI are the subcortical white matter, the corpus callosum, and the dorsolateral aspect of the upper brainstem. Other regions susceptible to TAI are the thalamus and basal ganglia, the internal and external capsules, the cerebellum, and various tracts in the brainstem and the cerebellar peduncles. It is believed that tissue density changes explain the

vulnerability of these locations to TAI (Graham & Gennarelli, 1997). Pathologically, TAI is traditionally graded according to the location of TAI lesions, which tends to become sequentially deeper with increasing severity of TBI: Grade I TAI with characteristic microscopic axonal abnormalities^{*}; grade II TAI characterized by macroscopically visible lesions in the corpus callosum in addition to grade I findings; and grade III TAI with macroscopically visible lesions in the dorsolateral quadrant of the brainstem in addition to grade II findings (Graham & Gennarelli, 1997).

Histopathologically, TAI is characterized by axonal retraction bulbs and axonal disruption, which may be immediate or delayed. These features are thought to be preceded by misalignments of the cytoskeletal network (Figure 2.1) and, in severe TAI, changes of axolemma permeability.

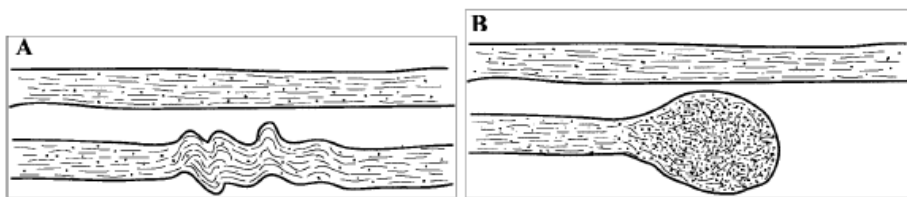


Figure 2.1. Schematic illustration of TAI. **A.** The top neuron is healthy. In the bottom neuron, neurofilamentous and, generally, cytoskeletal misalignment is visible a short time after injury. This impairs axonal transport. **B.** Organelles accumulate in the injured region, causing the axon to swell locally and subsequently disconnect from the rest. (Reprinted from Arfanakis et al, 2002)

Only a minority of TAI lesions are associated with macroscopically visible haemorrhages. The vast majority of TAI lesions are non-haemorrhagic but detectable on microscopic examination (preferably using immunostaining with β -amyloid precursor protein). Axonal disconnection following TAI leads to Wallerian-type degeneration, i.e. degeneration of the distal segment of the axon which has been separated from the cell body. Widespread atrophy of white matter ensues, with conspicuous microscopic changes in the brainstem pyramidal tract and medial lemnisci, and usually reduced bulk of lobar white matter, compensatory enlargement of the ventricles, and thinning of the corpus callosum (Graham & Gennarelli, 1997).

TAI is identified as one of the most important causes of morbidity and mortality in TBI. TAI is associated with immediate onset of unconsciousness, and it is assumed that in all cases of TBI with immediate loss of consciousness, some extent of TAI is present (Meythaler et al, 2001). In the acute phase of severe TBI, TAI of grade II or III causes diffuse brain oedema which, if severe, may cause herniation. TAI is the most important cause of persistent vegetative state following TBI, and is also thought to be associated with the syndrome of autonomic dysfunction. In patients who regain consciousness, a broad range of cognitive deficits following TAI are possible, the most frequent being deficits in memory (anterograde amnesia), information processing and executive functions (e.g. Meythaler et al, 2001; Povlishock & Katz, 2005; Scheid et al, 2006).

^{*} In radiology, the presence of visible TAI lesions confined to the lobar white matter is usually defined as grade I TAI (Gentry, 2002).

Cortical Contusions

The most frequently occurring primary focal brain lesions are cortical contusions. These primarily involve the superficial grey matter, occasionally with additional involvement of the underlying white matter. Cortical contusions are much more likely to be haemorrhagic than TAI lesions (Gentry, 2002). Contusions commonly occur in *coup* or *contre-coup* injuries. In *coup* injuries, the brain is injured directly under the area of impact, while in *contre-coup* injuries it is injured on the side opposite the impact. Areas of the brain particularly prone to contusion are those in the vicinity of sharp bony protuberances on the inside surface of the skull, namely the tips of the frontal and temporal lobes. Symptoms associated with contusions depend on location, size/depth, bilaterality, and secondary damage. Typical cognitive and behavioural symptoms related to frontal and temporal contusions are impairment of executive functioning, memory, attention, and behaviour modulation (Povlishock & Katz, 2005). Cerebral lacerations are related to contusions, but by definition lacerations involve the mechanical tearing of the pia/arachnoid and the underlying brain tissue. However, lacerations cannot easily be distinguished from contusions *in vivo* (except in penetrating injuries, not considered here).

Secondary Diffuse Injury

Secondary injuries are potentially amenable to therapeutic intervention and preventing or minimising secondary injury is crucial in the management of TBI patients. Secondary diffuse injury is most often hypoxic-ischemic, due to compromised oxygen supply and/or compromised global perfusion, insults which often occur in multi-trauma patients. The burst of excitatory transmitters released immediately following TBI is also believed to cause secondary brain injury at the cellular level. Some also consider late complications such as neuroinfection and obstructive hydrocephalus to be reckoned among the secondary injuries (Graham & Gennarelli, 1997).

Secondary hypoxic-ischemic injury has been estimated to occur in up to 30% of patients sustaining severe TBI (Chesnut, 1995). Compromised cerebral perfusion pressure can be caused by elevated intracranial pressure (due to brain oedema or haematomas), systemic hypotension (due to blood loss, compromised cardiac function, or loss of normal autoregulation response), or a combination of the two. Hypoxygenation can be caused by pulmonary injury or central hypoventilation. In clinical observational studies it has been found that the occurrence of these hypoxic-ischemic insults in TBI patients markedly influences outcome. Chesnut et al found overall morbidity to be increased by a factor of 10 if TBI patients had insults of hypotension (systolic < 90 mmHg) and hypoxia (PaO_2 < 60 mmHg) compared to TBI patients without any such secondary insults (Chesnut et al, 1993). Pathologically, fatal hypoxic-ischemic injury, as found isolated in non-resuscitated cardiac arrest, leads to laminar necrosis of the cerebral cortex and watershed infarction in the border zones of major arterial supply. The hippocampal formation seems to be particularly vulnerable to hypoxic-ischemic injury. However, in less severe hypoxic-ischemic injury, pathology may be subtle. Clinically, severe hypoxic-ischemic injury causes coma followed by persistent vegetative state, and often epileptic myoclonia due to the cortical involvement. Adults in a coma immediately after a hypoxic-ischemic injury generally have a poorer prognosis than those in a coma after a traumatic injury (The Multi-Society Task Force on PVS, 1994). In less severe hypoxic-ischemic injury, patients have symptoms of

amnesia. When hypoxic-ischemic injury occurs as secondary injury in TBI, these symptoms are usually indistinguishable from those caused by the primary injuries.

2.4 The Recovery Process

The course of clinical recovery after severe TBI is among the longest observed after neurological damage. Although the rate of improvement is usually highest within the first 6 months after injury, some degree of recovery may continue for years, and improvement of function has been reported up to 10 years after TBI (Sbordone et al, 1995). Obviously, knowledge of the neurobiological basis of recovery is of major interest as intervening with these processes could have immense treatment potential. The concept of neuroplasticity has attracted enormous interest during the recent decades and is the focus of intense research. Still, however, our understanding of the exact processes underlying recovery is quite limited. In this section, only a very brief introduction to the concept of recovery will be given.

Clinical Recovery

In patients with diffuse pathology, in particular TAI, clinical recovery is a gradual process which tends to follow a certain pattern. The time course of this recovery process seems to be related to the quantity of diffuse pathology. The phase of unconsciousness is followed by a proportionally longer phase of emerging consciousness and confusion, during which the patient is amnesic (PTA). Following resolution of PTA and confusion is a yet proportionally longer phase of post-confusional restoration of cognitive function (Povlishock & Katz, 2005). This sequence of recovery is reflected in the Ranchos Los Amigos Scale (see Appendix 4; Hagen, 1984) which describes the recovery process in eight stages. These Rancho levels are based on observations of the patient's response to external stimuli. Rehabilitation at this early phase during emergence from unconsciousness is mainly aimed at preventing, minimizing and treating cerebral and extracerebral complications, including spasticity, seizures, contractures, venous thrombosis, infections, autonomic dysfunction, etc. However, there is a growing amount of evidence to suggest that early intensive rehabilitation is also effective in terms of long-term functional outcome (e.g. Wagner et al, 2003; Engberg et al, 2006; Turner-Stokes et al, 2008). Once the patient has recovered to Ranchos level VIII, a more individualized and focused rehabilitation strategy, requiring the active cooperation of the patient, is feasible. This will usually involve cognitive and physical training.

Neurobiological Basis of Recovery

It is intuitively comprehensible that, with the resolution of brain oedema and restoration of other dynamic and reversible physiological events during the weeks following severe TBI, clinical recovery may follow. However, explaining late clinical improvements, which may occur several months or even years post-injury, is less straightforward. The concept of neuronal plasticity, the capacity of the nervous system to modify its organization in response to injury or environmental changes, was speculated upon as early as the mid-19th century. However, it was not until the 1980's that compelling evidence from accumulated experimental data made it

widely acceptable that the adult brain is capable of significant anatomical and physiological plasticity (Nudo & Dancause, 2006).

The main principles of adaptive neuroplasticity following injury are thought to be vicariation, the taking over of function of injured regions by spared healthy regions. The underlying mechanisms act at the molecular, synaptic, cellular, network and system levels. Examples of mechanisms underlying plasticity at the cellular and synaptic levels are axonal and dendritic sprouting, synaptogenesis, angiogenesis and possibly even neurogenesis (Nudo, 2006). These phenomena are again thought to be driven by adaptive molecular and electrical phenomena, including changes in gene expression, and long-lasting enhancement or reduction in synaptic transmission (long-term potentiation and long-term depression, respectively). It should be noted that most of the experimental research on adaptive plasticity after injury has been done in animal models of stroke, while much fewer studies were on models of TBI. Further, it should be stressed that in principle plasticity processes can be maladaptive as well as beneficial. For reviews of neuroplasticity after injury, see e.g. (Stein, 2006; Nudo, 2006; Nudo & Dancause, 2006).

2.5 Predictors of Outcome

As mentioned previously, long-term clinical outcome following severe TBI is highly variable and depends upon multiple factors, which makes prediction of outcome an extremely difficult and complex task. Particularly in patients who do not regain consciousness within a short time after TBI, the spectrum of final outcomes can range from nearly full recovery of function to persistent vegetative state or death. Although experienced clinicians may be able to predict a narrower spectrum of possible outcomes for the individual patient, a high degree of uncertainty is still related to prognostic assessments. Naturally, this uncertainty can be extremely stressful for the relatives, frustrating for the doctors and therapists – and from a socio-economical perspective, it complicates the economical priority of limited resources in our healthcare system.

The pathological heterogeneity of TBI along with the difficulties of characterizing diffuse-type injuries *in vivo*, probably represent the major challenges to prognostic assessment. Considering global parameters, in particular level of consciousness, diffuse-type injuries in general have much larger influence than do focal lesions (Povlishock & Katz, 2005). Further, as multiple factors seem to influence outcome, including age, genetic factors, the occurrence of secondary insults, and possibly a number of factors related to the trauma itself and to the immediate treatment, only more complexity is added to these challenges of outcome prediction.

Considering clinical prognostic indicators, initial GCS and length of coma are vaguely related to long-term outcome, while duration of PTA is a much stronger outcome predictor (e.g. Engberg, 1995; Greenwood, 1997). However, PTA is obviously not useful for early prognostic evaluation. Older age is associated with poorer long-term recovery (e.g. Marquez de la Plata et al, 2008), and there are some preliminary indications that females may recover better than males (Stein, 2007; Ratcliff et al, 2007). Abnormal pupillary reaction on admission to hospital is also associated with poor outcome (The Brain Trauma Foundation, 2000). The occurrence of secondary insults such as hypotension or hypoxia markedly worsens prognosis (Chesnut et al, 1993); however, these insults often escape registration, particularly in the pre-hospital setting.

There have been numerous attempts to identify genetic or biochemical markers of prognostic value in severe TBI. Apolipoprotein E (APOE) plays a number of roles in the CNS, including a possible role in neuronal protection, repair and remodelling (Horsburgh et al, 2000). Possession of the APOE E4 allele is known to carry risk for Alzheimer's disease. Although findings are inconsistent, in some studies possession of the E4 allele has been associated with worse outcome following TBI (see e.g. Kothari, 2006). Moderate or severe TBI is known to be associated with an increased risk of Alzheimer's disease, possibly through the deposition of β -amyloid, but whether any allele-specific interaction of APOE with β -amyloid is responsible for the possible association between APOE E4 and TBI outcome is yet unclear (Van Den Heuvel et al, 2007). However, any possible effect of APOE E4 on TBI outcome is probably too small to be of prognostic use. Nevertheless, unravelling the role of APOE in TBI could be of interest from a pathophysiological and a pharmacological intervention point of view.

Among the number of serum markers which have been proposed as prognostic variables in TBI, at present the astroglial protein S100b is the most promising (see e.g. Kothari, 2006). In the CNS, S100b is a parameter of glial activation and/or death. However, there are considerable extracranial sources of S100b, including bone and soft tissue which may also be injured by the same incident. Further, S100b levels must be drawn within a very short time after injury, precluding its use at later stages.

The prognostic value of early conventional imaging in severe TBI is rather disappointing, presumably due to the relative insensitivity to diffuse-type injuries. While highly useful for the identification of focal lesions requiring acute neurosurgical intervention, acute-care CT is not very helpful for determining long-term prognosis. The only acute CT findings which are associated with poor prognosis in severe TBI are compression of basal cisterns, presence of subarachnoidal haemorrhage, and significant midline shift / presence of mass lesion (The Brain Trauma Foundation, 2000). However, more specific conclusions about long-term prognosis cannot be made based on these findings.

Even though MRI is clearly superior to CT, particularly in detecting diffuse-type traumatic brain lesions, conventional MRI still highly underestimates the extent of TAI and also lacks sensitivity to subtle diffuse hypoxic-ischemic injuries. This probably explains why findings on conventional MRI are not closely related to prognosis. What seems to carry the most prognostic value on conventional MRI is the depth of identified lesions. While the finding of lesions in the cortex or subcortical white matter is not associated with worse prognosis, lesions indicating TAI in deep structures such as the corpus callosum and brainstem are associated with worse outcome (Wedekind et al, 1999; Firsching et al, 2001; Mannion et al, 2007). In particular the presence of bilateral brainstem lesions is strongly associated with poor outcome (Firsching et al, 2001).

As will be discussed later, some recent advanced MRI techniques are showing promise as prognostic tools, as they may improve the sensitivity to diffuse-type injuries.

CHAPTER 3

MAGNETIC RESONANCE IMAGING (MRI)

In this chapter a short introduction will be given to the basic principles of MRI. Following, the advanced MRI methods used in the present project will be described in brief.

3.1 Basic Principles

When performing an MR scan, the subject is placed in a strong homogeneous static magnetic field, B_0 . The field strength can range from low field, e.g. 0.5 Tesla (T) to high field, e.g. 7.0 T. Today most clinical scanners work at 1.0-3.0 T.

In the magnetic field, atomic nuclei with a magnetic moment (spin) will tend to align themselves along with B_0 . The MRI signal mainly comes from hydrogen nuclei (protons) in water molecules (except for some special MRI sequences not considered here). The protons precess around the direction of the magnetic field (the z-direction) with a frequency proportional to B_0 , the Larmor frequency.

By applying a brief radiofrequency (RF) pulse exactly at the Larmor frequency (the resonance frequency) protons can be brought out of equilibrium and the magnetization is flipped e.g. into the xy-plane, a process termed excitation. When the RF pulse ends, the magnetization returns to equilibrium by a process called relaxation. Relaxation follows an exponential course and can be described by two time constants, T1 and T2, which differ for different tissue types. T1 relaxation represents the regrowth of the magnetization in the z-direction, the longitudinal relaxation. T2 relaxation describes the loss of magnetization in the xy-plane, the transverse relaxation. (In physiological tissue, the transverse relaxation happens faster due to dephasing, caused by local field inhomogeneities, and is then termed T2*). The transverse component of the magnetization precesses around the z-axis emitting radio-waves at the Larmor frequency, which can be sampled by a receiver.

Spatial information is encoded by the use of gradients in the magnetic field. When images are acquired in 2D (slice-wise), slice selection is encoded during excitation, while in-plane spatial information is encoded subsequently by applying two additional gradients, a frequency-encoding and a phase-encoding gradient. Image reconstruction is then performed by use of Fourier transformation of the raw data (see e.g. Bushong, 2003).

MR image contrast is determined by a number of factors, some of which are related to the pulse sequence used and the selected sequence parameters. Some of the adjustable sequence parameters are the echo time (TE), the time from excitation to sampling; and the repetition time (TR), the time elapsed between two excitations. In general, with the choice of short TR along with short TE, T1-contrast is maximized, and the resulting images are said to be T1-weighted. With the choice of long TE along with long TR, T2-contrast is maximized, i.e. the images become T2-weighted. With the choice of long TR along with short TE, proton density weighting results.

A common category of MR pulse sequences are the spin-echo sequences, where a 90° excitation RF pulse is followed by a 180° refocusing RF pulse. In another type of pulse sequences, gradient echo sequences, the spins are refocused using gradients (instead of the 180° refocusing pulse used in spin-echo). As this does not eliminate effects from local magnetic field inhomogeneities, T2*-weighting is made possible, which is useful e.g. for the detection of blood (iron in haemoglobin and its derivatives induces field inhomogeneities). In inversion recovery sequences the magnetization is inverted by an inversion RF pulse prior to excitation, and thereby signal nulling is possible. For example, fluid-attenuated inversion recovery (FLAIR) produces heavily T2-weighted images but nulls the signal from CSF, with the advantage of improved lesion detection in tissue close to CSF.

Echo planar imaging (EPI) represents a sequence principle for very fast image acquisition, which can be either spin-echo or gradient-echo. The very short acquisition time allows for e.g. the acquisition of time series in functional MRI, but at the expense of spatial resolution and signal-to-noise-ratio.

For more information on the principles of MRI including a number of different conventional MRI sequences, the reader is referred to textbooks on this subject (e.g. Bushong, 2003; Bernstein et al, 2004).

3.2 Diffusion Imaging

Diffusion-weighted imaging (DWI), as well as its extension into diffusion tensor imaging (DTI), represents MRI techniques which are made sensitive to the self-diffusion of water molecules. The molecular diffusion, or Brownian motion, refers to the thermally driven random movement of molecules (e.g. water molecules) in a fluid. This movement is described by the diffusion coefficient (D), which is influenced by the temperature, the viscosity of the media and size of the molecules. In the unrestricted environment, as in a glass of water, diffusion is isotropic i.e. equal in all directions. However, in biological tissue, membranes etc. cause diffusion to be restricted, and in areas where diffusion is unequally restricted in different directions, diffusion is

described as anisotropic. In biological tissue the calculated diffusion coefficient is therefore termed the 'apparent diffusion coefficient' (ADC, sometimes termed the mean diffusivity, MD).

DWI and DTI are usually based on EPI spin-echo sequences in which pairs of diffusion-sensitising gradient pulses are introduced. Basic DWI, in which diffusion is measured along three orthogonal directions, provides diffusion-weighted images and maps of ADC. DTI provides additional information about the directional dependence of the diffusion signal, allowing diffusion to be considered in 3D. Imaging data is acquired while applying gradients that sensitise the signal to diffusion along a larger number of different directions (minimum of 6). For each direction, applying the first (defocusing) gradient pulse causes phase shifts of the protons along that direction. Typically 20-50 ms after the first pulse, a second (refocusing) gradient pulse is applied which, in absence of molecular diffusion, will refocus ('rewind') the phase perfectly and cause a high MR signal to be sampled. However, when water molecules move in between the two gradient applications, the second gradient will not refocus the phase perfectly, and consequently the sampled MR signal is attenuated (see Figure 3.1). This measured signal attenuation is then used to estimate the diffusion coefficient, D , from the following relationship (Stejskal-Tanner, see e.g. Le Bihan, 1995):

$$\frac{S}{S_0} = \exp(-bD) = \exp\left(-\gamma^2 G^2 \delta^2 \left(\Delta - \frac{1}{3}\delta\right)D\right)$$

where S and S_0 are the measured signals with and without the diffusion-sensitising gradient respectively, γ is the gyromagnetic ratio (specific for the nucleus), G the gradient amplitude, δ the duration of the gradient, and Δ the time interval between the leading edges of the gradient pulses. The b-value (b) is a summary parameter related to gradient strength.

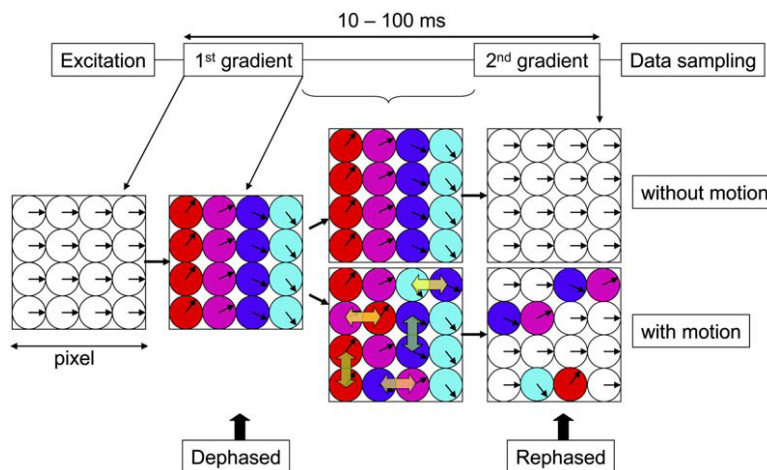


Figure 3.1. Diagram to explain the relationship between water motion and gradient applications in DTI. Circles represent water molecules, vectors in the circles indicate phases of the signal. If water molecules move in between the two gradient applications, the second gradient cannot perfectly refocus the phases, which leads to signal loss. In this example, horizontal motion leads to the signal loss, but vertical motion does not affect the signal intensity. (Reprinted from Mori & Zhang, 2006)

The successive application of diffusion-sensitising gradients in at least 6 directions with corresponding measurements of S allows for a mathematical model, known as a tensor, to be fitted to the measurements at each voxel. A tensor is a mathematical construct which can be expressed as a symmetric matrix (in this 3D case, the tensor is a 3x3 matrix). The diffusion tensor is fully characterised by the length and direction of its three major axes (Le Bihan 1995; Pierpaoli & Basser, 1996). As an illustration of the diffusion tensor (Figure 3.2) the probability

function of water displacement can be visualized as an ellipsoid, where the axes represent the three principal diffusion orientations (the eigenvectors, v_1, v_2, v_3) and $\lambda_1, \lambda_2, \lambda_3$ are the corresponding eigenvalues (diffusion coefficients). By convention, the eigensystem is ordered so that $\lambda_1 > \lambda_2 > \lambda_3$.

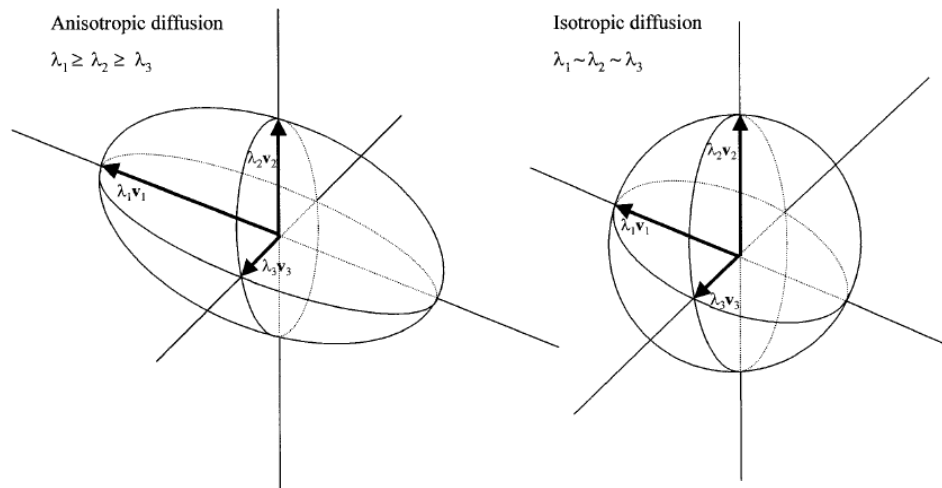


Figure 3.2. Probability function for water displacement, depicted as an ellipsoid. The axes are directed along the eigenvectors (v_1, v_2, v_3 , principal diffusion orientations), and the lengths are scaled by the corresponding eigenvalues ($\lambda_1, \lambda_2, \lambda_3$, diffusion magnitudes). The eigensystem is conventionally ordered so $\lambda_1 > \lambda_2 > \lambda_3$, with anisotropic diffusion characterised by $\lambda_1 \geq \lambda_2 \geq \lambda_3$ and isotropic diffusion by $\lambda_1 \sim \lambda_2 \sim \lambda_3$. (Reprinted from Wiegell et al, 2000)

The degree to which diffusion is directionally dependent can be expressed e.g. as the fractional anisotropy (FA), a parameter which can be calculated from the eigenvalues and takes values ranging from 0 (isotropic) to 1 (anisotropic) (Pierpaoli & Basser, 1996):

$$FA = \sqrt{\frac{1}{2} \frac{\sqrt{(\lambda_1 - \lambda_2)^2 + (\lambda_2 - \lambda_3)^2 + (\lambda_3 - \lambda_1)^2}}{\sqrt{\lambda_1^2 + \lambda_2^2 + \lambda_3^2}}}$$

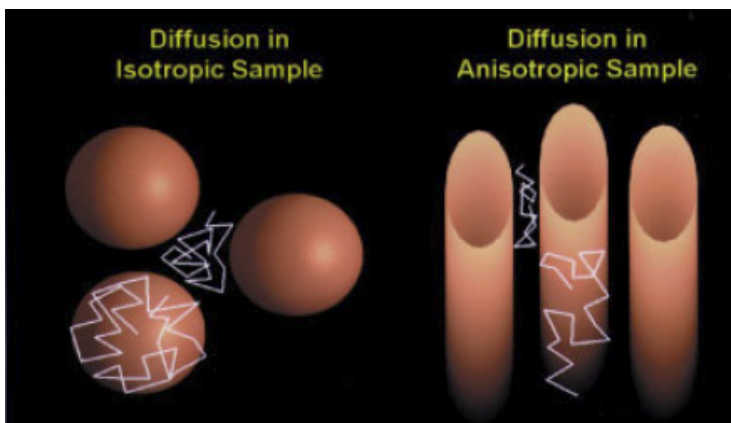


Figure 3.3. Schematic illustration of isotropic diffusion (similar molecular displacements in all directions) and anisotropic diffusion (greater molecular displacement along cylinders than across). In brain white matter, diffusion is anisotropic due to anatomical barriers causing diffusion to be restricted especially perpendicular to axonal fibre direction. (Reprinted from Beaulieu, 2002)

In the brain white matter, diffusion is anisotropic as it is greater along the axis of axons than across (see Figure 3.3). FA values are highest in regions where axons are organized in densely packed highly parallel fibre bundles (see Figure 3.4). This directional dependence is due to the presence of physical barriers to diffusion across axonal fibre bundles. Although the relative contribution of different components to white matter anisotropy has not been determined unequivocally, axonal membranes and myelin sheaths seem to compose the principal extracellular barriers (Beaulieu, 2002). In white matter, λ_1 is commonly termed the parallel diffusivity ($\lambda_{||}$) and the mean of λ_2 and λ_3 is termed the perpendicular diffusivity (λ_{\perp}).

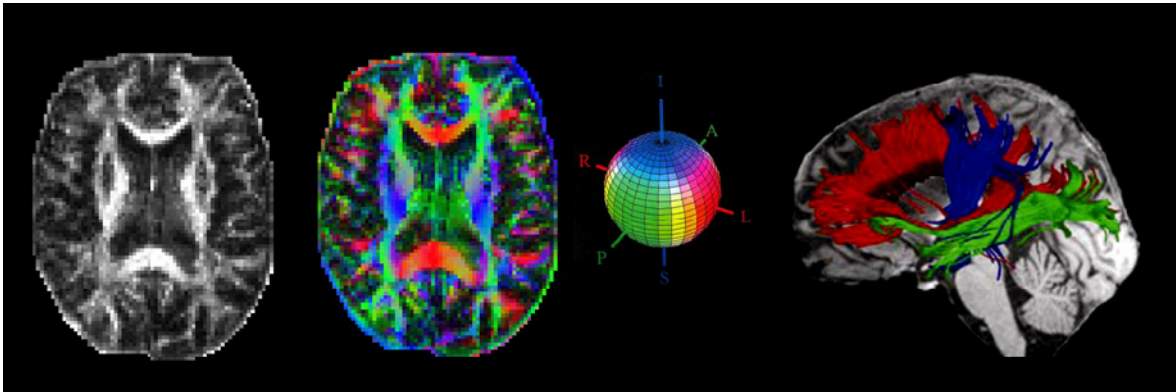


Figure 3.4. Examples of DTI maps. From left to right: Map of FA where intensity reflects FA (high intensity is high FA and vice versa). Colour map showing the dominating diffusion direction (v_1) masked by FA. As illustrated by the colour sphere, red represents the transverse direction, green the anterior-posterior and blue the superior-inferior direction. The information obtained from DTI can also be used for fibre tracking, by which axonal tracts are reconstructed. (Images are from the present study and from Wiegell et al, 2000).

Thus, in the brain white matter, the quantities derived from DTI are related to the micro-architecture of the tissue. Any pathological process which affects the barriers to diffusion could cause changes in the measured diffusion signal. However, there is not a clear-cut relationship between FA changes and any specific pathological change. Importantly, a decrease in FA could reflect a decrease in $\lambda_{||}$, an increase in λ_{\perp} , or a combination of these changes (and vice versa for FA increase). The pathological interpretation of changes in these underlying diffusivities is, however, also ambiguous (e.g. Sun et al, 2006; Budde et al, 2007).

3.3 Morphometry

Unlike techniques to measure diffusion, MRI techniques to measure brain morphology do not require a non-standard MRI sequence. Instead, these methods are based on conventional 3D high-resolution (usually T1-weighted) images processed with advanced software tools. In disease or in the normal brain (e.g. with ageing) neuroanatomical changes may be too subtle, diffuse or topologically complex to be detected by simple visual inspection or manually traced measurements of regions of interest (ROIs). With the continuous rapid development of computing power, the application of increasingly sophisticated software for morphometric image analysis is made possible. Manual ROI drawing for brain volume measurements is gradually getting replaced by unbiased and much less labour-intensive automated algorithms, and the field of computational neuroanatomy is developing rapidly. In the following, a short general

introduction to the main principles of voxel-wise computational neuroanatomy will be given. Note that, for convenience, the term MRI morphometry is used here as a joint designation for MRI techniques which measure brain volume changes as well as those measuring local shape changes.

Usually, computational techniques for morphometry involve some or all of the following steps: Brain extraction, tissue segmentation, co-registration/spatial normalization, smoothing, and statistical analysis (Ashburner et al, 2003). Brain extraction is necessary to eliminate the skull and exterior soft tissue. In tissue segmentation, voxels representing grey matter, white matter, and CSF are classified on the basis of intensity values. Co-registration/spatial normalization is a critical step in which the voxels of interest are matched to a template, a 'typical' brain (spatial normalization) or to a scan from the same individual acquired at another time point (co-registration). There are several approaches to coregistration/spatial normalization (see below), and this image registration step is typically what distinguishes different morphometry techniques. Smoothing is the spatial blurring of images by the averaging of signals from neighbouring voxels (usually done by applying a Gaussian filter). Smoothing is done to reduce registration imperfections, and to allow for parametric analysis. Finally, a statistical comparison is made of different groups of subjects or points in time.

Morphometry techniques can be classified into techniques designed for cross-sectional analysis versus those designed for longitudinal analysis. However, although one algorithm may have been developed for one purpose, it can also be useful in another (Ashburner et al, 2003). Further, techniques can be categorized according to whether they measure global or local changes of volume/shape (and whether analysis is based on intensity changes or deformation fields, see below).

One algorithm designed for longitudinal measurement of global volume changes is Structural Image Evaluation, using Normalisation, of Atrophy (SIENA; Smith et al, 2002). Here serial scans of the same individual are matched using linear registration. The method then finds all brain-surface edge points and estimates the perpendicular displacement of these edge points from one time point to the next (Figure 3.5), converting the mean edge displacement into an estimate of global brain volume change (%BVC). Measurement error of %BVC has been reported to be approximately $\pm 0.2\%$ (Smith et al, 2002). A modification of SIENA, termed SIENAX (Smith et al, 2002) is available for cross-sectional analysis.

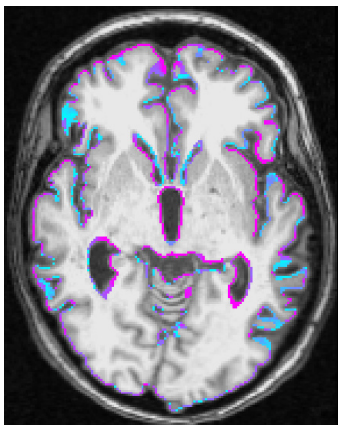


Figure 3.5. Structural Image Evaluation, using Normalisation, of Atrophy (SIENA). Example slice showing edge motion between two scan time points in the same subject, overlaid onto the original image. Here, red is atrophy, and blue is "growth". Edge displacement estimates are converted into percent brain volume change (%BVC). (From the present study)

In order to capture local changes of volume or shape, registration must be non-linear. The process of non-linear registration is often termed warping (Ashburner & Friston, 2007). Analysis of regional changes can be categorized into voxel-based* or deformation-based approaches, with tensor-based analysis being a special case of the latter. In voxel-based analysis, as e.g. in voxel-based morphometry (VBM; Ashburner & Friston, 2000), information on local volume differences are derived from intensity changes in each voxel upon registration. VBM is designed for cross-sectional analysis, and identifies regional differences in grey or white matter concentration between groups of subjects. In deformation-based methods, registration does not rely on tissue segmentation, and information on the extent of warping is stored in the computed deformation field (Figure 3.6). Statistical analysis is then performed on the deformation fields rather than on the registered images. In tensor-based morphometry (TBM; Ashburner et al, 2000), which is designed for longitudinal analysis, the Jacobian (see e.g. Press et al, 1992) of the deformation field is calculated for each voxel by taking the gradient of the deformation at each point. From this tensor field, the Jacobian determinant (JD), a scalar measure, is calculated for each voxel. In TBM, regional contraction or expansion can be expressed by the JD, e.g. if the JD takes the value of 2 in a particular voxel, that voxel has contracted from the first to the second scan by a factor of 2. Conversely, if the JD is -2, that voxel has expanded to double size. Thus, TBM allows for detailed quantitative information on regional changes of volume and shape over time.

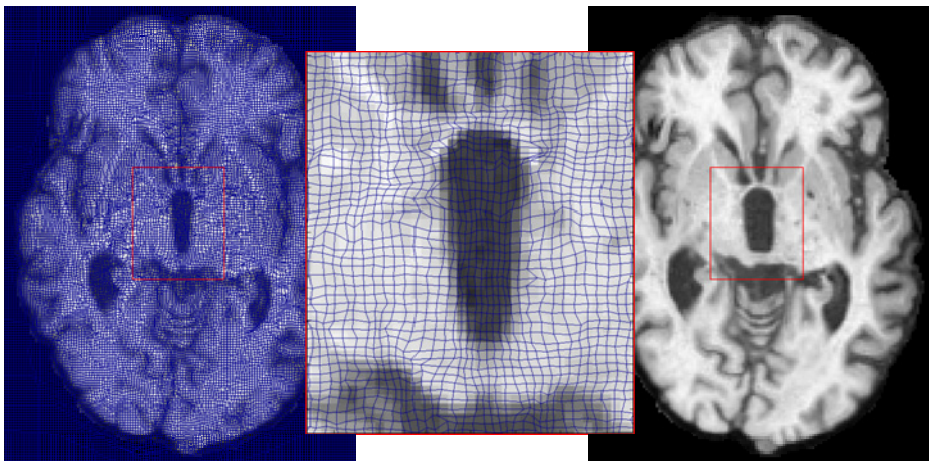


Figure 3.6. The deformation field illustrating the warping of one image to another. When the gradient of the deformation (the Jacobian) is used for statistical analysis, the method is termed tensor-based morphometry (TBM). (From the present study)

* Although changes in both tissue volume and shape are measured voxel-wise, techniques based on intensity changes are traditionally referred to as voxel-based morphometry (where intensity changes are translated into volume changes). Measurements of shape changes are correspondingly often referred to as deformation-based morphometry. This nomenclature is followed in this thesis.

CHAPTER 4

MRI OF TBI

In the previous two chapters, some background was given on TBI and on MRI, respectively. The present chapter now considers the application of MRI to TBI patients, with focus on the imaging of TAI and its structural consequences. First, some practical and ethical issues are mentioned. This is followed by an introduction to the imaging of TAI by conventional MRI. Thereafter, previous studies which have applied diffusion or morphometry MRI techniques in patients with severe TBI are reviewed. This leads finally to the motivation for the present studies.

4.1 Practical and Ethical Issues

Conventional MRI is far superior to CT for the diagnosis of traumatic lesions in the brain parenchyma, including the brainstem (e.g. Parizel et al, 1998). However, due to practical difficulties and risks of having unstabilized patients in the MR-scanner, MRI in the very acute phase cannot usually be performed for severely injured patients. Firstly, precautions need to be taken with MRI, particularly concerning metallic objects inside or outside the patient, including monitoring equipment. Secondly, the acquisition time of MRI is considerably longer than for CT, and MRI is much more sensitive to subject movement. CT is generally sufficient for the detection of focal intracranial (intra- or extracerebral) lesions which require acute neurosurgery. For these reasons CT is the recommended neuroimaging method for initial acute evaluation, and MRI is usually not performed until the patient has been stabilized.

When the patient is sufficiently stable for MRI, one issue which deserves special attention is subject movement. Sensitivity of MRI to subject movement is relevant even in the unconscious patient, but of course particularly problematic in patients in the confusional state, i.e. Rancho levels IV-VI (see Appendix 4). Also, patient cooperation may be a challenge at higher Rancho levels because of cognitive problems. Therefore, sedation or general anaesthesia is very often necessary in order to obtain a useful MR-scan in patients with severe TBI. Naturally, for the individual patient, this raises considerations about the risk associated with anaesthesia/sedation

versus the value of the diagnostic or prognostic information expected to be provided by MRI. Ethical issues arise particularly due to the inability of most patients to provide their own informed consent regarding anaesthesia/sedation. This is a major concern, not least if MRI is performed for research purposes.

4.2 Conventional MRI

Some classes of conventional MRI sequences were introduced in Chapter 3. Due to the diversity of possible lesion types in TBI, a number of MRI sequences are relevant in TBI patients. Covering this in detail for all lesion types is beyond the scope of this thesis; instead the reader is referred to textbooks of clinical MRI (e.g. Gentry, 2002). However, as the challenge of imaging diffuse-type lesions, in particular TAI, is one of the major issues motivating the present PhD project, a short review on conventional MRI for the detection of TAI is given below.

As noted earlier, conventional MRI highly underestimates the extent of TAI, particularly the non-haemorrhagic lesions (e.g. Jones et al, 1998). Yet, MRI is far superior to CT and represents the best tool to diagnose TAI presently available for routine clinical use. Appearance of TAI is very dependent on the MRI sequence used and is influenced by lesion age and presence/absence of haemorrhage or blood breakdown products (e.g. Parizel et al, 1998). T2*-weighted gradient echo sequences, with long echo time, are sensitive to iron-containing molecules such as haemoglobin and its degradation products, and therefore are suitable for detecting micro-haemorrhages associated with TAI (Figure 4.1). Haemosiderin, the end-stage haemoglobin derivate, causes marked hypointensities on T2*-weighted sequences. As haemosiderin cannot be processed by macrophages, these hypointensities on T2*-weighted gradient echo images may persist life-long (e.g. Parizel et al, 1998; Gentry, 2002).

However, as mentioned previously, the majority of TAI-lesions are non-haemorrhagic. T2-weighted imaging and particularly FLAIR may identify some of these lesions, or the oedema related to it, in the acute or sub-acute phase (Ashikaga et al, 1997; Parizel et al, 1998; Gentry, 2002). In the weeks and months following trauma, non-hemorrhagic TAI becomes less apparent, but might be identified as hyperintensities on FLAIR (Figure 4.1).

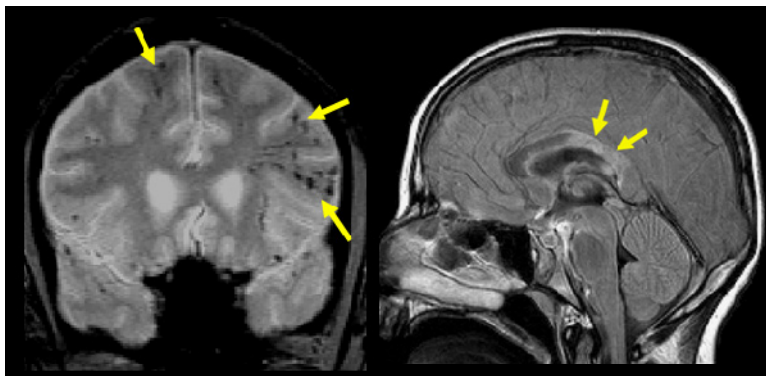


Figure 4.1. Conventional MRI of TAI. Left: Coronal T2*-weighted image showing multiple small haemorrhages at the subcortical grey-white matter junction. Right: Sagittal FLAIR showing a large hyperintense area in the corpus callosum. These images are examples of very pronounced abnormalities. (From the present study).

While TAI haemorrhagic lesion load, detected by T2*-weighted gradient echo imaging, has been found to be related to initial GCS (e.g. Scheid et al, 2003) there is poor correlation with long-term (>6 months) functional outcome. For example, Scheid et al studied the appearance of TAI at 3 Tesla in 66 patients in the chronic stage of TBI, and found no correlations between number and site of traumatic micro-bleeds and long-term outcome as measured by the extended Glasgow outcome scale (Scheid et al, 2003). Most other studies have found no or limited correlation between lesion load on conventional MRI and long-term outcome (e.g. Kelly et al, 1988; Levi et al, 1990).

Susceptibility-weighted imaging (SWI), although non-conventional, shall briefly be mentioned here. SWI has been shown to detect more TAI lesions than conventional T2*-weighted imaging, and lesion load on SWI may also be better related to clinical outcome (Tong et al, 2004). Still, SWI detects only the minority of TAI lesions which are associated with haemorrhage.

4.3 Diffusion Imaging

In recent years, diffusion imaging, in particular DTI, has attracted considerable attention for application in trauma and in a variety of diseases (see e.g. Assaf & Pasternak, 2008). Given the histopathological effects of TAI, with focal misalignment of the cytoskeletal network, changes of the axolemmal permeability and eventually disconnection of axons, changes of tissue diffusion properties are to be expected. Experimental studies have shown correlations between DTI and histology of TAI (Mac Donald et al, 2007), and the sensitivity of DTI to microstructural alterations makes this technique an obvious candidate for detecting and quantifying the histological effects of TAI *in vivo*. Before reviewing the previous literature regarding DTI in adult (mainly severe) TBI, studies using DWI will be mentioned for completeness.*

DWI performed within a few weeks post-trauma has been found to reveal TAI lesions that are not visible by conventional MRI (e.g. Hergan et al, 2002; Huisman et al, 2003, Ezaki et al, 2006; Hou et al, 2007). However, some TAI lesions detectable by conventional imaging may escape detection by DWI (Ezaki et al, 2006). Hyperintensities on diffusion weighted maps can be associated with either hyper- or hypointensity on ADC maps, and accordingly Hergan et al (Hergan et al, 2002) classified the DWI characteristics of TAI lesions into type 1 (increased ADC), type 2 (decreased ADC) and type 3 (complex with increased and decreased ADC within the same lesion). These variable ADC findings are thought to reflect a fast temporal evolution of the diffusion within TAI lesions in the acute phase. In experimental studies, a general rise in ADC apparently occurs immediately after trauma (reflecting vasogenic oedema), and within a few hours post-trauma ADC values decrease to below normal values (reflecting cytotoxic oedema) and remain decreased for up to two weeks. Thereafter ADC may again rise to above-normal values as a consequence of tissue degeneration with increased extracellular fluid content. However, the exact time course of ADC changes following TAI has not been delineated unequivocally (Assaf et al, 1997; Barzó et al, 1997) partly due to the lack of a good

* Since the submission of Paper I of the present thesis, a number of articles on DTI in TBI have emerged in the literature. These very recent studies are not considered as 'previous' and therefore will not be mentioned here. Instead these studies will be discussed in chapter 6 (section 6.1).

experimental model of TAI. In humans, acute/subacute whole-brain ADC values have been found to correlate with initial GCS score, with lower GCS being associated with higher ADC (Shanmuganathan et al, 2004). The relation between DWI acquired in the acute/subacute phase and long-term outcome has been investigated by Hou et al (Hou et al, 2007), who found that patients with unfavourable outcomes had significantly higher deep grey and white matter mean ADC values compared to those with favourable outcomes and to controls (Hou et al, 2007). Ezaki et al found that the number of DWI lesions in the brainstem was significantly higher in patients with unfavourable outcome than in patients with favourable outcome, a trend which could not be found based on conventional MRI (Ezaki et al, 2006).

The first paper applying DTI in clinical TBI was a case-study published in 1999 (Wieshmann et al, 1999), reporting areas of reduced FA along with increased ADC in a patient who had sustained severe TBI years previously. Following, Rugg-Gunn and colleagues published similar findings in two patients that had unremarkable conventional MRI (Rugg-Gunn et al, 2001). Both of these studies applied voxel-wise DTI analysis. Since then, a number of DTI studies have been published on groups of TBI patients who were studied in the acute, subacute or chronic phase (Arfanakis et al, 2002; Chan et al, 2003; Ptak et al, 2003; Huisman et al, 2004; Salmond et al, 2006; Nakayama et al, 2006; Benson et al, 2007; Xu et al, 2007). The number of patients in these studies ranged from 5 to 23, and injury severity was heterogeneous in most studies. The majority of studies applied an ROI-based approach (Arfanakis et al, 2002; Chan et al, 2003; Ptak et al, 2003; Huisman et al, 2004; Nakayama et al, 2006) with some applying a voxel-based approach (Salmond et al, 2006; Nakayama et al, 2006; Xu et al, 2007) or a whole-brain histogram analysis (Benson et al, 2007). Generally, FA was found to be reduced in TBI patients compared to controls, most consistently in the corpus callosum (Arfanakis et al, 2002; Chan et al, 2003; Ptak et al, 2003; Huisman et al, 2004; Nakayama et al, 2006; Xu et al, 2007), internal capsule (Arfanakis et al, 2002; Ptak et al, 2003; Huisman et al, 2004; Xu et al, 2007) and in white matter structures comprising the centrum semiovale (Ptak et al, 2003; Xu et al, 2007). ADC changes were reported to be both increased and decreased in studies of acute TBI, while studies on patients in the chronic phase generally reported widespread increases of ADC (Salmond et al, 2006; Xu et al, 2007).

Correlations between DTI measures and clinical measures of severity and outcome were investigated in a few of the above studies. In one study (Huisman et al, 2004) FA values in the splenium of corpus callosum and the internal capsule were found to be correlated with initial GCS and with the Rankin Scale score at discharge (on average only 18 days post-injury). Another study (Ptak et al, 2003) reported a correlation between DTI findings and short-term outcome parameters such as death or discharge to rehabilitation facility. Salmond et al investigated chronic TBI survivors and found high ADC to be associated with impaired neuropsychological test performance on learning and memory indices (Salmond et al, 2006). In a group of TBI patients with heterogeneous injury severity (mild to severe), scanned at a variable time from injury (3 days to 15 years) Benson et al found a correlation between FA histogram properties and injury severity indexed by GCS or PTA (Benson et al, 2007).

Longitudinal studies with serial application of DTI in TBI are sparse. A few studies have been published in which 2-3 scans were acquired in one or two patients (Arfanakis et al, 2002; Naganawa et al, 2004; Le et al, 2005; Voss et al, 2006). In these studies FA reductions were

most pronounced in the acute phase, gradually increasing to sub-normal values after some weeks. ADC was found to be reduced for up to a few days post-trauma, then gradually normalised, reaching supra-normal values after a few months. Le et al also reported the eigenvalues of the diffusion tensor measured in one patient, finding the major eigenvalue (λ_1) reduced and the minor eigenvalues (λ_2 and λ_3) slightly increased a few days post-trauma. At follow-up 12 weeks post-injury, λ_1 had increased to almost normal, while λ_2 and λ_3 had increased further to above normal (Le et al, 2005). Similar changes in the eigenvalues over time were reported for two patients with mild TBI studied within 24 hours of injury and again at one month by Arfanakis et al (Arfanakis et al, 2002).

4.4 Morphometry

Neuropathologists have long observed that the brains of patients who sustained severe TBI months or years before death usually show conspicuous atrophy on macroscopic examination. More recently it has become clear that the process of volume loss may continue for a long time after injury (e.g. Graham & Gennarelli, 1997), which is also indicated by animal studies (Smith et al, 1997; Rodriguez-Paez et al, 2005). Atrophy following severe TBI may not be homogeneously distributed, and knowledge of the regional distribution of late atrophy could potentially indicate the mechanism(s) accounting for the progressive volume loss. In the following, only morphometry studies on TBI which have applied voxel-wise analyses will be considered. For a review of ROI-based studies, see (Bigler, 2005).

Previously, only one longitudinal study investigated late brain volume changes by serial MRI in patients with severe TBI. Trivedi and colleagues (Trivedi et al, 2007) applied the SIENA software to evaluate global brain volume change between approximately 79 and 409 days post-TBI in 37 patients with TBI ranging from mild to severe (16 classified as severe). The authors found a change in brain volume of mean -1.43% (relative to $+0.1\%$ in healthy controls), with greater decline in brain volume being associated with longer duration of post-injury coma. Relation to clinical outcome was not reported in this study.

Four previous studies applied VBM to investigate the regional distribution of atrophy post-trauma (Gale et al, 2005; Tomaiuolo et al, 2005; Salmond et al, 2005; Bendlin et al, 2008), and of these one very recent study was longitudinal (Bendlin et al, 2008). In this latest study 35 patients with moderate TBI had MRI at about 2 months and again at about 12.7 months post-injury. In a group-wise statistical comparison between scan 1 and scan 2 (grey and white matter maps analyzed separately) significant volume loss over time was reported in corona radiata, corpus callosum, internal and external capsules, superior and inferior longitudinal fasciculus, cingulum, inferior fronto-occipital fasciculus, corticospinal tract, cerebellar peduncles, thalamus, and pallidum, as well as small areas with volume loss in the cerebellar white matter, right post-central and precentral gyri, supplementary motor area, and putamen (Bendlin et al, 2008). In the cross-sectional study by Gale et al, nine patients were examined about one year following TBI (severity ranging from mild to severe TBI). In comparison with healthy controls, the authors found decreased grey matter concentration in multiple brain regions including frontal and temporal cortices, cingulate gyrus, subcortical grey matter and cerebellum (Gale et al, 2005). Tomaiuolo et al compared white matter concentration in 19 severely injured patients and 19 controls. Patients were scanned 3-113 months following injury. The authors reported

significant volume reduction in corpus callosum, fornix, anterior limb of the internal capsule, superior frontal gyrus, para-hippocampal gyrus, optic radiation and chiasma (Tomaiuolo et al, 2005). Salmond and colleagues studied both grey and white matter density in 22 patients with moderate or severe TBI, compared with controls. They reported grey matter reduction in the basal forebrain nuclei, the hippocampal formation and regions of the neocortex (parietal, temporal, occipital lobes). White matter reduction was found in the lateral capsular pathway and in the medial pathway (Salmond et al, 2005).

As introduced in Chapter 3, TBM allows for high-dimensional within-subject registration and therefore is particularly suitable for longitudinal studies. When instead compared to a template brain, TBM is also useful for cross-sectional analysis. Particularly when studying TBI, where focal lesions may cause regional distortions in brain shape and intensity changes, VBM has important limitations which are partly overcome by TBM. Firstly, misregistration during normalization of highly heterogeneous brains is reduced using the high-dimensional warping of TBM, and when used for longitudinal analysis, the within-subject registration approach further minimizes registration errors. Secondly, lesioned areas easily cause errors in tissue segmentation, and as opposed to VBM, TBM does not require segmentation. Mainly for these reasons TBM would be expected to be more robust in the analysis of TBI brains than would VBM.

One cross-sectional TBM study on TBI was recently published (Kim et al, 2008). The population consisted of 29 patients with moderate or severe TBI, scanned at least 3 months (ranging between 4 months and 27.5 years) following injury, and compared to 20 controls matched in terms of age, gender, education and ethnicity. Using an advanced normalization algorithm followed by TBM with warping of each patient's brain to a study-specific template, the authors found localized volume reduction most prominently in the thalamus, the midbrain, the corpus callosum, the cingulate cortex, and the caudate (at a false discovery rate, FDR, of 0.05). Significant volume increase was found mainly in the ventricles. It should be emphasized that, since this was a cross-sectional study of patients with chronic TBI, no distinction could be made between early and late atrophy.

4.5 Motivation for the Present Studies

In considering the previous literature there is an obvious paucity of longitudinal studies on TBI, in particular studies of DTI or morphometry which have correlated imaging findings with clinical outcome parameters. In general, very few studies have applied serial MRI in groups of TBI patients. Moreover, in most previous cross-sectional MRI studies, injury severity was heterogeneous and data on long-term clinical outcome were not reported. In particular, no previous studies on DTI or morphometry in TBI patients enabled comparison between imaging findings and measures of clinical function at different time points during rehabilitation. Such information is warranted, as it could add to our understanding of the macro- and microstructural brain changes occurring during recovery from severe TBI, and how this relates to clinical variables. Further, in search of prognostic markers in TBI, some previous studies have suggested that DTI may be a candidate tool. However, no previous studies investigated correlations of relatively early DTI findings with long-term (>6 months) clinical outcome in severe TBI.

In consideration of the above, the present project was conducted as a prospective longitudinal study with acquisition of MRI, including DTI, at two time points (~2 months and ~1 year post-trauma) and frequent clinical functional assessments, including outcome evaluation at ~1-year post-injury.

It was hypothesized that:

- DTI abnormalities (reduced FA) in white matter would be present at the first scan time point in patients as compared to healthy controls
- At both scan time points, DTI would be more abnormal in patients with unfavourable long-term outcome as compared to patients with favourable long-term outcome
- During recovery, initial DTI abnormalities might partly normalise, at least in some regions
- The extent of late atrophy would be larger in patients with clinical indices of more severe injury (based on duration of coma and PTA) and with unfavourable outcome
- The most pronounced late volume changes would be found in regions susceptible to TAI and resulting Wallerian degeneration

In the following chapters, methods and results of the present project will be described, followed by a discussion of the results. As the two papers constituting the basis of this thesis are included as appendices (Appendices 1 and 2), only brief summaries of the results will be given. The discussion implies acquaintance with the articles, and it is therefore recommended that these are read in detail before proceeding to the discussion (Chapter 6).

CHAPTER 5

METHODS AND RESULTS

In this chapter methods and results of the present project will be described. Only brief summaries of the results presented in the papers (Appendices 1 and 2) will be given here. Some additional results, not included in the papers, will be provided in this chapter.

5.1 Design and Subjects

This project was designed as a prospective longitudinal study of patients with severe TBI, with a healthy control group for comparison. MRI was acquired at two time points at which patients were evaluated clinically, as illustrated by the study time line below (Figure 5.1).

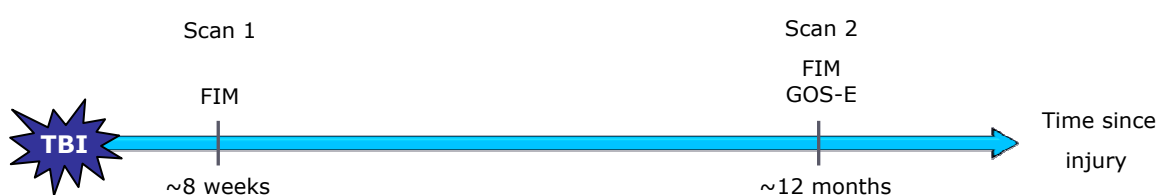


Figure 5.1. Study time line illustrating the data sampling time points.
FIM = functional independence measure; GOS-E = extended Glasgow outcome scale.

The cohort of patients was recruited from the Brain Injury Unit, Department of Neurorehabilitation at Hvidovre Hospital, Denmark, which receives patients for early intensive rehabilitation. The inclusion criteria of this project were as follows: Severe TBI within 12 weeks, age ≥ 18 years, and informed consent from patient or from closest relative. If sedation/anaesthesia was required for MRI, patients were included only if conventional MRI was requested for clinical purposes. MRI sequences for research purposes (including DTI) were then acquired in the same session. For patients with impaired consciousness, informed consent was

Table 5.1. Demographics and clinical characteristics (patients)

Patient	Age at scan1 (years)	Sex	APOE	Cause of trauma	Initial GCS	Neuro-surgery ^a	ISS	Secondary insults ^b	Days to GCS >8	Duration of PTA (days)	FIM at scan1	FIM at scan2	GOS-E at ~1 year
1	19	M	NA	MVA	4	-	35	+	10	>FU	29	83	3 (3)
2	23	F	2/3	MVA	3	-	43	+	36	79	47	120	4 (3)
3	23	F	3/3	Fall	3	-	45	+	>FU	>FU	18	18	2 (2)
4	21	F	4/4	MVA	6	+	25	-	12	39	79	117	4 (3)
5	34	M	3/3	MVA	3	-	66	+	126	>FU	18	30	3 (3)
6	40	F	3/3	Fall	3	+	25	+	9	>FU	18	20	3 (3)
7	40	M	3/3	Assault	3	-	29	+	4	88	87	122	6 (4)
8	60	M	3/4	Fall	3	+	25	-	21	>FU	34	35	3 (3)
9	28	M	3/3	MVA	≤8	-	25	-	24	66	122	125	8 (5)
10	54	M	3/3	Fall	≤8	-	34	-	14	119	60	125	5 (4)
11	23	M	3/3	MVA	4	+	43	-	18	47	117	124	6 (4)
12	26	M	3/3	MVA	3	-	35	-	2	25	110	126	7 (5)
13	24	M	3/4	MVA	3	-	26	-	1	39	93	125	5 (4)
14	65	M	3/3	Fall	3	-	29	-	3	39	116	120	6 (4)
15	31	M	2/3	MVA	5	+	25	+	7	48	38	102	5 (4)
16	37	M	3/3	MVA	≤8	+	38	-	14	40	117	122	7 (5)
17	22	M	2/3	MVA	≤8	-	43	-	7	31	120	125	7 (5)
18	19	M	2/3	MVA	6	-	33	-	2	23	113	124	7 (5)
19	41	F	3/3	MVA	6	+	34	-	10	65	55	113	5 (4)
20	26	M	4/4	MVA	6	+	25	+	22	65	106	124	6 (4)
21	60	M	3/3	Fall	3	-	26	+	18	289	31	30	3 (3)
22	22	M	3/3	MVA	3	-	43	+	9	178	18	103	4 (3)
23	61	M	NA	Fall	5	+	25	+	22	>FU	18	25	3 (3)
24	23	M	3/3	MVA	3	-	29	+	11	107	23	111	4 (3)
25	18	F	3/3	MVA	3	+	29	+	15	66	24	105	4 (3)
26	40	M	3/4	Fall	3	+	25	-	10	84	100	117	5 (4)
27	53	M	3/4	Fall	4	+	25	+	5	171	18	111	5 (4)
28	28	M	3/3	Fall	3	-	38	+	15	180	18	36	3 (3)
29	31	M	2/4	MVA	3	-	48	+	33	>FU	18	22	3 (3)
30	27	M	3/3	MVA	6	-	35	+	10	77	49	113	5 (4)
31	26	F	2/3	MVA	7	-	29	-	4	58	59	126	8 (5)

APOE=apolipoprotein genotype; MVA=motor vehicle accident; GCS=Glasgow coma scale; NA=not available; >FU=exceeds ~1 year follow-up; ISS=injury severity score (>25 indicates extra-cranial injury); PTA=post-traumatic amnesia; FIM=functional independence measure; GOS=Glasgow outcome scale; GOS-E=extended Glasgow outcome scale.

^a Surgery that involved craniotomy, excluding insertion of intracranial pressure monitoring devices.

^b Occurrence of hypotension (systolic blood pressure < 90 mmHg), hypoxia (oxygen saturation < 90% or cyanosis in field) or intracranial pressure > 20 mmHg.

obtained from the closest relative. If the patient regained consciousness during the time of the study, the continued participation depended on consent from the patient him-/herself.

Exclusion criteria were: Previous history of TBI or other neurological disorder, presence of contraindications to MRI or to sedation/anaesthesia during MRI. Further, patients were excluded from the study if, for safety or practical reasons, the first MRI could not be acquired within 12 weeks from injury. Finally, lack of informed consent for participation/continued participation excluded patients from the study, as did lack of clinical request for the initial MRI in patients unable to cooperate for MRI without sedation/anaesthesia.

Patients were not excluded based on their use of alcohol or drugs, as in particular alcohol was frequently involved in the accidents causing TBI, and history of abuse was often subject to considerable uncertainty. However, estimated use of alcohol and drugs, as reported by relatives, was recorded and considered in the selection of healthy controls (see below).

All patients with severe TBI, according to initial GCS, who were admitted to the Brain Injury Unit during the recruitment period (2003-2005) were evaluated for study eligibility. The most frequent causes of exclusion were logistic problems in acquiring MRI within 12 weeks from injury, and the presence of extracranial metal implants considered unsafe for MRI. A total of 31 patients were included (Table 5.1). The patient population of this study represented the most severe end of the spectrum of severe TBI, reflecting the admission criteria of the Brain Injury Unit (Engberg et al, 2006).

For comparison in terms of quantitative MRI measures, 30 healthy controls were included. Of these, 6 participated as part of another project (led by Henrik Kahr Mathiesen). The controls were recruited through announcements on the internet, in supermarkets, garages, etc., and by use of an introductory questionnaire they were selected to approximately match the patient group on the parameters age, sex, education, and use of alcohol and drugs (Table 5.2). Exclusion criteria were a history of TBI, any significant medical illness, or contraindications to MRI.

Table 5.2. Demographics of patient and control groups (all subjects*)

	Patients (n = 31)	Controls (n = 30)	Group differences
Age, scan 1 (years) [mean (SD)]	33.7 (14.2)	34.0 (13.9)	$P > 0.91^a$
Sex: M/F	24/7	23/7	$P = 1.02^b$
Education (years) [mean (SD)]	13.3 (3.0)	13.4 (2.3)	$P > 0.91^a$
Excessive alcohol intake (> 21 drinks per week for men, > 14 for women), Y/N	5/26	4/26	$P = 1.02^b$
Use of drugs (cannabinoids or psycho-stimulants) > once a month, Y/N	3/28	1/29	$P > 0.62^b$

* Similar comparisons for subjects included in the longitudinal analyses are found in Table 2 of Paper I and in Table 1 of Paper II. ^a Independent-samples *t*-test ^b Fishers Exact test.

5.2 Clinical Assessments

The clinical assessments reported in this study were performed by trained staff as part of routine assessments. Data from the acute phase were obtained from medical files of the neuro-intensive units. Ratings and evaluations throughout inpatient rehabilitation, at discharge, and at follow-up were documented in the Brain Injury Unit's rating files. The reported functional assessments do therefore not reflect choices of scales made for the present study. The personnel performing the ratings were unaware of quantitative MRI results.

For details on how various clinical parameters were defined or assessed, please see Paper I (Material and methods, subsection on clinical assessments). Note that while in Paper I the original Glasgow outcome scale (GOS) was reported, we chose to report the extended GOS (GOS-E) in Paper II as these additional data were available for all patients. How GOS-E translates into GOS can be found in Appendix 4.

In Appendix 4, English versions of some of the applied assessment scales are provided, including GCS, functional independence measure (FIM) and GOS/GOS-E. For more information on the various rating scales which are commonly used in TBI, the reader is referred to the following website: <http://www.tbims.org/combi/>

5.3 MRI Acquisition

All patients and controls were scanned on the same 1.5 Tesla Siemens Magnetom Vision MR scanner at the Danish Research Centre for Magnetic Resonance (DRCMR), Hvidovre Hospital. Preceding the inclusion period, a pilot MRI of two patients (not included in the study) was acquired to decide on the final MRI protocol. During the study period, MRI sessions for patients and controls were interleaved in time, and no major upgrades were carried out on the scanner.

The MRI protocol comprised the following conventional sequences: T1-weighted 3D high-resolution (1 mm^3), T2-weighted double spin-echo, T2*-weighted gradient-echo, and FLAIR sequences (for sequence parameters, see Paper I). The DTI sequence was a spin-echo single-shot EPI sequence with diffusion encoding in 6 non-collinear directions averaged over 6 datasets. Sequence parameters were as follows: echo time = 60 ms, field of view = 230×230 mm, matrix 128×128 , 30 axial slices of 5 mm thickness, b-values of 0 and $\sim 740 \text{ s/mm}^2$ with duration of diffusion sensitizing gradient pulse, $\delta=29$ ms, and gradient separation, $\Delta=52$ ms. This DTI sequence had been developed and implemented on the scanner as part of a previous PhD project (by Mette Wiegell). In some patients, additional measurements of proton spectroscopy and perfusion were also acquired (not included in this thesis). Total acquisition time was around 60 minutes (around 90 minutes when additional sequences were acquired).

The conventional sequences and DTI were acquired for the first scan of all patients. For the follow-up scan, and for controls, not all of the conventional sequences were necessarily acquired, but a minimum of DTI and 3D T1-weighted images were obtained.

Table 5.3. MRI acquisition and findings on conventional images (patients)

	Scan 1			Scan 2			Conventional MRI findings (scan 1)		
	Sedation	T1-W	DTI	Sedation	T1-W	DTI	TAI grade ^a	Focal lesions ^b	
1	+	+	+	NA	- ¹	- ¹	II	Haem L putamen	
2	+	+	+	NA	- ²	- ²	III	Haem R temporal	
3	+	+	+	+	+	+	II	-	
4	+	+	+	-	+	+	II	Cont L+R temporal	
5	+	+	+	+	+	+	III	-	
6	+	+	+	+	+	+	II	Cont L+R mesial incl. thalamus	
7	+	+	+	-	+	+	0	-	
8	+	+	+	+	+	+	II	Cont L+R temporal, Inf R PCA	
9	+	+	+	-	+	+	III	-	
10	+	+	+	-	+	+	II	Cont L+R frontal	
11	-	+	(+) ⁴	-	+	(+) ⁴	II	Cont R frontal + L temporal	
12	-	+	+	-	(+) ⁴	+	II	-	
13	+	+	+	-	+	+	I	-	
14	-	+	+	-	+	+	I	Cont L temporal	
15	+	+	+	-	+	+	II	Cont L+R frontal, abscess R frontal, Inf R ACA+PCA, Inf L mesencephalon	
16	-	+	+	-	+	+	I	Cont L temporal	
17	-	+	+	-	+	+	II	-	
18	-	+	+	-	+	+	I	-	
19	+	+	+	-	+	+	II	Cont L+R frontal+L temporal	
20	+	+	+	-	+	+	I	Cont R frontal + L temporal	
21	+	+	+	NA	- ¹	- ¹	III	-	
22	+	+	+	-	+	+	II	-	
23	+	+	+	NA	- ¹	- ¹	II	Cont L+R temporal, Inf L parietal	
24	+	+	+	-	+	+	III	Cont L temporal	
25	+	+	+	-	+	+	III	Cont L frontal + R temporal	
26	+	+	(+) ⁵	-	+	+	II	Cont R frontal + R temporal	
27	+	+	+	-	+	+	III	Cont L+R frontal, Inf L PCA	
28	+	+	+	NA	- ³	- ³	III	Cont R temporal	
29	+	+	+	NA	- ¹	- ¹	III	Haem L+R frontal	
30	+	+	+	-	+	+	II	-	
31	+	+	+	-	+	+	II	-	

¹ Insufficient patient cooperability; ² MRI-incompatible implants; ³ Patient relocation; ⁴ Movement artifacts; ⁵ Acquisition error.
^a According to location of microhaemorrhages on T2*-weighted images (0=none, I=subcortical only, II=callosal, III=brainstem).
^b Parenchymal lesions only. Note: General atrophy and signs of pyramidal tract degeneration in the brainstem were found in many patients, in particular at scan 2. L=left, R=right; Cont=contusion; Haem=haemorrhage; Inf=infarction; ICA=internal carotid artery; ACA=anterior cerebral artery; PCA=posterior cerebral artery; T1-W=T1-weighted (3D sequence); NA=not applicable.

For all patients included, the first MRI was acquired between 5 weeks and 11 weeks (mean 8 weeks) post-injury. Of the 31 patients, 25 had follow-up MRI between 9 months and 15 months (mean 12 months) post-injury. For the remaining patients a second MRI could not be acquired for reasons listed in Table 5.3. Of the 30 controls, 14 were scanned twice, and with a similar time interval as that of patients.

As mentioned in Chapter 3, sedation/anaesthesia during MRI acquisition is often necessary in patients with impairment of consciousness or cognition. This turned out to be necessary in the majority of patients (25 out of 31) at the first scan. However by the time of the follow-up scan, most patients were able to cooperate for MRI without sedation/anaesthesia, and only a few (4 out of 25) were sedated. Although from a research perspective it would have been desirable if this factor could have been kept constant within the study population and over time, for ethical reasons patients were only sedated if necessary and if MRI was requested for clinical purposes.

The choice of scan time points was partly a matter of what was practically feasible, and partly based upon considerations of pathophysiology and the effects under investigation. At around 8 weeks post-injury, patients were usually stable enough for MRI and had been transferred from the neuro-intensive departments (at other hospitals) to rehabilitation at Hvidovre Hospital. Another clear advantage of a delayed first scan time point was to avoid major effects of tissue oedema on the measured MRI quantities. The second scan time point, around 1 year post-injury, was practical, as patients were routinely admitted for 1-day clinical follow-up in the Brain Injury Unit about 1 year from injury. Also, structural changes would be expected to have occurred during this relatively long time interval between scans.

5.4 MRI Data Processing

Before initiating analysis of MRI data, all images were visually checked for quality and excluded if image quality was insufficient. Prior to quantitative analyses, conventional images of patients were qualitatively evaluated by an experienced neuroradiologist (Margrethe Herning) unaware of clinical ratings.

The processing of MRI data in this study has been described in detail in the methods sections of Papers I and II. Figure 5.2 and 5.3 provide schematic overviews of MRI data processing steps preceding statistical analyses. For an explanation of the principles of some key data processing steps, such as spatial normalization and coregistration, see e.g. the following MRI online tutorial by de Haan & Rorden (although concerning functional MRI, basic processing steps are similar in structural MRI) http://www.sph.sc.edu/comd/rorden/fmri_guide/index.html

The analysis of DTI data was ROI-based, mainly because more advanced and reliable voxel-wise approaches for DTI analysis (such as Tract-based spatial statistics; Smith et al, 2006) were not developed at the time when DTI analysis of this project was initiated. The ROIs were manually outlined on each of the normalized 3D T1-weighted images, and were positioned by anatomical guidance, not lesion guidance. ROIs in the most frontal cerebral areas were avoided, since frontal regions were susceptible to misregistration (stemming from EPI-related susceptibility artifacts). Although ROI drawing was performed blinded to subject status, the presence/absence of visible lesions and central atrophy usually revealed subject status as patient/control. White

matter ROIs included: Posterior aspect of corpus callosum (PCC), posterior limb of internal capsule (PLIC), centrum semiovale (CSO) and cerebral peduncle (CP). Additionally, ROIs were positioned in deep grey matter (putamen) and in CSF. Details of ROI positioning are described in Paper I. Diffusion parameter results were summarized as median values for voxels comprising the ROI, values for bilateral ROIs being averaged.

The software tools applied for morphometry (SIENA and TBM) were chosen because these techniques were designed for longitudinal analysis, and because they were judged to be the most robust available methods for handling the challenges of TBI brains, in particular the frequent presence of focal lesions.

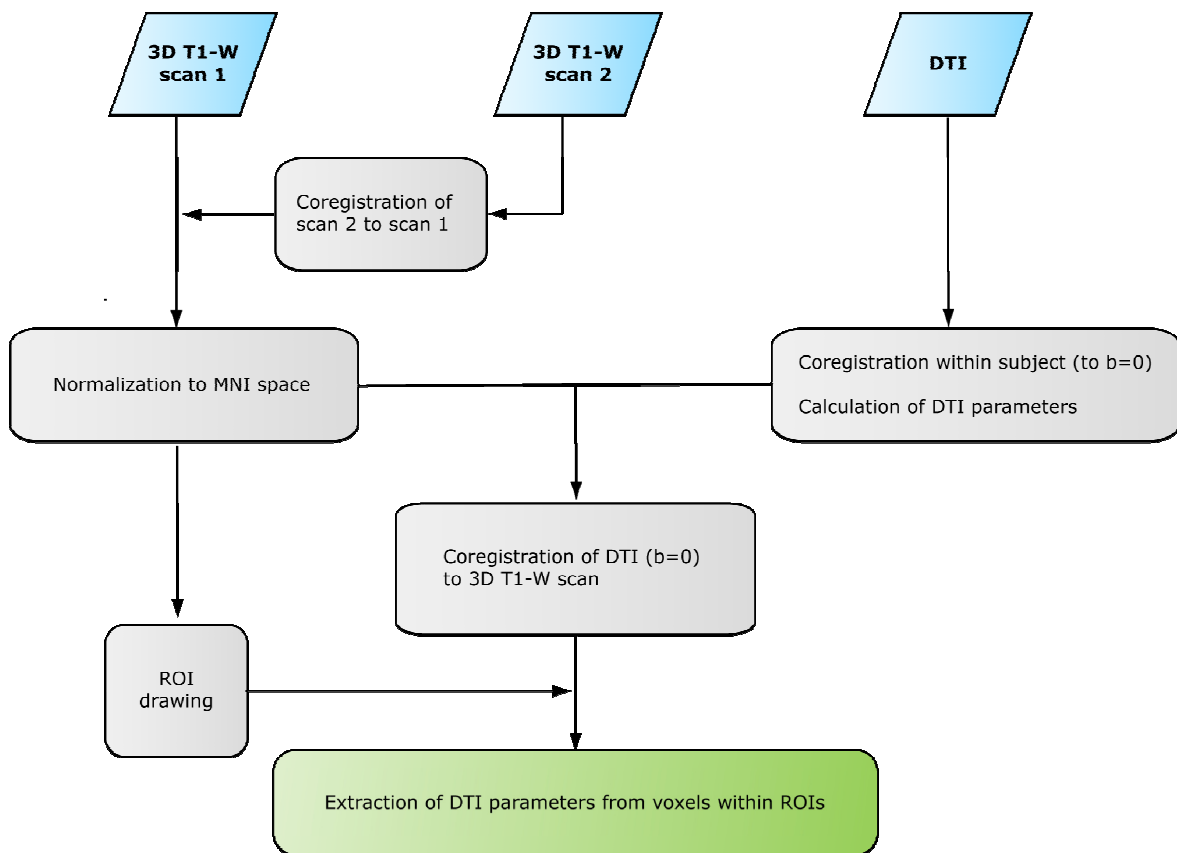


Figure 5.2. Overview of data processing for DTI analysis. Subsequent statistical analyses are described in Paper I. T1-W = T1-weighted; MNI = Montreal Neurological Institute.

5.5 Results, Paper I (Diffusion Study)

At the initial scan time point, DTI data of acceptable quality were available for 29 patients and 30 controls. In 22 of the patients and in 14 of the controls, DTI data of sufficient quality were available at both time points. Reproducibility of DTI parameter results regarding ROI positioning (intra-rater only), as well as between successive DTI acquisitions, was satisfactory in white matter, see Paper I for details. As PCC is particularly prone to partial voluming from neighbouring CSF, successive erosion of the exterior of this ROI was performed. This indicated partial voluming (Table 5, Paper I), but statistical results remained significant following erosion.

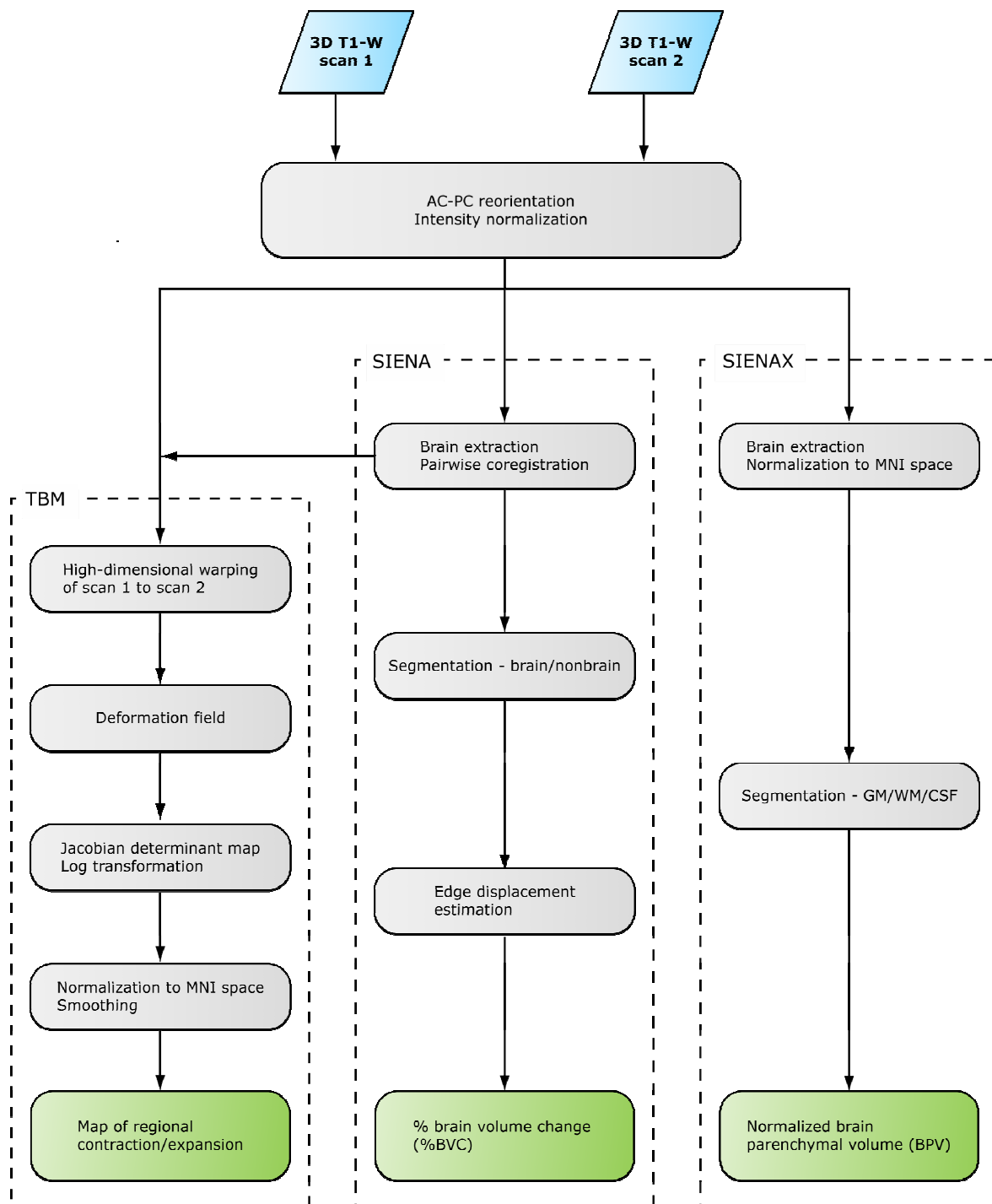


Figure 5.3. Overview of data processing for morphometry. Subsequent statistical analyses are described in Paper II. T1-W = T1-weighted; AC-PC = anterior commissure - posterior commissure; MNI = Montreal Neurological Institute; GM = grey matter; WM = white matter.

Initial scan

In all of the four white matter regions studied, FA was significantly decreased in patients as compared to controls. This was caused by the combined effects of $\lambda_{||}$ decrease and λ_{\perp} increase (significant except in CSO) with relatively unaffected MD (Table 3, Paper I).

Longitudinal findings

In controls, no significant changes of DTI parameters were observed over time. In patients, FA had partly normalised at follow-up in PLIC and CSO due to a selective increase of $\lambda_{||}$. Conversely, in PCC and CP, FA decreased further as both $\lambda_{||}$ and λ_{\perp} increased (λ_{\perp} relatively more than $\lambda_{||}$). Consequent increases of MD were found (Table 4, Paper I).

Clinical correlations

At the initial scan, FA in CP was positively correlated with GOS (Figure 3, Paper I). When included in a logistic regression model to predict dichotomized GOS, FA in CP predicted dichotomized outcome with 76% accuracy when taken alone. Further, FA in CP significantly added predictive accuracy to FIM evaluated at the initial scan time point, so that a model consisting of initial FIM and FA in CP yielded a predictive accuracy of 100% in this sample.

At follow-up there was a positive correlation between $\lambda_{||}$ in PLIC and GOS. In PCC and CP, FA values were lower in patients with unfavourable outcome than in patients with favourable outcome, according to dichotomized GOS.

5.6 Results, Paper II (Morphometry Study)

For 24 patients and 14 controls, good-quality 3D high-resolution T1-weighted images were available at both time points. Result images of within-subject registration (SIENA and TBM) and of segmentation (SIENAX) were inspected for every subject.

Initial scan

As a rough estimate of the volume loss occurring before the first scan time point, patients were compared to controls on global volume measures, using SIENAX. Normalized brain parenchymal volume (BPV) was on average 8.4% smaller in the patients than in the controls (mean \pm SD: 1506 ml \pm 85 ml and 1645 ml \pm 85 ml, respectively).

Longitudinal findings

During the scan interval, patients exhibited continued atrophy with percent brain volume change (%BVC), derived from SIENA, ranging between -0.6% and -9.4% (mean -4.0%, median -2.9%). In controls %BVC ranged between -0.9% and +0.3% (mean -0.18%, median -0.13%).

As seen in Figure 5.4, regional distribution of this late atrophy in patients (relative to controls), investigated using TBM, revealed widespread symmetric volume loss in the brainstem and cerebellar peduncles, thalamus, putamen, internal and external capsules, inferior and superior longitudinal fasciculus, corpus callosum and corona radiata, with additional small clusters of volume loss mainly in the cerebellum and in the frontal lobes. Significant volume expansion was found in the ventricles and scattered in the subarachnoid space (permutation test, FDR 0.05). Individual TBM result images for all subjects (one axial slice only) are displayed in Figure 5.5.

Clinical correlations

BPV at the initial scan correlated with concomitantly evaluated FIM, and with duration of PTA. Initial-scan BPV also correlated with the full-scale GOS-E, although it did not significantly distinguish patients with favourable versus unfavourable outcome based on dichotomized GOS-E, and did not improve prediction of FIM at follow-up in a linear regression model.

Longitudinal %BVC correlated with duration of coma and of PTA, and with FIM evaluated at both scan time points. With respect to outcome, %BVC correlated with GOS-E and distinguished favourable and unfavourable outcome groups. In a linear regression model to predict FIM at follow-up, adding %BVC significantly improved a model based on FIM at the initial scan.

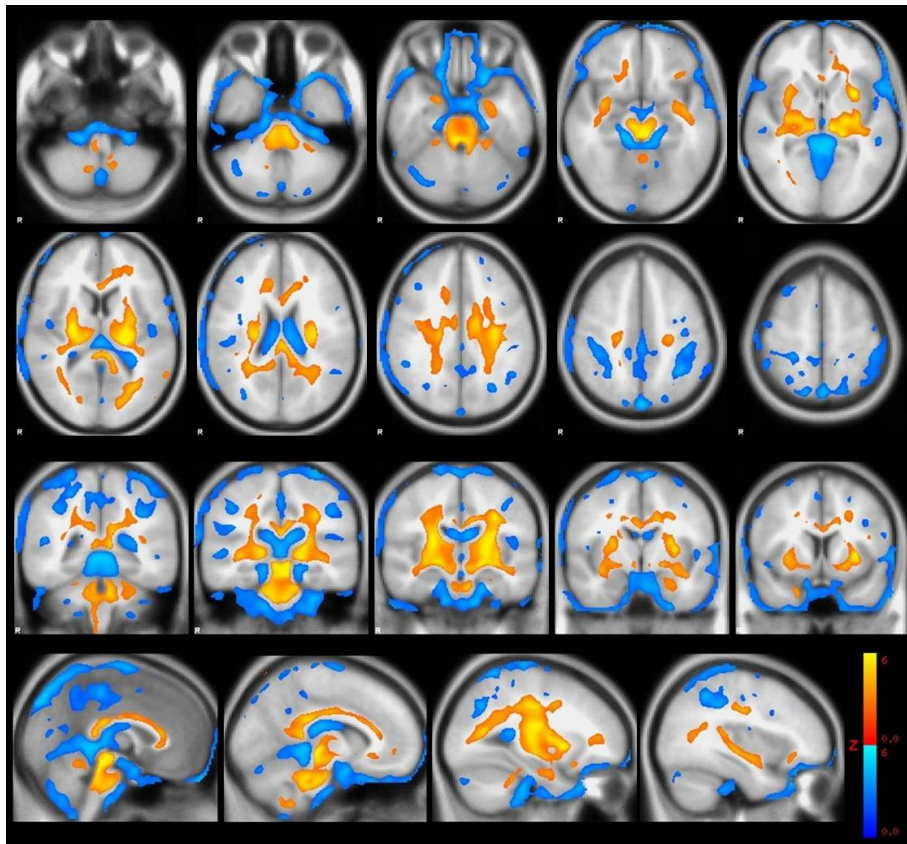


Figure 5.4. Regions of significant volume changes in TBI patients between ~8 weeks and ~12 months post-injury, as compared to controls, thresholded at false discovery rate (FDR) 0.05 (clusters of < 33.5 voxels rejected). Longitudinal volume reduction is coded with hot colours, volume expansion with cold colours. Results are overlaid onto the Montreal Neurological Institute (MNI) standard template.

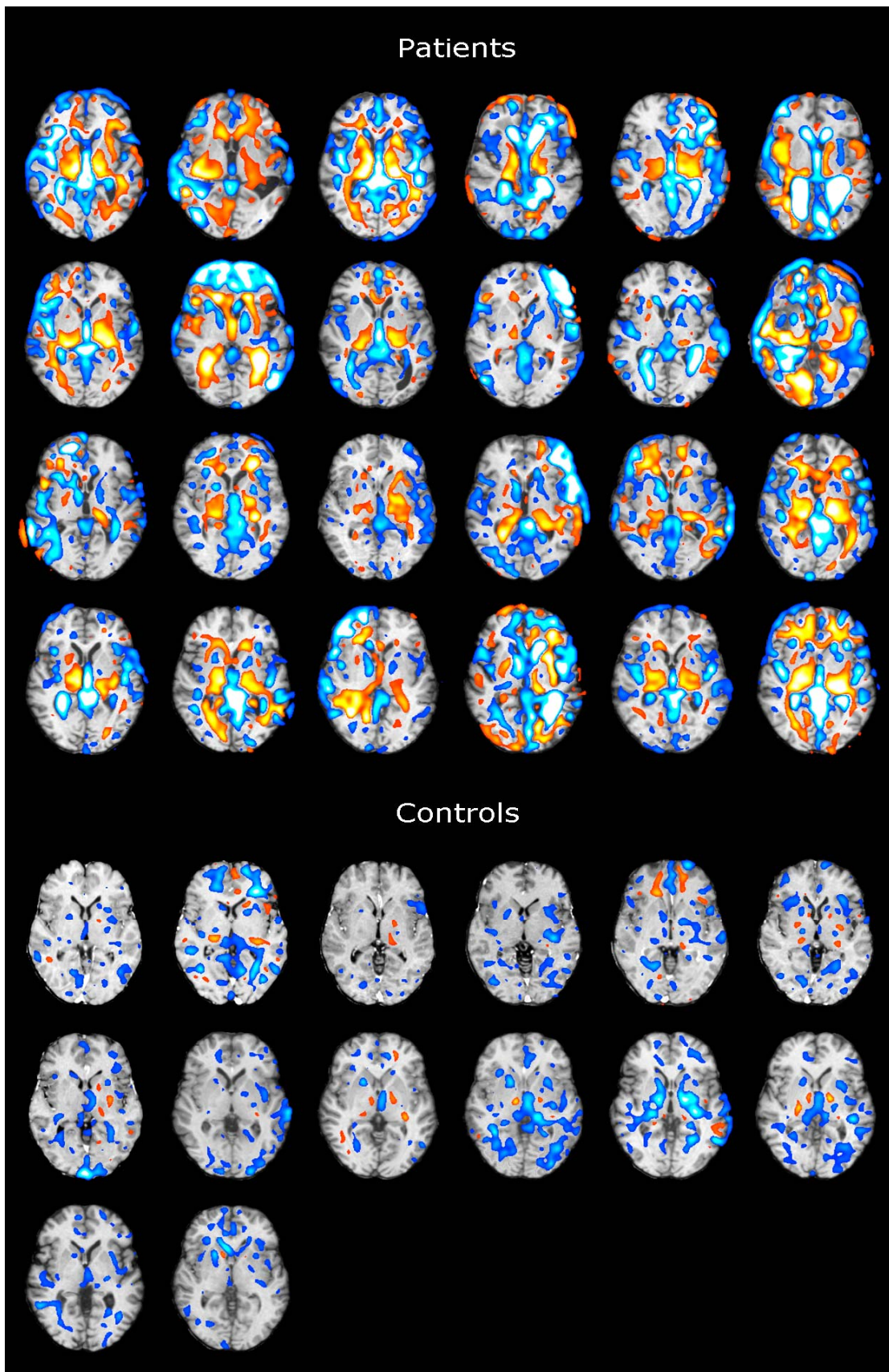


Figure 5.5. Individual TBM result images (one slice per subject) for the 24 patients and 14 controls. Normalized and smoothed log Jacobian determinant maps overlaid onto normalized T1-weighted images (scan 2). Longitudinal volume reduction is coded with hot colours, volume expansion with cold colours.

5.7 Supplemental Results

Regional Volume Changes and Outcome

Additional analysis of the TBM results of patients was made in order to investigate whether a different pattern of late atrophy would be found in patients with unfavourable outcome (GOS-E = 1-4) in comparison with patients with favourable outcome (GOS-E = 5-8). Limited by the small number of subjects in each group (16 with favourable outcome and 8 with unfavourable outcome) it was expected that, if any detectable differences existed, there might be more extensive atrophy in the brainstem in patients with unfavourable outcome as compared to patients with favourable outcome, reflecting the supposedly more frequent occurrence of brainstem TAI and extensive Wallerian degeneration with unfavourable outcome.

Statistical analysis was performed similarly as for the main TBM analysis (permutation test, same nuisance variables). Since no voxels of volume loss survived the FDR 0.05 threshold, we applied a threshold of $p < 0.001$, uncorrected for multiple comparisons. The results are seen in Figure 5.6. Apart from clusters of volume expansion in the subarachnoidal CSF, this shows a generally asymmetrical pattern of small clusters of volume loss scattered mainly in deep white matter and brainstem. However, one bilateral cluster of volume reduction in the brainstem was found at the level of pons and the middle cerebellar peduncles, indicating more extensive volume loss over time in this area for patients with unfavourable outcome as compared to patients with favourable outcome.

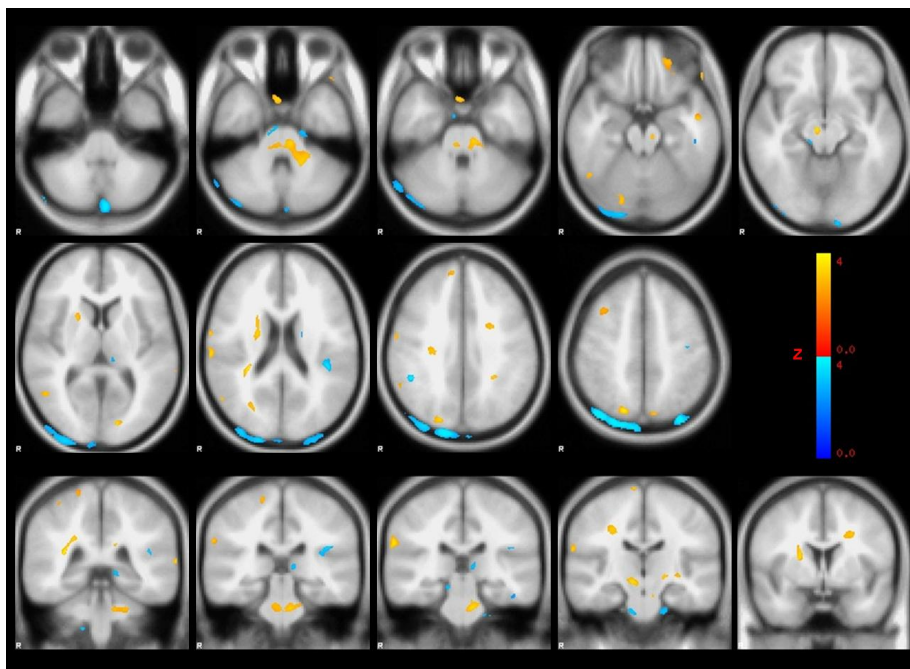


Figure 5.6. Areas in which patients with unfavourable outcome (GOS-E = 1-4; $n = 8$) exhibited more longitudinal volume change as compared to patients with favourable outcome (GOS-E = 5-8; $n = 16$), thresholded at $p < 0.001$, uncorrected (clusters of < 33.5 voxels rejected). Longitudinal volume reduction is coded with hot colours, volume expansion with cold colours. Results are overlaid onto the Montreal Neurological Institute (MNI) standard template.

Relation between Diffusional and Volume Changes

One might speculate whether the longitudinal change of DTI parameters could be explained by the volume changes. Therefore the longitudinal results for DTI and SIENA were compared for the 22 patients who had good quality 3D T1-weighted images as well as DTI images at both scan time points. Simple correlation analyses (Spearman's correlation) of %BVC versus FA in each of the 4 white matter ROIs did not reveal any significant or near-significant correlations ($p > 0.2$). Unfortunately, more detailed analysis of this problem was not possible because of the different approaches for analysis (ROI-based versus voxel-based) in the DTI and morphometry studies.

Apolipoprotein E (APOE) Genotype

As mentioned in Chapter 2, in some studies the APOE E4 allele has been associated with worse outcome following TBI. In the present study, APOE genotype was determined for the patients in order to check for any possible confounding effect by APOE genotype in statistical analyses of clinical outcome. For method of APOE genotyping on blood, see (Wenham et al, 1991). APOE results are displayed in Table 5.1.

Due to the small sample size of this study, only presence or absence of the APOE E4 allele was analysed statistically. The APOE E4 allele occurred with a frequency comparable to that reported for the general Danish population (Gerdes et al, 1992). Among the 29 patients in whom APOE E4/non-E4 status was available, there were no significant differences regarding the occurrence of APOE E4 in patients with favourable versus unfavourable outcome (Fishers Exact test, $p = 1.0$). When included as a covariate in the regression analyses reported in Papers I and II, presence/absence of APOE E4 did not show any statistical tendency for influencing clinical outcome. Further, there were no significant (or near-significant) relationships between APOE E4/non-E4 status and key DTI parameters, e.g. FA in CP ($p > 0.8$, independent samples t-test), or between APOE E4 status and %BVC ($p > 0.9$, independent samples t-test).

CHAPTER 6

DISCUSSION

In this chapter the results of the present studies are discussed in relation to current knowledge within the field, including results of very recent publications not available at the time of submission of Papers I and II. Regarding limitations of the present studies, mainly issues which have not been thoroughly dealt with in Paper I or Paper II will be discussed here. This chapter requires detailed acquaintance with Papers I and II.

6.1 Interpretation of Results

In this section Papers I and II are not discussed separately, but instead the section is divided into a discussion of the early cross-sectional findings followed by a discussion of the longitudinal results. Finally, the supplemental unpublished results are considered.

Early Cross-sectional Findings

At the first scan time point, approximately 8 weeks post-injury, a comparison with matched healthy control brains yielded an average parenchymal volume reduction of 8.4%. Although this should be regarded as a fairly rough estimate, it does indicate massive atrophy within the first weeks to months following severe TBI, in accordance with general pathological and radiological experience (Graham & Genarelli, 1997; Gentry, 2002). This measure of early volume loss, however, correlated only weakly with clinical long-term outcome.

At the microstructural level, DTI at the first scan time point revealed significantly reduced FA in all four investigated white matter regions (PCC, PLIC, CSO, CP) in patients as compared to controls. Generally, this is in agreement with previous studies (Arfanakis et al, 2002; Chan et al, 2003; Ptak et al, 2003; Huisman et al, 2004; Salmond et al, 2006; Nakayama et al, 2006; Benson et al, 2007; Xu et al, 2007) and also with some very recent studies (Bendlin et al, 2008; Miles et al, 2008; Niogi et al, 2008; Rutgers et al, 2008). In the longitudinal DTI and VBM study

by Bendlin and colleagues (Bendlin et al, 2008) a voxel-wise DTI analysis of TBI patients at the first scan time point, about 2 months post-injury, showed FA reductions in the same regions as found in our study, plus in several additional regions (forceps major and minor, anterior corona radiata, anterior limb of internal capsule, external capsule, cingulum, inferior fronto-occipital fasciculus, uncinate fasciculus, and portions of the thalamus). Recent studies of mild TBI also revealed significant FA reductions in white matter, even in patients with normal findings on conventional imaging (Miles et al, 2008; Niogi et al, 2008; Rutgers et al, 2008). This indicates that DTI is sensitive even to subtle injury.

Given that DTI quantities capture biological severity it is likely that these are related to clinical outcome. In the present study it was found that FA in CP correlated with 1-year outcome and improved prediction of dichotomized outcome in a logistic regression model. Our finding of FA in CP being related to outcome is very preliminary and certainly needs confirmation in larger studies. One might speculate why the correlation with outcome was found specifically for FA in CP. One explanation may be that FA in CP reflects the microstructural integrity of the entire pyramidal tract above the level of the mesencephalon. TAI anywhere in the cerebral part of the pyramidal tract will eventually lead to Wallerian degeneration involving the CP, so DTI of the CP may capture much of the biological severity related to TAI.

Although DTI seems to carry high sensitivity towards TAI, as also demonstrated in experimental studies (Mac Donald et al, 2007), it should be emphasized that the specificity is limited. FA decrease in white matter has been found in a number of different diseases (reviewed e.g. by Assaf & Pasternak, 2008) and is by no means specific to TAI. Experimental studies have indicated that information on the eigenvalues could potentially provide more specificity in terms of the underlying pathology. In particular, experimental axonal injury has been found to selectively decrease $\lambda_{||}$ while demyelination has been reported to selectively increase λ_{\perp} (Song et al, 2002; Song et al, 2003; Sun et al, 2006). However, it is still unclear and a matter of debate to which extent this eigenvalue information can be used to infer underlying pathology. In the present study we found that the observed FA decrease in TBI patients as compared to controls was caused by a combination of $\lambda_{||}$ decrease and λ_{\perp} increase. Similar findings have been found in previous case reports of TBI (Arfanakis et al, 2002; Le et al, 2005). Although this could reflect the combination of axonal injury ($\lambda_{||}$ decrease) and demyelination (λ_{\perp} increase), other types of pathology, e.g. gliosis, would cause similar changes of the eigenvalues. Thus, with the current knowledge, no characteristic pattern of DTI parameter change can be regarded as pathognomonic for TAI.

This naturally leads to the question of whether or not the observed DTI abnormalities can be assumed to reflect TAI. Indeed TAI and consequent Wallerian degeneration cannot be distinguished based on DTI, as brainstem Wallerian degeneration secondary to hemispherical stroke produces a similar pattern of eigenvalue changes as does TAI (Pierpaoli et al, 2001). In studies of mild TBI in otherwise healthy subjects, with no visible lesions found on conventional MRI, FA values below the normal range would be likely to reflect the effects of subtle TAI and its consequences. However, in more severe TBI where different lesion types very often coexist, it is not necessarily possible to distinguish between effects of TAI/Wallerian degeneration and effects of other lesions on the DTI parameters. In particular, secondary diffuse lesions, such as hypoxic-ischemic injury, often go undetected by conventional MRI but may very well affect DTI

values. Although no studies have been published which applied DTI on hypoxic-ischaemic injury in adults, one study of infants with non-traumatic hypoxic-ischemic encephalopathy found reduced FA in a number of regions including centrum semiovale and internal capsule (Ward et al, 2006), regions which are also affected by TAI.

To summarize, considerable atrophy occurs during the first weeks to months following severe TBI. DTI seems to provide high sensitivity towards the detection of TAI, but lacks specificity. Still, DTI is very promising as a marker of biological injury severity and a candidate prognostic indicator in TBI. Further studies are clearly needed to determine the prognostic value of DTI in TBI.

Longitudinal Findings

While the early cross-sectional results have a clinical application perspective, the longitudinal data are interesting from a neurobiological point of view as it may reveal some mechanisms of change during recovery from TBI. Such insight may, in turn, have future clinical interventional implications.

During the scan interval, between ~8 weeks and ~12 months post-injury, patients exhibited on average 4% brain volume reduction. In principle one cannot completely exclude the possibility that resolution of residual oedema partly accounted for this change. However oedema resolution is considered unlikely to be of any major significance, since considerable reduced brain volumes (compared to controls) were found already at the first scan time point, and moreover, radiological evidence of oedema at the first scan time point was absent. Therefore, this finding strongly suggests that atrophy continues beyond the first few months post-trauma in severely injured patients. This is in agreement with the finding by Trivedi et al, although in their study the possible influence of oedema resolution was not studied, as initial volume estimates were not available (Trivedi et al, 2007).

The application of TBM enabled the investigation of the regional distribution of this late atrophy, and we found widespread volume loss predominantly in the deep white matter and in the thalamus (patients compared to controls at FDR 0.05). The pyramidal tract was continuously involved from the corona radiata to pons. This pattern of late volume change is in general agreement with two recent studies (Kim et al, 2008; Bendlin et al, 2008). However, the study by Kim and colleagues was a cross-sectional study of patients in the chronic phase of TBI, and therefore early and late atrophy were conflated. The study by Bendlin et al was longitudinal with similar scan time points as in our study; however the method applied was VBM, not TBM.

The observed pattern of late volume loss resembles the characteristic distribution of TAI and the consequent Wallerian degeneration of the affected white matter tracts. This may suggest that TAI is the dominating pathological feature responsible for this progressive atrophy. However, with only two scan time points our study does not reveal the time course of this late atrophy, which may be, e.g., a continuous process throughout the scan interval or may end after a short time. Further, the observed late atrophy could result from, e.g., continued Wallerian degeneration or merely the removal of cell debris without further degeneration. Animal studies,

however, do suggest that Wallerian-like processes of degeneration continue for at least 1 year after experimental TBI (Smith et al, 1997; Rodriguez-Paez et al, 2005).

Regarding the clinical significance of the observed longitudinal volume changes, the degree of late atrophy (%BVC) was found to correlate with duration of coma and of PTA, with FIM at the two scan time points and finally with GOS-E at 1-year post-injury. Furthermore, in a linear regression model to predict FIM at 1-year post-trauma, %BVC improved the model. Given the above interpretation of the regional findings, it is likely that %BVC mainly reflects the severity of TAI, which in turn is a major determinant of clinical outcome. In spite of continued volume decline, the vast majority of patients exhibited remarkable functional improvement during the scan interval (reflected e.g. in change of FIM values). This apparent paradox indicates some concurrently acting regenerative processes which are not detectable at the macrostructural level.

The longitudinal DTI data revealed significant changes of DTI values during the scan interval. In all the investigated white matter ROIs, $\lambda_{||}$ increased over time. In PCC and CP, this was accompanied by relatively larger increases of λ_{\perp} and consequently FA decreased to even lower levels than at the first scan, while MD increased. In PLIC and CSO, however, λ_{\perp} remained unchanged during the scan interval, with resulting FA increase towards normal values and moderate MD increase. As several possible limitations could potentially influence these results (see below and the discussion section of Paper I) interpretation should be cautious. However, if assuming that these findings do represent true changes, the results are intriguing. The increase of all eigenvalues in PCC and CP most likely would represent accumulation of extracellular fluid, but the selective $\lambda_{||}$ increase and consequent increase of FA in PLIC and CSO might reflect microstructural reorganization. In the recent study by Bendlin et al (Bendlin et al, 2008), a voxel-wise analysis of longitudinal DTI data also showed FA decrease over time in the corpus callosum and in the cerebral peduncle, as well as in additional regions (inferior longitudinal fasciculus, middle cerebellar peduncle, temporal white matter, and inferior frontal white matter), but no regions of FA increase over time. A more diffuse and widespread pattern of MD increase was found over time in the Bendlin-study, however some areas of MD decrease were also reported (internal capsule, superior and inferior longitudinal fasciculus, portions of corona radiata, anterior thalamic radiations, putamen, portions of hippocampus and small cortical areas). In their discussion, Bendlin et al suggest that the regional decreases of MD may represent regenerative changes, which taken together with our findings of regional FA increases, point toward the possibility of functional reorganization following TBI.

To summarize, atrophy continues beyond ~8 weeks post-injury in severe TBI, with a regional distribution suggesting that TAI and consequent Wallerian degeneration represent the main underlying pathology. Paradoxically, concurrent clinical recovery may occur. DTI may be able to track microstructural changes over time, including possible regenerative changes. Although important limitations and pitfalls of DTI warrant very cautious interpretation of longitudinal changes, findings of the present and other recent studies may suggest regional microstructural reorganization.

Supplemental Findings

The supplemental TBM analysis (patients only) did not reveal profound differences between patients with unfavourable versus favourable outcome. Apart from clusters of volume expansion in CSF and small asymmetrical clusters of volume loss predominantly in lobar white matter and brainstem, one bilateral cluster of volume loss was found in the pons/middle cerebellar peduncles, indicating more extensive atrophy in this area for patients with unfavourable outcome as compared to patients with favourable outcome. However, the results were not highly significant, possibly owing to the small sample size (few degrees of freedom in the statistical analysis). Therefore, further conclusions cannot be drawn from this analysis, and larger studies will be needed to clarify if the pattern of atrophy differs according to outcome.

In this patient sample, simple correlation analysis did not reveal any relationships between the longitudinal DTI changes and volume changes. This issue is discussed further in the following section of MRI methodological limitations.

Regarding APOE E4, the sample size of the present study was clearly too small for the detection of any possible influence of APOE E4 on clinical outcome. Nevertheless, knowledge of APOE status of the patients enabled us to exclude the possibility of this genetic factor being a major confounding variable responsible for the observed relationships between imaging parameters and outcome.

6.2 MRI Methodological Limitations

Some limitations of the applied MRI methods have been discussed in Papers I and II and will only briefly be mentioned here.

Certain artifacts and pitfalls are related to DTI acquisition and interpretation (for an overview see Le Bihan, 2006 or Mori & Zhang, 2006). One issue of particular importance in relation to our study is that of partial voluming. The DTI voxel dimensions were relatively large, particularly in the z-direction, and although attempts were made to minimize partial voluming by erosion of PCC, any influence of partial voluming certainly cannot be excluded. Further, the tensor model is unable to model different fibre populations within one voxel, and in particular the crossing of fibres within a voxel can easily lead to errors in the calculated DTI metrics (Figure 6.1). It should always be kept in mind that while voxel dimensions are in the order of a few millimeters,

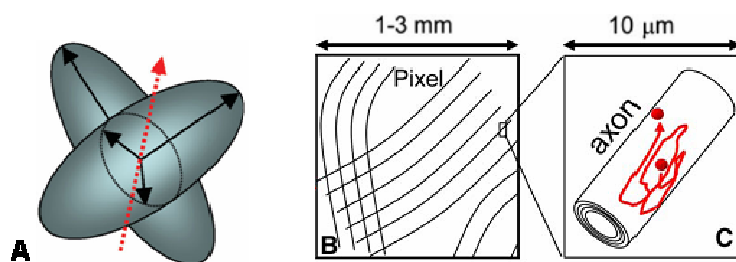


Figure 6.1. Illustration of some of the limitations of DTI. **A.** Two fibre bundles are crossing inside a voxel at 90° leading to the direction of highest diffusivity (red arrow) that does not fit with any of the actual bundle directions (From Le Bihan et al, 2006). **B** and **C.** Typical relative size of pixels in clinical DTI and individual axons (From Mori & Zhang, 2006).

the diffusion process is in the order of micrometer (1–10 μm during typically 20–100 ms of diffusion time). Thus, microscopic information is averaged over the large voxel volume, and we observe diffusion anisotropy only when there are microscopic sources of diffusion anisotropy *and* there is macroscopic homogeneity of the structures within a voxel (Mori & Zhang, 2006).

In the present DTI study, intra-rater and between-scan reproducibility of manual ROI delineation were found satisfactory for all white matter ROIs (coefficients of variation $\leq 4\%$, for ROI medians of FA and MD). However, in a recent study using kappa-statistics to assess intra- and inter-observer agreement in ROI-based DTI analysis, the CSO and internal capsule exhibited poor reproducibility, while other white matter regions including the corpus callosum exhibited much better reproducibility (Ozturk et al, 2008). As pointed out by the authors, a possible explanation of the higher variability in the internal capsule and CSO may be related to section shifts of the ROI location. In consideration with the above, even small section shifts may cause e.g. differences in partial voluming (particularly for internal capsule) or addition/subtraction of voxels in which fibre crossing results in erroneously low FA values (particularly for CSO). In principle, small section shifts could similarly influence longitudinal findings in these regions, further emphasizing the need for very cautious interpretation of the longitudinal DTI changes that we observed therein. It should be noted, however, that the reproducibility measures reported by Ozturk et al were based on mean DTI parameter values of voxels within ROIs. The use of median values instead of mean values may be less influenced by small sections shift.

Other types of limitations apply to the voxel-wise morphometric analyses performed in this study. One limitation of TBM, which applies to VBM as well, is that the sensitivity to areas with high anatomical variability between subjects, such as cortical gyri and sulci, is less than to areas exhibiting little inter-subject variability (Tisserand et al, 2002; Kim et al, 2008). Combined with the frequent presence of focal lesions in frontal and temporal cortices, possibly complicating registration, the relative sparing of cortex observed in our group analysis in terms of volume loss over time could be a false-negative result. However, the individual TBM results only revealed cortical atrophy in a minority of the patients, thus suggesting white matter atrophy generally being more pronounced than cortical grey matter atrophy.

In our patient population most subjects had visible focal lesions on conventional MRI. Possible confounding of focal lesions on the pattern of longitudinal volume loss found with TBM cannot be ruled out. In the cross-sectional TBM study by Kim et al, a subgroup analysis was performed for the patients without focal lesions, showing a pattern of volume loss comparable to that of the whole patient group (Kim et al, 2008). However, similar subgroup analysis was not made in the present study because of the small number of patients without focal lesions.

Certain limitations relate to the use of SIENAX for estimation of volume loss in the patients prior to the first scan. Although the patients and controls were fairly well matched with respect to demographic parameters, the assumption that brain volume of the patients prior to injury was comparable to that of the controls is a rough approximation. Further, the segmentation algorithm of SIENAX tended to misclassify focal lesions as grey matter, which prevented us from studying grey and white matter separately. Since lesions were never misclassified as CSF, the sum of grey and white matter volume estimates was considered as a relatively valid estimate of

parenchymal volume. However, in consideration of these limitations, the SIENAX results should be regarded only as rough estimations of initial volume loss.

One overall limitation of the present project is that fundamentally different approaches were applied for the DTI and the morphometry analyses (ROI approach versus voxel-wise approach, respectively). This prevented a detailed analysis of the relation between DTI and volume changes. In the recent study by Bendlin et al, both 3D T1-weighted images and DTI were analysed using voxel-based approaches (Bendlin et al, 2008). While at ~2 months post-injury they found that DTI revealed more regions of abnormalities than did VBM, widespread volume loss as well as MD increase dominated in the longitudinal analysis, with a seemingly overlapping although not identical pattern. Unfortunately, Bendlin et al did not report whether DTI changes and volume changes were interrelated at the voxel level.

While voxel-wise as opposed to ROI-based approaches have the clear advantages of enabling unbiased analyses of the entire brain, one major advantage of ROI-based analysis is that it can be hypothesis-driven and therefore statistically more sensitive (fewer corrections for multiple comparisons are required). For analysis of DTI data, ROI-based analysis also avoids the problems related to between-subject coregistration of FA images, and partial voluming introduced by smoothing. The particular challenges of between-subject registration of FA maps are addressed in recent advanced registration approaches for DTI data (e.g. tract-based spatial statistics; Smith et al, 2006). Very recently, a multivariate registration algorithm was proposed, in which registration is based on both high-resolution T1-weighted images and DTI (Avants et al, 2008). The authors studied limbic regions using this method and found reduced volume and increased MD at coincident locations in the mediodorsal thalamus and anterior hippocampus in TBI survivors as compared to controls. Similar analysis of other brain regions could presumably uncover the interrelationship between DTI and volume changes following TBI.

Finally, one limitation of the present project is the potential bias introduced by the need for sedation/anaesthesia during MRI in some patients, primarily at the first scan. Although no tendency was found towards any systematic differences between sedated versus non-sedated individuals regarding the MRI images or the derived quantitative parameters, the possibility of any such effects cannot be entirely excluded (see discussion in Paper I).

6.3 Limitations of Clinical Ratings

The clinical rating instruments used for the comparison with MRI parameters in the present study were not a result of deliberate considerations for this particular study, but were a subset of the ratings routinely performed for all patients in the Brain Injury Unit, Hvidovre Hospital. Currently there is not international consensus on which functional assessment scales are best suited to monitor clinical progress during rehabilitation following TBI, and the optimal scales for research and for clinical use are not necessarily the same. For thumbnail descriptions of some of the most widely used rating scales in TBI rehabilitation, the following web site is recommended: <http://www.tbims.org/combi/>

One general problem of functional assessment in TBI is the extremely broad range of function in TBI patients. No single scale (which can be performed within a reasonable amount of time) is

able to capture this large variability of type and severity of impairment, and yet still be sensitive to subtle individual changes over time. The FIM total score (sum of scores on 18 items) was reported in this study as a measure of clinical function at the two scan time points. Besides satisfactory reliability and validity, the FIM has the advantage of being relatively sensitive to individual change. However, the FIM was not developed specifically for TBI and has few cognitive, behavioural, and communication related functional items relevant to assessing TBI patients (Dijkers & Greenwald, 2006). Moreover, FIM suffers from ceiling effects which was a particular problem in the present study. At the time of the initial scan total FIM exhibited high variability between patients, whereas there was little variability in FIM scores at follow-up, as the majority of patients grouped close to the maximum. The same applied to the motor subscore (13 of 18 items) and the cognitive subscore (5 of 18 items) when considered separately (data not shown). One unfortunate consequence of this was that it did not allow a meaningful investigation of the relationship between change in MRI-measured quantities and change in clinical function during the scan interval. No other relevant clinical measure recorded at both scan time points, which could enable such interesting comparisons, was available.

In this study, clinical outcome was evaluated by GOS-E, which was applied at the time of the follow-up scan ~1 year post-injury. The 8-point GOS-E (which includes guidelines for a structured interview) has been found to be more reliable and sensitive than the original 5-point GOS (Dijkers & Greenwald, 2006). In Paper I only GOS was reported, however similar results were found using GOS-E (data not shown). The Disability Rating Scale (DRS; Rappaport et al, 1982) is more widely used than GOS and GOS-E, particularly in the U.S. Although with a total score ranging from 0-29 the DRS may have offered additional sensitivity as compared to GOS-E, the relatively small sample size of the present study limited most statistical analyses to consider only dichotomized outcome.

CHAPTER 7

CONCLUSIONS

In this final chapter, the main conclusions of the present project are summarized, and some clinical and neuroscientific perspectives of this and related work are outlined. Finally, directions for future studies are proposed.

7.1 Conclusions

In this prospective longitudinal MRI study of patients with severe TBI, DTI at ~8 weeks post-trauma revealed decreased FA in all four white matter regions investigated, caused by decreased $\lambda_{||}$ and increased λ_{\perp} . FA in the CP was predictive of 1-year clinical outcome. Together with recent related studies, this suggests that DTI provides a sensitive (albeit not specific) and clinically relevant marker of white matter microstructural integrity following severe TBI, which unlike conventional imaging captures biological severity of injury. DTI has high potential as a quantitative diagnostic marker of TAI, and may have prognostic value in TBI.

At the initial scan as well as at the follow-up scan ~12 months post-injury, FA values tended to be more abnormal in patients with unfavourable outcome as compared to patients with favourable outcome. When longitudinal comparison was made between DTI acquired at ~8 weeks and ~12 months post-injury, patients generally exhibited further FA decrease in some regions (PCC and CP), but partial normalization of FA values in other regions (PLIC and CSO). While interpretation of the longitudinal findings should be cautious due to methodological limitations, DTI might provide a candidate tool for the *in vivo* tracking of microstructural reorganization during recovery from TBI.

Longitudinal morphometric analyses of the present study demonstrated that late macrostructural volume loss was most pronounced in regions susceptible to TAI and resulting Wallerian degeneration. This is in accordance with other very recent studies and suggests that TAI is a major factor responsible for progressive volume loss following severe TBI. The extent of

late global volume loss correlated with a number of clinical parameters including duration of coma and PTA, and 1-year outcome. This further supports that clinical severity and outcome, as well as the degree of atrophy following severe TBI, are highly influenced by the severity of TAI.

Together, these quantitative MRI analyses of micro- and macrostructural changes complemented each other in this study of severe TBI. Applied in the late subacute/early chronic phase of TBI, DTI may capture biological severity at the microstructural level and provide prognostic information. Serial application of these MRI techniques enables the monitoring of the extent and distribution of micro- and macrostructural changes during TBI rehabilitation. This project contributed to the evolving research area of advanced imaging of TBI, providing new insight into the possibilities of measuring and monitoring structural brain changes following TBI.

7.2 Perspectives

The potential of DTI to measure and monitor microstructural changes *in vivo* following TBI has a number of clinical implications. As DTI seems to provide high sensitivity for the detection of TAI, DTI has important perspectives for the diagnosis of TAI. Particularly in mild TBI without abnormalities on conventional imaging, DTI might be useful to detect subtle TAI, which could have a wide range of consequences. As biological severity of injury may be reflected in DTI quantities, DTI might provide prognostic information in TBI, as suggested by the results of the present study. Naturally, if this is confirmed and a valid and reliable prognostic DTI index is developed, this would be of large clinical significance. Additionally, the present and other studies indicated that with serial application, DTI may offer a tool for tracking degenerative and regenerative changes during recovery from TBI. Although particular pitfalls apply to the measurement of DTI changes over time, if these are overcome DTI may provide important insight into the microstructural reorganization following TBI, and eventually DTI may offer a supplement for monitoring response to new therapies. DTI may be useful for the evaluation of a number of diseases affecting white matter, and this technique is expected to be widely implemented for routine clinical practice in the near future.

The macrostructural longitudinal findings of the present study have implications for the neuroscientific understanding of the biological processes underlying late volume change following TBI. Uncovering the mechanisms underlying progressive volume loss may identify possible targets of therapeutic intervention with these processes.

Taken together, DTI and morphometry techniques such as TBM and SIENA represent complementary tools for the advanced MRI evaluation of micro- and macrostructural changes following TBI. With further advancements of these techniques in the future, even more sophisticated and less error-prone measurements will probably be available for clinical use.

7.3 Future Directions

For future studies, larger patient populations are required, in particular in order to determine the diagnostic and prognostic potential of DTI in TBI. Prospective longitudinal studies with serial imaging at multiple time points, concomitant appropriate clinical evaluation, and a follow-up

period of more than one year would be extremely interesting for following micro- and macrostructural brain changes over time and relating these to clinical change.

Ideally, DTI should be acquired with higher resolution (preferably cubic voxels) and more diffusion-encoding directions than in the present study, however under the consideration of acquisition time. For voxel-wise analyses, registration algorithms optimised for DTI should be applied, ideally using a multi-variate statistical framework which could disambiguate the interrelationship between e.g. volume and diffusion changes. Finally, multi-modal imaging with the additional voxel-wise analysis of e.g. whole-brain MR spectroscopy and perfusion measurements would be of particular interest and presumably unravel more aspects of TBI pathophysiology. With the rapid advancements in the field of neuroimaging, detailed characterisation of injury following TBI, and insight into the cellular and subcellular dynamics during recovery, may ultimately lead to therapeutic improvements.

REFERENCES

Arfanakis K, Haughton VM, Carew JD, et al. Diffusion tensor MR imaging in diffuse axonal injury. *Am J Neuroradiol* 2002; 23: 794-802.

Ashburner J, Andersson JL, Friston KJ. Image registration using a symmetric prior – in three dimensions. *Hum Brain Mapp* 2000; 9: 212-25.

Ashburner J, Csernansky JG, Davatzikos C, et al. Computer-assisted imaging to assess brain structure in healthy and diseased brains. *Lancet Neurol* 2003; 2: 79-88.

Ashburner J, Friston KJ. Voxel-based morphometry - the methods. *Neuroimage* 2000; 11: 805-21.

Ashburner J, Friston K. Computational anatomy. In: Friston K (Ed.). *Statistical parametric mapping: The analysis of functional brain images*. 1st edn., London: Academic Press; 2007. p. 49-98.

Ashikaga R, Araki Y, Ishida O. MRI of head injury using FLAIR. *Neuroradiology* 1997; 39: 239-42.

Assaf Y, Beit-Yannai E, Shohami E, et al. Diffusion- and T2-weighted MRI of closed-head injury in rats: a time course study and correlation with histology. *Magn Res Imaging* 1997; 15: 77-85.

Assaf Y, Pasternak O. Diffusion tensor imaging (DTI)-based white matter mapping in brain research: a review. *J Mol Neurosci* 2008; 34: 51-61.

Avants B, Duda JT, Kim J, et al. Multivariate analysis of structural and diffusion imaging in traumatic brain injury. *Acad Radiol* 2008; 15: 1360-75.

Barzó P, Marmarou A, Fatouros P, et al. Contribution of vasogenic and cellular edema to traumatic brain swelling measured by diffusion-weighted imaging. *J Neurosurg* 1997; 87: 900-07.

Beaulieu C. The basis of anisotropic water diffusion in the nervous system - a technical review. *NMR Biomed* 2002; 15: 435-55.

Bendlin BB, Ries ML, Lazar M, et al. Longitudinal changes in patients with traumatic brain injury assessed with diffusion-tensor and volumetric imaging. *Neuroimage* 2008; 42: 503-14.

Benson RR, Meda SA, Vasudevan S, et al. Global white matter analysis of diffusion tensor images is predictive of injury severity in traumatic brain injury. *J Neurotrauma* 2007; 24: 446-59.

Bernstein MA, King KF, Zhou XJ. *Handbook of MRI pulse sequences*. Elsevier Academic Press, 2004.

Bigler ED. Structural imaging. In: Silver JM, McAllister TW, Yudofsky SC (Eds.). *Textbook of traumatic brain injury*. American Psychiatric Publishing, Inc., Washington, DC, 2005. p. 79-105.

Budde MD, Kim JH, Liang HF, et al. Toward accurate diagnosis of white matter pathology using diffusion tensor imaging. *Magn Reson Med* 2007; 57: 688-95.

Bushong SC. *Magnetic resonance imaging: Physical and biological principles*. 3rd edn., Mosby, USA, 2003.

Chan JH, Tsui EY, Peh WC, et al. Diffuse axonal injury: detection of changes in anisotropy of water diffusion by diffusion-weighted imaging. *Neuroradiology* 2003; 45: 34-8.

Chesnut RM, Marshall LF, Klauber MR, et al. The role of secondary brain injury in determining outcome from severe head injury. *J Trauma* 1993; 34: 216-22.

Chesnut RM. Secondary brain insults after head injury: clinical perspectives. *New Horiz* 1995; 3: 366-75.

Dijkers M, Greenwald B. Functional assessment in TBI rehabilitation. In: Zasler ND, Katz DI, Zafonte RD (Eds.). *Brain injury medicine: Principles and practice*. Demos Medical Publishing, LLC, 2006. p. 225-45.

Engberg A. Severe traumatic brain injury - epidemiology, external causes, prevention, and rehabilitation of mental and physical sequelae. *Acta Neurol Scand Suppl* 1995; 164: 1-151.

Engberg AW, Liebach A, Nordenbo A. Centralized rehabilitation after severe traumatic brain injury- a population-based study. *Acta Neurol Scand* 2006; 113: 178-84.

Ezaki Y, Tsutsumi K, Morikawa M, et al. Role of diffusion-weighted magnetic resonance imaging in diffuse axonal injury. *Acta Radiol* 2006; 47: 733-40.

Firsching R, Woischneck D, Klein S, et al. Classification of severe head injury based on magnetic resonance imaging. *Acta Neurochir (Wien)* 2001; 143: 263-71.

Gale SD, Baxter L, Roundy N, et al. Traumatic brain injury and grey matter concentration: a preliminary voxel based morphometry study. *J Neurol Neurosurg Psychiatry* 2005; 76: 984-8.

- Geddes JF, Whitwell HL, Graham DI. Traumatic *or* diffuse axonal injury? Author's response. *Neuropathol Appl Neurobiol* 2000; 26, 491.
- Gerdes LU, Klausen IC, Sihm I, et al. Apolipoprotein E polymorphism in a Danish population compared to findings in 45 other study populations around the world. *Genet Epidemiol* 1992; 9: 155-67.
- Gentry LR. Head trauma. In: Atlas SW, (Ed.). *Magnetic resonance imaging of the brain and spine*. 3rd edn., Philadelphia: Lippincott Williams & Wilkins; 2002. p. 1059-98.
- Graham DI, Gennarelli TA. Trauma. In: Graham DI, Lantos PL, (Eds.). *Greenfield's neuropathology*. 6th edn., London: Arnold; 1997. p. 197-262.
- Greenwood R. Value of recording duration of post-traumatic amnesia. *Lancet* 1997; 349: 1041-2.
- Hagen C. Language disorders in head trauma. In: Holland A, (Ed.). *Language disorders in adults*. San Diego, California: College Hill Press; 1984. p. 245-81.
- Hergan K, Schaefer PW, Sorensen AG, et al. Diffusion-weighted MRI in diffuse axonal injury of the brain. *Eur Radiol* 2002; 12: 2536-41.
- Horsburgh K, McCarron MO, White F, et al. The role of apolipoprotein E in Alzheimer's disease, acute brain injury and cerebrovascular disease: evidence of common mechanisms and utility of animal models. *Neurobiol Aging* 2000; 21: 245-55.
- Hou DJ, Tong KA, Ashwal S, et al. Diffusion-weighted magnetic resonance imaging improves outcome prediction in adult traumatic brain injury. *J Neurotrauma* 2007; 24: 1558-69.
- Huisman TAGM, Schwamm LH, Schaefer PW, et al. Diffusion tensor imaging as potential biomarker of white matter injury in diffuse axonal injury. *Am J Neuroradiol* 2004; 25: 370-76.
- Huisman TAGM, Sorensen AG, Hergan K, et al. Diffusion-weighted imaging for the evaluation of diffuse axonal injury in closed head injury. *J Comp Ass Tomogr* 2003; 27: 5-11.
- Jennett B, Snoek J, Bond MR, et al. Disability after severe head injury: observations on the use of the Glasgow Outcome Scale. *J Neurol Neurosurg Psychiatr* 1981; 44; 285-93.
- Jones NR, Blumbergs PC, Brown CJ, et al. Correlation of postmortem MRI and CT appearances with neuropathology in brain trauma: a comparison of two methods. *J Clin Neurosci* 1998; 5: 73-9.
- Kelly AB, Zimmerman RD, Snow RB, et al. Head trauma: comparison of MR and CT-experience in 100 patients. *Am J Neuroradiol* 1988; 9: 699-708.
- Kim J, Avants B, Patel S, et al. Structural consequences of diffuse traumatic brain injury: a large deformation tensor-based morphometry study. *Neuroimage* 2008; 39: 1014-26.

Kothari S. Prognosis after severe TBI: a practical evidence-based approach. In: Zasler ND, Katz DI, Zafonte RD, (Eds.). Brain injury medicine: Principles and practice. Demos Medical Publishing, LLC, 2006. p.169-200.

Le Bihan D (Ed.). Diffusion and perfusion magnetic resonance imaging: Applications to functional MRI. New York: Raven Press, Ltd.; 1995.

Le Bihan D, Poupon C, Amadon A, et al. Artifacts and pitfalls in diffusion MRI. J Magn Reson Imaging 2006; 24: 478-88.

Le TH, Mukherjee P, Henry RG, et al. Diffusion tensor imaging with three-dimensional fiber tractography of traumatic axonal shearing injury: an imaging correlate for the posterior callosal "disconnection" syndrome: case report. Neurosurgery 2005; 56: 189.

Levi L, Guilburd JN, Lemberger A, et al. Diffuse axonal injury: analysis of 100 patients with radiological signs. Neurosurgery 1990; 27: 429-32.

Levin HS, O'Donnell VM, Grossman RG. The Galveston Orientation and Amnesia Test. A practical scale to assess cognition after head injury. J Nerv Ment Dis 1979; 167: 675-84.

Mac Donald CL, Dikranian K, Song SK, et al. Detection of traumatic axonal injury with diffusion tensor imaging in a mouse model of traumatic brain injury. Exp Neurol 2007; 205: 116-31.

MacKenzie EJ. Epidemiology of injuries: current trends and future challenges. Epidemiol Rev 2000; 22: 112-9.

Mannion RJ, Cross J, Bradley P, et al. Mechanism-based MRI classification of traumatic brainstem injury and its relationship to outcome. J Neurotrauma. 2007; 24: 128-35.

Marquez de la Plata CD, Hart T, Hammond FM, et al. Impact of age on long-term recovery from traumatic brain injury. Arch Phys Med Rehabil 2008; 89: 896-903.

Meythaler JM, Peduzzi JD, Eleftheriou E, et al. Current concepts: diffuse axonal injury-associated traumatic brain injury. Arch Phys Med Rehabil 2001; 82: 1461-71.

Miles L, Grossman RI, Johnson G, et al. Short-term DTI predictors of cognitive dysfunction in mild traumatic brain injury. Brain Inj 2008; 22: 115-22.

Mori S, Zhang J. Principles of diffusion tensor imaging and its applications to basic neuroscience research. Neuron 2006; 51: 527-39.

Naganawa S, Sato C, Ishihara S, et al. Serial evaluation of diffusion tensor brain fiber tracking in a patient with severe diffuse axonal injury. Am J Neuroradiol 2004; 25: 1553-6.

Nakayama N, Okumura A, Shinoda J, et al. Evidence for white matter disruption in traumatic brain injury without macroscopic lesions. J Neurol Neurosurg Psychiatry 2006; 77: 850-5.

- Niogi SN, Mukherjee P, Ghajar J, et al. Extent of microstructural white matter injury in postconcussive syndrome correlates with impaired cognitive reaction time: a 3T diffusion tensor imaging study of mild traumatic brain injury. *AJNR Am J Neuroradiol* 2008; 29: 967-73.
- Nudo RJ. Mechanisms for recovery of motor function following cortical damage. *Curr Opin Neurobiol* 2006; 16: 638-44.
- Nudo RJ, Dancause N. Neuroscientific basis for occupational and physical therapy interventions. In: Zasler ND, Katz DI, Zafonte RD, (Eds.). *Brain injury medicine: Principles and practice*. Demos Medical Publishing, LLC, 2006. p.913-28.
- Ozturk A, Sasson AD, Farrell JA, et al. Regional differences in diffusion tensor imaging measurements: assessment of intrarater and interrater variability. *AJNR Am J Neuroradiol* 2008; 29: 1124-7.
- Parizel PM, Özsarlak Ö, Van Goethem JW, et al. Imaging findings in diffuse axonal injury after closed head trauma. *Eur Radiol* 1998; 8: 960-5.
- Pierpaoli C, Barnett A, Pajevic S, et al. Water diffusion changes in Wallerian degeneration and their dependence on white matter architecture. *Neuroimage* 2001; 13: 1174-85.
- Pierpaoli C, Basser PJ. Toward a quantitative assessment of diffusion anisotropy. *Magn Reson Med* 1996; 36: 893-906.
- Povlishock JT, Katz DI. Update of neuropathology and neurological recovery after traumatic brain injury. *J Head Trauma Rehabil* 2005; 20: 76-94.
- Press WH, Teukolsky SA, Vetterling WT, Flannery BP. *Numerical recipes in C: The art of scientific computing*. 2nd edn., Cambridge, Cambridge University Press, 1992.
- Ptak T, Sheridan RL, Rhea JT, et al. Cerebral fractional anisotropy score in trauma patients: a new indicator of white matter injury after trauma. *Am J Radiol* 2003; 181: 1401-7.
- Rappaport M, Hall KM, Hopkins K, et al. Disability rating scale for severe head trauma: coma to community. *Arch Phys Med Rehabil* 1982; 63: 118-23.
- Ratcliff JJ, Greenspan AI, Goldstein FC, et al. Gender and traumatic brain injury: do the sexes fare differently? *Brain Inj* 2007; 21: 1023-30.
- Rodriguez-Paez AC, Brunschwig JP, Bramlett HM. Light and electron microscopic assessment of progressive atrophy following moderate traumatic brain injury in the rat. *Acta Neuropathol* 2005; 109: 603-16.
- Rugg-Gunn FJ, Symms MR, Barker GJ, et al. Diffusion imaging shows abnormalities after blunt head trauma when conventional magnetic resonance imaging is normal. *J Neurol Neurosurg Psychiatry* 2001; 70: 530-3.
- Rutgers DR, Toulgoat F, Cazejust J, et al. White matter abnormalities in mild traumatic brain injury: a diffusion tensor imaging study. *AJNR Am J Neuroradiol* 2008; 29: 514-9.

Salmond CH, Chatfield DA, Menon DK, et al. Cognitive sequelae of head injury: involvement of basal forebrain and associated structures. *Brain* 2005; 128, 189-200.

Salmond CH, Menon DK, Chatfield DA, et al. Diffusion tensor imaging in chronic head injury survivors: correlations with learning and memory indices. *Neuroimage* 2006; 29: 117-24.

Sbordone RJ, Liter JC, Pettler-Jennings P. Recovery of function following severe traumatic brain injury: a retrospective 10-year follow-up. *Brain Inj* 1995; 9: 285-99.

Scheid R, Preul C, Gruber O, et al. Diffuse axonal injury associated with chronic traumatic brain injury: evidence from T2*-weighted gradient-echo imaging at 3 T. *Am J Neuroradiol* 2003; 24: 1049-56.

Scheid R, Walther K, Guthke T, et al. Cognitive sequelae of diffuse axonal injury. *Arch Neurol* 2006; 63: 418-24.

Shanmuganathan K, Gullapalli RP, Mirvis SE, et al. Whole-brain apparent diffusion coefficient in traumatic brain injury: correlation with Glasgow Coma Scale score. *AJNR Am J Neuroradiol* 2004; 25: 539-44.

Smith DH, Chen XH, Pierce JE, et al. Progressive atrophy and neuron death for one year following brain trauma in the rat. *J Neurotrauma* 1997; 14: 715-27.

Smith SM, Jenkinson M, Johansen-Berg H, et al. Tract-based spatial statistics: voxelwise analysis of multi-subject diffusion data. *Neuroimage* 2006; 31: 1487-505.

Smith SM, Zhang Y, Jenkinson M, et al. Accurate, robust and automated longitudinal and cross-sectional brain change analysis. *Neuroimage* 2002, 17: 479-89.

Stein DG. Concepts of CNS plasticity and their implications for understanding recovery after brain damage. In: Zasler ND, Katz DI, Zafonte RD, (Eds.). *Brain injury medicine: Principles and practice*. Demos Medical Publishing, LLC, 2006. p.169-200.

Stein DG. Sex differences in brain damage and recovery of function: experimental and clinical findings. *Prog Brain Res* 2007; 161: 339-51.

Strich SJ. Diffuse degeneration of the cerebral white matter in severe dementia following head injury. *J Neurol Neurosurg Psychiatry* 1956; 19: 163-85.

Song SK, Sun SW, Ju WK, et al. Diffusion tensor imaging detects and differentiates axon and myelin degeneration in mouse optic nerve after retinal ischemia. *Neuroimage* 2003; 20: 1714-22.

Song SK, Sun SW, Ramsbottom MJ, et al. Demyelination revealed through MRI as increased radial (but unchanged axial) diffusion of water. *Neuroimage* 2002; 17: 1429-36.

Sun SW, Liang HF, Trinkaus K, et al. Noninvasive detection of cuprizone induced axonal damage and demyelination in the mouse corpus callosum. *Magn Reson Med* 2006; 55: 302-8.

Teasdale G, Jennett B. Assessment of coma and impaired consciousness. A practical scale. *Lancet* 1974; 2: 81-4.

The Brain Trauma Foundation. The American Association of Neurological Surgeons. The Joint Section of Neurotrauma and Critical Care. Part 2: Early indicators of prognosis in severe traumatic brain injury. *J Neurotrauma* 2000; 17: 557-627.

The Multi-Society Task Force on PVS. Medical aspects of the persistent vegetative state, Part 1 and Part 2. *N Engl J med* 1994; 330: 1499-508 (part 1) + 1572-79 (part 2).

Thurman DJ, Coronado V, Selassie A. The epidemiology of TBI: Implications for public health. In: Zasler ND, Katz DI, Zafonte RD, (Eds.). *Brain injury medicine: Principles and practice*. Demos Medical Publishing, LLC, 2006. p.45-55.

Thurman DJ, Sniezek JE, Johnson D, et al. Guidelines for surveillance of central nervous system injury. Atlanta, Georgia: National Center for Injury Prevention and Control, Centers for Disease Control and Prevention, U.S. Department of Health and Human Services, 1995.

Tisserand DJ, Pruessner JC, Sanz Arigita EJ, et al. Regional frontal cortical volumes decrease differentially in aging: an MRI study to compare volumetric approaches and voxel-based morphometry. *Neuroimage* 2002; 17: 657-69.

Tomaiuolo F, Worsley KJ, Lerch J, et al. Changes in white matter in long-term survivors of severe non-missile traumatic brain injury: a computational analysis of magnetic resonance images. *Neurotrauma*. 2005; 22: 76-82.

Tong KA, Ashwal S, Holshouser BA, et al. Diffuse axonal injury in children: clinical correlation with hemorrhagic lesions. *Ann Neurol*. 2004; 56: 36-50.

Trivedi MA, Ward MA, Hess TM, et al. Longitudinal changes in global brain volume between 79 and 409 days after traumatic brain injury: relationship with duration of coma. *J Neurotrauma* 2007; 24: 766-71.

Turner-Stokes L. Evidence for the effectiveness of multi-disciplinary rehabilitation following acquired brain injury: a synthesis of two systematic approaches. *J Rehabil Med* 2008; 40: 691-701.

Van Den Heuvel C, Thornton E, Vink R. Traumatic brain injury and Alzheimer's disease: a review. *Prog Brain Res* 2007; 161: 303-16.

Van Zomeren AH, Brouwer WH, Deelman BG. Attentional deficits: the riddles of selectivity, speed, and alertness. In: Brooks N (Ed.). *Closed head injury: Psychological, social, and family consequences*. Oxford: Oxford University Press; 1984. p. 74-107.

Voss HU, Uluc AM, Dyke JP, et al. Possible axonal regrowth in late recovery from the minimally conscious state. *J Clin Invest* 2006; 116: 2005-11.

Wagner AK, Fabio T, Zafonte RD, et al. Physical medicine and rehabilitation consultation: relationships with acute functional outcome, length of stay, and discharge planning after traumatic brain injury. *Am J Phys Med Rehabil.* 2003; 82: 526-36.

Ward P, Counsell S, Allsop J, et al. Reduced fractional anisotropy on diffusion tensor magnetic resonance imaging after hypoxic-ischemic encephalopathy. *Pediatrics* 2006; 117: e619-30.

Wedekind C; Fischbach R, Pakos P, et al. Comparative use of magnetic resonance imaging and electrophysiologic investigation for the prognosis of head injury. *J Trauma* 1999; 47: 44-9.

Wenham PR, Price WH, Blandell G. Apolipoprotein E genotyping by one-stage PCR. *Lancet* 1991; 337: 1158-9.

Wiegell MR, Larsson HB, Wedeen VJ. Fiber crossing in human brain depicted with diffusion tensor MR imaging. *Radiology* 2000; 217: 897-903.

Wieshmann UC, Symms MR, Clark CA, et al. Blunt-head trauma associated with widespread water-diffusion changes. *Lancet* 1999; 353: 1242-3.

Wilson JT, Pettigrew LE, Teasdale GM. Structured interviews for the Glasgow Outcome Scale and the Extended Glasgow Outcome Scale: Guidelines for their use. *J Neurotrauma* 1998; 15: 573-85.

Xu J, Rasmussen IA, Lagopoulos J, et al. Diffuse axonal injury in severe traumatic brain injury visualized using high-resolution diffusion tensor imaging. *J Neurotrauma.* 2007; 24: 753-65.

APPENDICES

A1: Paper I

A2: Paper II

A3: Supplemental short review in Danish (summary in English)

A4: Clinical rating scales

Appendix 1

PAPER I

Diffusion tensor imaging during recovery from severe traumatic brain injury and relation to clinical outcome: a longitudinal study

Annette Sidaros,^{1,2} Aase W. Engberg,² Karam Sidaros,¹ Matthew G. Liptrot,¹ Margrethe Herning,¹ Palle Petersen,³ Olaf B. Paulson,^{1,4} Terry L. Jernigan^{1,5} and Egill Rostrup¹

¹Danish Research Centre for Magnetic Resonance, Copenhagen University Hospital, Hvidovre, Denmark, ²Brain Injury Unit, Department of Neurorehabilitation, Copenhagen University Hospital, Hvidovre, Denmark, ³Department of Neurology, Copenhagen University Hospital, Rigshospitalet, Denmark, ⁴Neurobiology Research Unit, Copenhagen University Hospital, Rigshospitalet, Denmark and ⁵Laboratory of Cognitive Imaging, Department of Psychiatry, University of California, San Diego, CA, USA

Correspondence to: Annette Sidaros (previously Annette S. Nielsen), MD, Danish Research Centre for Magnetic Resonance, Copenhagen University Hospital, Hvidovre, Department 340, 2650 Hvidovre, Denmark
E-mail: annettes@drcmr.dk

Diffusion tensor imaging (DTI) has been proposed as a sensitive biomarker of traumatic white matter injury, which could potentially serve as a tool for prognostic assessment and for studying microstructural changes during recovery from traumatic brain injury (TBI). However, there is a lack of longitudinal studies on TBI that follow DTI changes over time and correlate findings with long-term clinical outcome. We performed a prospective longitudinal study of 30 adult patients admitted for subacute rehabilitation following severe traumatic brain injury. DTI and conventional MRI were acquired at mean 8 weeks (5–11 weeks), and repeated in 23 of the patients at mean 12 months (9–15 months) post-trauma. Using a region-of-interest-based approach, DTI parameters were compared to those of healthy matched controls, scanned during the same time period and rescanned with a similar interval as that of patients. At the initial scan, fractional anisotropy was reduced in all the investigated white matter regions in patients compared to controls ($P \leq 0.01$) due to decreased diffusivity parallel (λ_{\parallel}) and increased diffusivity perpendicular (λ_{\perp}) to axonal fibre direction. Fractional anisotropy in the cerebral peduncle correlated with ~ 1 year Glasgow outcome scale score ($r = 0.60$, $P < 0.001$) and in this sample predicted dichotomized outcome with 76% accuracy when taken alone, and with 100% accuracy in combination with clinical evaluation by functional independence measure at the time of the first scan. At follow-up DTI, fractional anisotropy in patients had increased in the internal capsule and in centrum semiovale ($P \leq 0.01$) due to an interval increase of λ_{\parallel} with unchanged λ_{\perp} . In these regions, fractional anisotropy and λ_{\parallel} reached normal or supranormal levels, primarily in patients with favourable outcome. In the cerebral peduncle and in corpus callosum, λ_{\parallel} and λ_{\perp} both increased during the scan interval and, particularly in patients with unfavourable outcome, fractional anisotropy remained depressed. No significant DTI parameter changes over time were found in controls, or in CSF of patients. These findings support that DTI is a clinically relevant biomarker in TBI, which may have prognostic value and also might serve as a tool for revealing changes in the neural tissue during recovery.

Keywords: diffusion tensor imaging (DTI); traumatic brain injury (TBI); magnetic resonance imaging (MRI); outcome prediction; neuroplasticity

Abbreviations: CP = cerebral peduncle; CSO = centrum semiovale; DAI = diffuse axonal injury; DTI = diffusion tensor imaging; FA = fractional anisotropy; FLAIR = fluid-attenuated inversion recovery; FIM = functional independence measure; GCS = Glasgow coma scale; GOS = Glasgow outcome scale; ISS = injury severity score; MD = mean diffusivity; PCC = posterior aspect of corpus callosum; PLIC = posterior limb of internal capsule; PTA = post-traumatic amnesia; PUT = putamen; ROIs = regions of interest; TBI = traumatic brain injury

Received May 20, 2007. Revised November 6, 2007. Accepted November 7, 2007. Advance Access publication December 14, 2007

Introduction

Traumatic brain injury (TBI) is a major cause of death and severe disability under the age of 45 years in Western countries (MacKenzie, 2000). Diffuse-type (non-focal) injuries are generally the most devastating, yet their assessment *in vivo* is hampered by the low sensitivity of conventional imaging. The key mechanism of primary injury is diffuse axonal injury (DAI), which results from rotational acceleration–deceleration causing shear strain deformation and subsequent disconnection of axons. DAI is characterized by microscopic lesions scattered throughout the white matter, with the parasagittal white matter, corpus callosum and the dorsolateral upper brainstem being most commonly involved. Secondary hypoxic-ischaemic injury due to, e.g. insults of hypotension, hypoxia and/or increased intracranial pressure, is known to markedly worsen prognosis following TBI (see e.g. Chesnut *et al.*, 1993). With time both of these diffuse-type injuries lead to Wallerian-like degeneration of white matter (Graham and Gennarelli, 1997).

Recently, much interest has been directed towards the potential of diffusion tensor imaging (DTI) as a tool for *in vivo* quantification of white matter microstructural alterations following TBI (see e.g. Schiff, 2006). DTI is a relatively new MRI modality that non-invasively provides information regarding the degree and directionality of tissue water diffusion (Basser *et al.*, 1994). This technique describes the diffusion process using three eigenvectors, of which the magnitudes, the eigenvalues (λ_1 , λ_2 , λ_3), quantify the diffusion in three orthogonal directions. Due to barriers to water diffusion imposed by e.g. myelin and membranes, hindrance of diffusion is larger across than along axonal fibres, causing diffusion in white matter to be anisotropic. Anisotropy is commonly expressed relative to the magnitude of the diffusion tensor as the fractional anisotropy (FA) (Pierpaoli and Basser, 1996), and this index ranging from 0 to 1 is found to be higher in intact white matter consisting of highly parallel fibres. Mean diffusivity (MD), or ‘apparent diffusion coefficient’, refers to the average of the three eigenvalues. While commonly only these summary parameters, FA and MD, are reported, the underlying eigenvalues hold additional valuable information as they may be selectively affected with certain pathological processes (Song *et al.*, 2002).

In a recent experimental study, correlations between DTI and histology of DAI were demonstrated (Mac Donald *et al.*, 2007). Prior clinical DTI-studies on TBI have found reduced FA in several white matter areas, both within lesions and in tissue appearing normal on conventional MRI (Rugg-Gunn *et al.*, 2001; Arfanakis *et al.*, 2002; Chan *et al.*, 2003; Ptak *et al.*, 2003; Huisman *et al.*, 2004; Inglese *et al.*, 2005; Salmond *et al.*, 2006; Nakayama *et al.*, 2006). At post-acute stages, MD in areas of decreased FA has been found to be normal or increased (Rugg-Gunn *et al.*, 2001; Chan *et al.*, 2003; Inglese *et al.*, 2005; Salmond *et al.*, 2006; Nakayama *et al.*, 2006). The eigenvalues were reported

in one of the aforementioned studies of five patients with mild TBI (Arfanakis *et al.*, 2002) and in one case study (Le *et al.*, 2005), suggesting that decrease of the major eigenvalue, λ_1 , and increase of the minor eigenvalues λ_2 and λ_3 may underlie FA (and MD) alterations. Some association has been reported between DTI values (in splenium and internal capsule) and short-term outcome (Huisman *et al.*, 2004). However, as most prior studies were cross-sectional, few investigated correlations of DTI with long-term (>6 months) clinical outcome. Moreover, little is known about the long-term evolution of diffusion abnormalities during recovery from TBI. Apart from reports on one or two patients (Arfanakis *et al.*, 2002; Naganawa *et al.*, 2004; Le *et al.*, 2005; Voss *et al.*, 2006), longitudinal DTI studies in TBI have not, to our knowledge, been published previously. DTI repeated during rehabilitation and correlated with long-term clinical outcome may add to our understanding of the natural course of diffuse traumatic injuries and of the mechanisms of neuroplasticity and repair operating during recovery from TBI.

We performed a prospective longitudinal study of 30 patients with severe TBI, comparing results to 30 healthy matched controls. With the current study we sought to examine the correlation between white matter DTI measures in the late subacute (or early chronic) phase and 1-year clinical outcome, and to investigate whether DTI repeated about 1 year post-trauma would detect white matter microstructural alterations. Additionally, we wished to determine which diffusivity changes underlie FA (and MD) abnormalities in severe TBI. We hypothesized that, for one or more of the investigated white matter areas, (i) FA would be reduced in TBI patients in the late subacute phase, (ii) FA would increase in patients during the scan interval, (iii) FA would deviate more from control values, at both scan time points, in patients with poorer long-term clinical outcome.

Material and Methods

Subjects

The study was approved by the local Scientific Ethics Committee (KF 01-038/03). Informed consent was obtained from the participants or from next of kin, meeting criteria of the Helsinki Declaration.

Thirty adult patients (age 18–65 years, mean 34 years; 23 males, 7 females) with severe TBI were recruited from the Brain Injury Unit at Copenhagen University Hospital Hvidovre, Denmark, to which they were admitted for subacute rehabilitation between 2003 and 2005. Severe TBI was defined as a post-resuscitation Glasgow Coma Scale (GCS; Teasdale and Jennett, 1974) score ≤ 8 measured within 24 h post-injury and prior to the initiation of paralytics or sedatives. Patients were referred from neuro-intensive units, and admitted for rehabilitation only if they had subnormal GCS after cessation of sedation. All adult patients with severe TBI admitted during the recruitment period were evaluated for study eligibility. Patients were excluded if they had any previous history of TBI or other neurological disorder, if contraindications to MRI or to sedation

Table 1 Clinical characteristics of patients

Patient	Age at scan I (years)	Sex	Cause of trauma	Post-resuscitation GCS	Neuro-surgery	ISS	Secondary insults	Days to GCS > 8	Duration of PTA (days)	FIM at scan I	FIM at 1 year	GOS at 1 year
1	19	M	MVA	4	—	35	+	10	>FU	29	83	3
2	23	F	MVA	3	—	43	+	36	79	47	120	3
3 ^a	23	F	Fall	3	—	45	+	>FU	>FU	18	18	2
4 ^a	21	F	MVA	6	+	25	—	12	39	79	117	3
5 ^a	34	M	MVA	3	—	66	+	126	>FU	18	30	3
6 ^a	40	F	Fall	3	+	25	+	9	>FU	18	20	3
7 ^a	40	M	Assault	3	—	29	+	4	88	87	122	4
8 ^a	60	M	Fall	3	+	25	—	21	>FU	34	35	3
9 ^a	28	M	MVA	NA	—	34	—	24	66	122	125	5
10	54	M	Fall	NA	—	25	—	14	119	60	125	4
11 ^a	26	M	MVA	3	—	35	—	2	25	110	126	5
12 ^a	24	M	MVA	3	—	26	—	1	39	93	125	4
13 ^a	65	M	Fall	3	—	29	—	3	39	116	120	4
14 ^a	31	M	MVA	5	+	25	+	7	48	38	102	4
15 ^a	37	M	MVA	NA	+	38	—	14	40	117	122	5
16 ^a	22	M	MVA	NA	—	43	—	7	31	120	125	5
17 ^a	19	M	MVA	6	—	33	—	2	23	113	124	5
18 ^a	41	F	MVA	6	+	34	—	10	65	55	113	4
19 ^a	26	M	MVA	6	—	25	+	22	65	106	124	4
20	60	M	Fall	3	—	26	+	18	289	31	30	3
21 ^a	22	M	MVA	3	—	43	+	9	178	18	103	3
22	61	M	Fall	5	+	25	+	22	>FU	18	25	3
23 ^a	23	M	MVA	3	—	25	+	11	107	23	111	3
24 ^a	18	F	MVA	3	—	29	+	15	66	24	105	3
25 ^{a, b}	40	M	Fall	3	+	25	—	10	84	100	117	4
26 ^a	53	M	Fall	4	+	25	+	5	171	18	111	4
27	28	M	Fall	3	—	38	+	15	180	18	36	3
28	31	M	MVA	3	—	38	+	33	>FU	18	22	3
29 ^a	27	M	MVA	6	—	45	+	10	77	49	113	4
30 ^a	26	F	MVA	7	—	29	—	4	58	59	126	5

^aPatients who had follow-up DTI; ^bexcluded from DTI analysis (acquisition error). MVA = motor vehicle accident; GCS = Glasgow coma scale; NA = not available (GCS ≤ 8 but exact GCS not documented); > FU = exceeds ~1 year follow-up; ISS = injury severity score (> 25 indicates extra-cranial injury); PTA = post-traumatic amnesia; FIM = functional independence measure; Scan I = initial MRI; GOS = Glasgow outcome scale. See text for details.

during MRI were present, or if MRI could not be performed within 12 weeks post-trauma for safety or practical reasons.

After discharge, patients were re-admitted for clinical follow-up on average 12 months (9–15 months) post-injury (one patient who moved far away was instead visited and evaluated in his home by the treating physician). During, or as close as possible, to this stay a second scan was obtained in 23 of the patients. For the remaining patients follow-up DTI could not be acquired due to: relocation (*n* = 1), inability to complete the repeat examination because of poor cooperation (*n* = 4), insertion of MRI-incompatible implants (*n* = 1), or scanner failure (*n* = 1). Table 1 summarizes clinical data for the patients studied.

Thirty healthy controls, without any history of significant TBI or neurological disorder, were selected to match the patient group with respect to distribution of age, sex, educational level and abuse of alcohol and drugs (Table 2). Of these, 14 were investigated longitudinally with a time interval comparable to that of the patients.

Clinical assessments

For all patients, clinical data and ratings were documented in medical files. Cause of trauma was classified as motor vehicle

accident (*n* = 19), fall (*n* = 10) or assault (*n* = 1). Accidents with any direct involvement of a motor vehicle (including pedestrian or bicyclist hit by car) were classified as motor vehicle accident. GCS was registered frequently in the acute phase and daily during rehabilitation, only to be discontinued if stable at 15. As an indicator of the total injury severity to all organ systems, Injury Severity Score (ISS, Greenspan *et al.*, 1985) was assessed based on clinical data from the acute phase (ISS >25 indicates extracranial injury). Secondary insults were defined as the occurrence of any of the following in the acute or subacute phase: hypotension (systolic blood pressure <90 mmHg), hypoxia (oxygen saturation <90% or cyanosis in field) or high intracranial pressure (ICP >20 mmHg) (Jones *et al.*, 1994). Neurosurgery was defined as surgery that involved craniotomy, excluding insertion of ICP monitoring devices.

The number of days from TBI until GCS >8 was registered as a measure of coma duration, and the Galveston Orientation and Amnesia Test (Levin *et al.*, 1979) was repeatedly applied to establish duration of post-traumatic amnesia (PTA). Functional Independence Measure (FIM; Granger *et al.*, 1986) was documented regularly, including at both scan time points (sum score ranges from 18 indicating ‘total assist’, to 126 indicating ‘complete independence’). Functional outcome at ~12 months post-TBI was

Table 2 Demographic characteristics of patient and control groups

	Scan 1			Scan 2		
	Patients (n = 30)	Controls (n = 30)	Group differences	Patients (n = 23)	Controls (n = 14)	Group differences
Age, scan 1 (years), mean (SD)	34.1 (14.3)	34.0 (13.9)	$P > 0.99^a$	32.4 (12.9)	31.2 (8.1)	$P > 0.7^a$
Sex: M/F	23/7	23/7	$P = 1.0^b$	17/6	9/5	$P > 0.7^b$
Education (years), mean (SD)	13.3 (3.1)	13.4 (2.3)	$P > 0.99^a$	13.4 (3.1)	13.7 (2.7)	$P > 0.7^a$
Excessive alcohol intake (> 21 drinks per week for men, > 14 for women), Y/N	5/25	4/26	$P = 1.0^b$	4/19	0/14	$P = 0.3^b$
Use of drugs (cannabinoids or psycho-stimulants) $>$ once a month, Y/N	3/27	1/29	$P > 0.6^b$	3/20	0/14	$P = 0.3^b$

^aIndependent-samples t-test; ^bFishers exact test. Scan 1 = initial MRI; Scan 2 = follow-up MRI.

evaluated using the 5-point Glasgow Outcome Scale (GOS; Jennett and Bond, 1975), ranging from 1 = dead to 5 = good recovery. Based on previous literature (see e.g. Choi *et al.*, 2002), GOS = 1–3 was considered as unfavourable outcome and GOS = 4–5 as favourable outcome, thus distinguishing whether or not patients were able to live independently. All clinical ratings were performed by trained staff, neurologists and neuropsychologists unaware of DTI results.

MRI data acquisition

MRI including DTI was acquired 5–11 weeks (mean 8 weeks) after trauma. A more uniform time interval was not achievable, mainly because patients had to be medically stable when scanned. All patients were referred to conventional MRI for clinical purposes. DTI and other sequences not reported here were performed as an extension of the MRI examination. The majority of patients ($n = 25$) were sedated for the initial MRI, since they were unable to cooperate for MRI. Intravenously administered propofol was used for sedation, and patients were monitored by anaesthesiology staff. Oxygen supply and mechanical ventilation were provided when necessary.

All patients and controls were scanned on the same 1.5 T MRI scanner (Magnetom Vision; Siemens Medical Solutions, Erlangen, Germany) using a standard circular-polarized head coil. During the study period, MRI sessions for patients and controls were interleaved in time, and no major upgrades were carried out on the scanner. A 3D sagittal T1-weighted sequence (TR/TE/TI = 13.5/7/100 ms, flip angle 15°, spatial resolution of $\sim 1 \text{ mm}^3$) was acquired in all subjects. For patients, additional conventional sequences included: axial T2-weighted images (spin-echo, TR/TE = 5400/99 ms, 27 contiguous, 5 mm thick slices, $0.5 \times 0.5 \text{ mm}^2$ in-plane resolution), coronal T2*-weighted gradient-echo images (TR/TE = 544/15 ms, 34 contiguous, 5 mm thick slices, $0.9 \times 0.9 \text{ mm}^2$ in-plane resolution), axial and sagittal FLAIR (TR/TE/TI = 9000/110/2500 ms, 34 contiguous, 5 mm thick slices, $0.9 \times 0.9 \text{ mm}^2$ in-plane resolution).

All subjects underwent DTI using a diffusion-weighted spin-echo single-shot echo-planar imaging (EPI) sequence acquired with diffusion encoding in 6 non-collinear directions and averaged over six datasets for a total acquisition time of ~ 15 min. The sequence parameters were as follows: TE = 60 ms, field of view 230 mm, matrix 128×128 , 30 axial slices, 5 mm slice thickness, b values 0 and $\sim 740 \text{ s/mm}^2$ with diffusion sensitizing gradient pulses of duration = 29 ms (δ) and separation = 52 ms (Δ).

Follow-up MRI was acquired in 23 of the patients (9–15 months post-injury, mean 12 months), and in 14 of the controls. A minimum of DTI and 3D T1-weighted images were obtained at follow-up with the parameters described earlier. Subjects were repositioned as close as possible to their position in the previous scan. For ethical reasons patients were sedated only if follow-up MRI was requested for clinical purposes and patients were unable to cooperate for MRI because of cognitive impairment. While 19 patients were fully cooperative, four were sedated for the follow-up MRI. Four patients were not sufficiently cooperative to complete the follow-up MRI but could not be sedated.

For one patient, careful inspection of the diffusion-weighted images acquired at the initial scan revealed an abnormally low signal-to-noise ratio (most likely due to miscalibration of the radio-frequency transmitter reference). We therefore excluded DTI data for this patient (initial and follow-up scan) from statistical analysis.

MRI data analysis

Evaluation of conventional MRI

The conventional images were qualitatively evaluated for all patients by an experienced neuroradiologist (M.H.) blinded to the DTI findings and clinical ratings. This evaluation included classification of all visible lesions based on their signal characteristics (see e.g. Gentry, 2002). Additional careful inspection of the regions of interest (ROIs) was done subsequently.

Regions of interest

Images were transferred to an offline workstation for post-processing, and were visually checked for quality. All ROIs were outlined manually on spatially normalized 3D T1-weighted structural images (Fig. 1). Spatial normalisation of the T1-weighted images according to the MNI template was performed using a 12 parameter transformation in SPM2 (<http://www.fil.ion.ucl.ac.uk/spm>). Using image display software (MIPAV, version 2.0, <http://mipav.cit.nih.gov>) the following white matter ROIs were positioned for each individual scan: posterior aspect of the corpus callosum (PCC), posterior limb of internal capsule (PLIC), centrum semiovale (CSO) and cerebral peduncle (CP). Additional ROIs in ventricular CSF and in the putamen (PUT), expected to be relatively unaffected by TBI, served as internal references for MD. In order to minimize misregistration stemming from

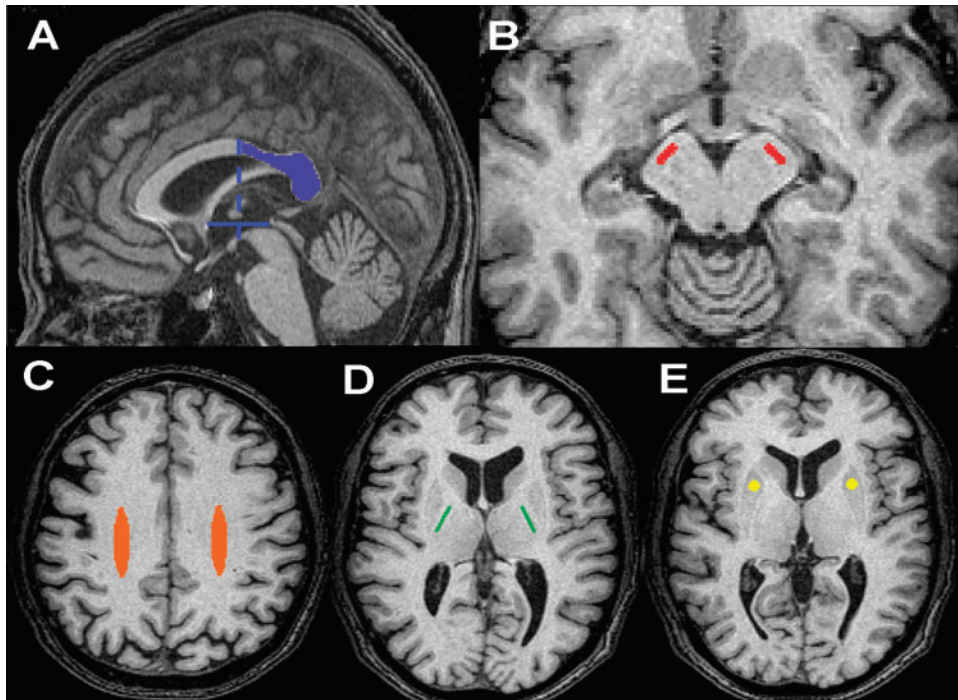


Fig. 1 ROIs used in the study. ROIs were drawn on normalized 3D T1-W images (shown) for each individual scan. (A) Posterior aspect of corpus callosum (PCC). Anterior border is defined by midpoint of the AC–PC line; (B) cerebral peduncle (CP); (C) centrum semiovale (CSO); (D) posterior limb of internal capsule (PLIC); (E) putamen (PUT). See text for details.

EPI-related susceptibility artifacts, we avoided ROIs in the most frontal cerebral areas. As structural changes were expected to occur over time, ROIs were redrawn/repositioned for all follow-up scans to ensure identical anatomical positioning for initial and follow-up scans. ROIs were positioned by anatomic guidance, not lesion guidance, and were outlined bilaterally in the axial plane, except for PCC which was outlined in the sagittal plane. For statistical analysis, bilateral measurements were averaged.

The PCC ROI [volume (mean \pm SD) = 2513 \pm 479 μ l] was drawn according to the callosal borders on the midsagittal slice plus the four adjacent parasagittal slices on each side, with the anterior border being defined arbitrarily by a line perpendicularly crossing the midpoint of the anterior-posterior commissural (AC–PC) line. Anatomically, the PCC included the splenium, isthmus and posterior part of the body of corpus callosum. The PLIC (171 \pm 2 μ l) was sampled by a rectangle in the centre of the structure on the four axial slices where it appeared broadest. For the CSO (4820 \pm 46 μ l) an ellipse was placed centrally in the hemispherical white matter on 8–10 axial slices. The CP (150 \pm 0 μ l) was sampled by a polygonal ROI on five slices of the upper mesencephalon. For reference (MD only), a circular ROI was placed in the centre of the PUT (672 \pm 0 μ l), transversing 10–12 axial slices and ventricular CSF was sampled on one axial slice (43 \pm 5 μ l).

Except for the PCC, the borders of the ROIs were kept distant from adjacent tissue/CSF. For PCC a step-wise erosion algorithm, with each step eroding the exterior voxel layer in the sagittal plane, was subsequently applied to test for possible partial volume effects, i.e. the unintentional inclusion in the ROIs of other than the tissue of interest. Due to global atrophy during the scan interval, the volumes of some ROIs (particularly the PCC) were smaller at the follow-up scan in many patients.

All ROIs were outlined by the same rater (A.S.). For evaluation of intra-rater reproducibility, ROIs were positioned 3 times (with evaluations separated by 1–2 days) in four subjects (two controls, two patients). Between-scan reproducibility was estimated using additional data from three healthy subjects scanned twice with a maximum interval of 4 weeks.

Every individual ROI was inspected carefully for lesions visible on conventional sequences (T1, T2, T2*, FLAIR). Since DAI lesions were often punctate and multiple we did not attempt to eliminate DAI lesions from the ROIs. Instead, individual ROIs were excluded from statistical analysis (both initial and follow-up) only if they contained non-DAI lesions. If one ROI was excluded, the contralateral one was used for analysis (bilateral ROIs).

DTI post-processing

Diffusion-weighted images were coregistered to the $b=0$ images using a 12 parameter algorithm in SPM2. The six repetitions for each measured direction were averaged to increase the signal-to-noise ratio. The diffusion tensor (D) and its eigenvalues ($\lambda_1, \lambda_2, \lambda_3$) and eigenvectors were then estimated for each voxel (Basser *et al.*, 1994), the calculations being performed in native space prior to spatial normalization. By sorting the eigenvalues in order of decreasing magnitude for each voxel ($\lambda_1 > \lambda_2 > \lambda_3$), λ_1 represents the diffusivity along the primary diffusion direction, i.e. along the fibre axis, and is referred to as the *axial* diffusivity, $\lambda_{||}$. The averaged water diffusivities perpendicular to the axonal fibres, λ_2 and λ_3 , are referred to as $\lambda_{\perp} = (\lambda_2 + \lambda_3)/2$, or the *radial* diffusivity (Song *et al.*, 2002). The summary parameters MD and FA were calculated voxel-wise according to (Pierpaoli and Basser, 1996).

Coregistration and extraction of DTI values

For each scan the $b=0$ images were coregistered to the corresponding spatially normalized 3D structural T1-weighted images using normalized mutual information. This transformation was then applied to the calculated diffusion parameter maps and these were resliced using tri-linear interpolation in SPM2. For all scans coregistration was visually checked by superimposing the images (including the ROIs). The coregistration was done after calculating the diffusion parameters in order to avoid any effects this spatial normalization step might have on the calculation of the diffusion tensor. The only effect the normalization has on the diffusion parameter maps is therefore a slight smoothing due to the reslicing. Following coregistration, diffusion parameters (FA, MD, λ_{\parallel} and λ_{\perp}) were extracted from each ROI and summarized as the median value of the voxels comprising the ROI.

For those subjects who had a follow-up scan, a pairwise coregistration of the second to the first 3D T1-weighted volume was performed, followed by the normalization applied in the first scan. The calculated diffusion images were then coregistered to the T1-weighted images as described earlier.

Statistical analysis

Statistical analyses were performed with SPSS (v.15.0), and the threshold for statistical significance was set at $P < 0.05$. Shapiro–Wilk’s test was used to test the distribution of DTI parameters, and since deviation from normality was not found parametric statistics were applied. For measures of intra-rater and between-scan reproducibility, the coefficient of variation (CV) was computed ($CV = SD/mean$). To test the principal hypotheses, independent-samples t -tests (two-tailed) were conducted to compare FA between patients and controls as well as between favourable and unfavourable outcome subgroups, while paired t -tests (two-sided) were used to examine changes over time. Bonferroni correction for multiple comparisons was made for tests of the principal hypotheses regarding FA (four white matter ROIs were tested, hence $P < 0.0125$ was considered significant following correction).

To further examine the basis of any FA differences, we conducted secondary comparisons on the additional diffusion parameters MD, λ_{\parallel} and λ_{\perp} . Additional secondary analyses of clinical and conventional imaging variables relative to dichotomized outcome were performed using independent-samples t -test (continuous normally distributed variables), Mann–Whitney U-test (continuous non-normally distributed variables) and Fisher’s exact test (categorical variables). Finally, we employed a binary logistic regression analysis (forward step-wise, likelihood ratio) to determine the ability of DTI at the initial scan (~8 weeks post-trauma) to predict dichotomized ~1-year outcome, and to assess the added value of DTI compared to prediction of outcome by clinical evaluation (FIM) only.

Results

Conventional MRI

All but one patient exhibited signal abnormalities consistent with DAI on one or more conventional sequences, presenting as petechial haemorrhages on T2*-weighted images and/or hyperintensities on FLAIR within typical locations. These abnormalities however ranged from a few subtle

lesions identified in a single anatomic location to multiple clear and widespread lesions. Graded according to location (Graham and Gennarelli, 1997), 5 patients had visible DAI lesions confined to the hemispheres (grade I), 15 had visible DAI lesions in the corpus callosum but not in the brainstem (grade II) and 9 had additional DAI-related lesions in the brainstem (grade III).

Residual lesions other than DAI were found on conventional MRI in 26 of 30 patients (initial scan); frequently several types of lesions coexisted. The following intracranial abnormalities were found (number of patients): cortical contusion(s) (15), small subdural haematoma (7), intracerebral haematoma (3), arterial dissection (1), abscess (1), territorial arterial infarction (4), focal brainstem infarct (1), diffuse hypoxic injury (1) and pyramidal tract degeneration in the brainstem (4). Individual ROIs containing non-DAI lesions on conventional MRI and therefore excluded from statistical analysis were: one left PLIC, one left CSO, two right CSO, one left CP, one right CP, one left PUT and two right PUT. Controls all had unremarkable T1-weighted images within and outside ROIs.

At follow-up general atrophy was pronounced in many patients, notably ventricular size had increased and callosal thickness decreased compared to the initial MRI. In many patients the pyramidal tract in the brainstem exhibited bilateral degenerative abnormalities at follow-up.

DTI

Reproducibility of DTI measures was satisfactory for all white matter ROIs, regarding both intra-rater ($CV \leq 3\%$ for FA) and between-scan ($CV \leq 4\%$ for FA) measurements. As expected, in areas of low anisotropy (PUT and CSF), variation of FA was much higher (intra-rater CV up to 26%, between-scan CV up to 19%), whereas MD showed good reproducibility (intra-rater $CV \leq 2\%$, between-scan $CV < 3\%$).

Table 3 lists DTI results for the initial and follow-up scans of the patients (mean 8 weeks and 12 months post-injury) as compared to the controls. DTI values in controls were in the same range as those reported previously (e.g. Pierpaoli *et al.*, 1996; Marenco *et al.*, 2006). At the initial scan, FA was found to be significantly decreased in all white matter ROIs (PCC, PLIC, CSO, CP) in patients as compared with controls ($P < 0.000001$ for PCC and CP, $P \leq 0.01$ for PLIC and CSO). These results remained significant following Bonferroni correction. Except for CP, MD in patients was not significantly different from controls at the initial scan. Investigating the underlying axial (λ_{\parallel}) and radial (λ_{\perp}) diffusivities, for PCC, PLIC and CP this revealed significantly decreased λ_{\parallel} ($P < 0.00001$ for PCC, $P < 0.001$ for PLIC, $P < 0.000001$ for CP) as well as increased λ_{\perp} ($P < 0.0001$ for PCC, $P < 0.05$ for PLIC, $P < 0.001$ for CP). Hence, decrease of FA was caused by the combined effects of λ_{\parallel} decrease and λ_{\perp} increase. MD was relatively unaffected as these effects counterbalanced.

Table 3 Diffusion parameters, mean (SD) for each ROI, initial and follow-up scans

ROI	Scan	FA		MD [$\times 10^{-3}$ mm ² /s]		λ_{\parallel} [$\times 10^{-3}$ mm ² /s]		λ_{\perp} [$\times 10^{-3}$ mm ² /s]	
		Controls	Patients	Controls	Patients	Controls	Patients	Controls	Patients
PCC	1	0.55 (0.06)	0.42 (0.08) ***	1.08 (0.10)	1.10 (0.07)	1.85 (0.14)	1.67 (0.12)***	0.72 (0.11)	0.84 (0.10)***
	2	0.57 (0.06)	0.37 (0.08) ***	1.06 (0.09)	1.27 (0.11)***	1.85 (0.10)	1.80 (0.13)	0.68 (0.11)	1.02 (0.14)***
PLIC	1	0.68 (0.05)	0.64 (0.06) **	0.80 (0.06)	0.80 (0.05)	1.55 (0.07)	1.48 (0.09)***	0.43 (0.07)	0.46 (0.06)*
	2	0.69 (0.05)	0.67 (0.05)	0.79 (0.05)	0.84 (0.07)**	1.53 (0.08)	1.59 (0.08)*	0.41 (0.07)	0.46 (0.08)
CSO	1	0.39 (0.08)	0.35 (0.06) **	0.88 (0.08)	0.89 (0.08)	1.28 (0.09)	1.24 (0.10)	0.68 (0.11)	0.71 (0.08)
	2	0.40 (0.08)	0.39 (0.08)	0.87 (0.07)	0.92 (0.09)	1.27 (0.12)	1.33 (0.10)	0.67 (0.09)	0.71 (0.11)
CP	1	0.70 (0.03)	0.60 (0.07) ***	0.84 (0.06)	0.80 (0.07)*	1.66 (0.09)	1.41 (0.15)***	0.43 (0.06)	0.50 (0.07)***
	2	0.72 (0.03)	0.59 (0.07) ***	0.80 (0.07)	0.90 (0.10)***	1.62 (0.10)	1.58 (0.13)	0.40 (0.05)	0.57 (0.11)***
PUT	1	0.21 (0.04)	0.23 (0.07)	0.79 (0.07)	0.80 (0.05)	0.95 (0.08)	0.99 (0.09)	0.71 (0.06)	0.71 (0.05)
	2	0.20 (0.03)	0.26 (0.05)***	0.78 (0.05)	0.82 (0.07)	0.93 (0.05)	1.03 (0.11)**	0.71 (0.05)	0.71 (0.06)
CSF	1	0.13 (0.05)	0.12 (0.04)	3.21 (0.11)	3.20 (0.12)	3.63 (0.19)	3.61 (0.25)	2.98 (0.11)	2.98 (0.08)
	2	0.12 (0.04)	0.12 (0.07)	3.20 (0.19)	3.22 (0.18)	3.59 (0.31)	3.64 (0.38)	3.00 (0.15)	3.00 (0.14)

Initial scan (scan 1): *n* = 29 patients, 30 controls; follow-up Initial scan (scan 2): *n* = 22 patients, 14 controls **P* < 0.05 ***P* ≤ 0.01 ****P* ≤ 0.001 (uncorrected), independent-samples *t*-tests, patients compared with controls. For principal analyses (FA in white matter ROIs), bold values indicate that patients remained significantly different from controls following Bonferroni correction (*P* < 0.0125). Secondary analyses (MD, λ_{\parallel} , λ_{\perp}) are displayed on the right; reference ROIs for MD (PUT and CSF) at the bottom (shaded). PCC = posterior aspect of corpus callosum; PLIC = posterior limb of internal capsule; CSO = centrum semiovale; CP = cerebral peduncle; PUT = putamen; CSF = cerebrospinal fluid; FA = fractional anisotropy; MD = mean diffusivity; λ_{\parallel} = axial diffusivity; λ_{\perp} = radial diffusivity.

Table 4 Longitudinal DTI findings in 22 patients, mean (SD)

ROI	FA		MD [$\times 10^{-3}$ mm ² /s]		λ_{\parallel} [$\times 10^{-3}$ mm ² /s]		λ_{\perp} [$\times 10^{-3}$ mm ² /s]	
	Scan 1	Scan 2	Scan 1	Scan 2	Scan 1	Scan 2	Scan 1	Scan 2
PCC	0.42 (0.07)	0.37 (0.08) ***	1.10 (0.07)	1.27 (0.11)***	1.66 (0.11)	1.80 (0.13)***	0.84 (0.09)	1.02 (0.14)***
PLIC	0.64 (0.05)	0.67 (0.05) **	0.79 (0.05)	0.84 (0.07)***	1.47 (0.10)	1.59 (0.08)***	0.46 (0.06)	0.46 (0.08)
CSO	0.35 (0.07)	0.39 (0.08) **	0.88 (0.08)	0.92 (0.09)*	1.24 (0.11)	1.33 (0.10)***	0.71 (0.08)	0.71 (0.11)
CP	0.61 (0.07)	0.59 (0.07)*	0.80 (0.07)	0.90 (0.10)***	1.42 (0.16)	1.58 (0.13)***	0.49 (0.07)	0.57 (0.11)***
PUT	0.22 (0.07)	0.26 (0.05)**	0.79 (0.05)	0.82 (0.07)	0.97 (0.08)	1.03 (0.11)**	0.70 (0.05)	0.71 (0.06)
CSF	0.11 (0.04)	0.12 (0.07)	3.19 (0.13)	3.22 (0.18)	3.62 (0.24)	3.64 (0.38)	2.99 (0.11)	3.00 (0.14)

P* < 0.05; *P* ≤ 0.01; ****P* ≤ 0.001 (uncorrected), paired *t*-tests. For principal analyses (FA in white matter ROIs), bold values indicate that results remained significant following Bonferroni correction (*P* < 0.0125). Secondary analyses (MD, λ_{\parallel} , λ_{\perp}) are displayed on the right; reference ROIs for MD (PUT and CSF) at the bottom (shaded). Scan 1 = initial MRI; Scan 2 = follow-up MRI; PCC = posterior aspect of corpus callosum; PLIC = posterior limb of internal capsule; CSO = centrum semiovale; CP = cerebral peduncle; PUT = putamen; CSF = cerebrospinal fluid; FA = fractional anisotropy; MD = mean diffusivity; λ_{\parallel} = axial diffusivity; λ_{\perp} = radial diffusivity.

For the CSO, λ_{\parallel} and λ_{\perp} were not significantly different from controls (*P* > 0.1). MD was not significantly different between patients and controls in the grey matter ROI (PUT) or in CSF (*P* > 0.4). For these reference ROIs FA, λ_{\parallel} and λ_{\perp} are listed for completeness.

The DTI changes over time are further presented in Table 4 for the 22 patients who were rescanned ~12 months post-injury. During the scan interval FA increased in PLIC and CSO (*P* ≤ 0.01). However in PCC, FA decreased further (*P* < 0.0001). These findings remained significant following Bonferroni correction. Investigating the changes of the underlying eigenvalues revealed that λ_{\parallel} increased in all white matter ROIs (*P* < 0.00001 for PCC, *P* < 0.00001 for PLIC, *P* < 0.0001 for CSO and CP). In PCC and CP this was accompanied by significant increase of λ_{\perp} (*P* < 0.00001 for PCC, *P* < 0.001 for CP), i.e. all eigenvalues changed in the same direction and consequently

large increases of MD were seen in these ROIs (*P* < 0.000001 for PCC, *P* < 0.0001 for CP). However, in PLIC and CSO, λ_{\perp} did not change over time, and so the observed FA (and MD) increase was caused by a selective λ_{\parallel} increase in these ROIs. For each ROI the direction of change in each DTI parameter was the same in almost all patients individually. However, in a few cases values were unchanged or went slightly in the opposite direction.

In CSF no significant changes over time were seen. In PUT however, an unexpected increase of FA over time was found (*P* < 0.01). Computing FA in isotropic or nearly isotropic areas, such as in CSF and PUT, is subject to considerable noise (cf. the poor reproducibility in these areas), which makes it difficult to interpret this latter finding.

Controls had comparable DTI parameter values at the initial and follow-up scans in all ROIs, with no trends of any systematic effects over time. Additional testing of change over

Table 5 Erosion of PCC, effect on DTI metrics, initial and follow-up scans, mean (SD)

	Scan	FA		MD [$\times 10^{-3}$ mm ² /s]		λ_{\parallel} [$\times 10^{-3}$ mm ² /s]		λ_{\perp} [$\times 10^{-3}$ mm ² /s]	
		Controls	Patients	Controls	Patients	Controls	Patients	Controls	Patients
0 erosions	1	0.55 (0.06)	0.42 (0.08) ***	1.08 (0.10)	1.10 (0.07)	1.85 (0.14)	1.67 (0.12)***	0.72 (0.11)	0.84 (0.10)***
	2	0.57 (0.06)	0.37 (0.08) ***	1.06 (0.09)	1.27 (0.11)***	1.85 (0.10)	1.80 (0.13)	0.68 (0.11)	1.02 (0.14)***
1 erosion	1	0.61 (0.06)	0.48 (0.08) ***	1.00 (0.08)	1.03 (0.07)	1.83 (0.14)	1.64 (0.13)***	0.60 (0.10)	0.74 (0.10)***
	2	0.64 (0.05)	0.43 (0.08) ***	0.98 (0.08)	1.17 (0.11)***	1.83 (0.10)	1.74 (0.15)*	0.57 (0.09)	0.89 (0.14)***
2 erosions	1	0.67 (0.06)	0.54 (0.09) ***	0.93 (0.07)	0.96 (0.06)	1.80 (0.14)	1.61 (0.15)***	0.50 (0.09)	0.64 (0.10)***
	2	0.69 (0.05)	0.50 (0.09) ***	0.92 (0.07)	1.07 (0.10)***	1.82 (0.11)	1.70 (0.16)**	0.48 (0.08)	0.76 (0.13)***
3 erosions	1	0.70 (0.06)	0.58 (0.09) ***	0.90 (0.07)	0.91 (0.07)	1.80 (0.14)	1.59 (0.17)***	0.45 (0.09)	0.57 (0.10)***
	2	0.72 (0.05)	0.54 (0.09) ***	0.88 (0.07)	1.01 (0.10)***	1.82 (0.11)	1.68 (0.18)**	0.42 (0.08)	0.68 (0.12)***

Initial scan (scan 1): $n = 29$ patients, 30 controls; follow-up scan (scan 2): $n = 22$ patients, 14 controls. * $P < 0.05$ ** $P \leq 0.01$ *** $P \leq 0.001$ (uncorrected), independent-samples t -tests, patients compared to controls. For principal analyses (FA), bold values indicate that patients remained significantly different from controls following Bonferroni correction ($P < 0.0125$). PCC = posterior aspect of corpus callosum; FA = fractional anisotropy; MD = mean diffusivity; λ_{\parallel} = axial diffusivity; λ_{\perp} = radial diffusivity.

time in patients compared to change over time in controls (independent-samples t -test, data not shown) therefore yielded statistical differences comparable to those in Table 4.

As DAI lesions visible on conventional MRI were frequently present within PCC, supplemental analysis was made for the subgroup of patients without any visible abnormalities in PCC on conventional MRI ($n = 6$, corresponding to DAI grade I or no DAI). For this subgroup FA was still significantly lower in PCC compared to the controls, both at the initial scan and at follow-up ($P < 0.02$).

To test and correct for partial volume effects of the PCC, a step-wise (up to 3 times) erosion of the exterior voxel layer of PCC was performed in the sagittal plane. As displayed in Table 5, this could indicate partial voluming of the uneroded ROI (FA increased, while MD, λ_{\perp} and, to a lesser extent, λ_{\parallel} decreased with each erosion step). However, when repeating statistical analysis on the eroded PCC, differences between patients and controls remained significant, even after three erosions.

Volumes of the PCC ROI in patients were generally smaller at follow-up compared to the initial scan (mean 2.1 versus 2.5 ml, $P < 0.00001$, paired t -test), since in most patients callosal thinning occurred during the scan interval. As this could introduce systematic differences in partial voluming, the longitudinal analysis was repeated using the eroded PCC (data not shown). Changes over time in patients remained significant following three erosions for all DTI parameters ($P < 0.01$, paired t -tests).

Potential influence of the occurrence of secondary insults on DTI parameters was examined, and although FA values in some ROIs appeared to be more depressed in patients with secondary insults, this did not approach significance. Additionally, careful data inspection revealed no trends towards the influence of sedation upon DTI parameters.

Clinical outcome correlations

Table 6 summarizes statistical analysis on demographic, clinical and conventional imaging variables when

comparing patients according to dichotomized ~ 1 -year outcome (favourable: GOS = 4–5, corresponding to good recovery or moderate disability; unfavourable: GOS = 1–3, corresponding to severe disability, vegetative state or death). Clinical features significantly related to outcome were post-resuscitation GCS, occurrence of secondary insults, duration of coma, duration of PTA and FIM (measured at the time of the initial MRI). Presence of DAI grade III, as based on conventional MRI, just yielded significance as being associated with unfavourable outcome. The occurrence of focal contusions on conventional MRI was not significantly different between outcome groups.

Figure 2 illustrates the DTI findings at ~ 8 weeks post-TBI in relation to dichotomized 1-year outcome, with control values shown for comparison. There was a general tendency for patients with unfavourable outcome to deviate more from control DTI values than patients with favourable outcome, not only for FA but also for the underlying diffusivities. Following Bonferroni correction FA in CP remained significantly different between outcome groups. Further examination of the relationship between FA in CP and 1-year GOS revealed significant correlations, with higher FA being related to higher GOS ($r = 0.60$, $P < 0.001$, Spearman's correlation), see Fig. 3.

When FA in CP was included in a logistic regression model to predict dichotomized 1-year outcome, a moderately good predictive accuracy was found (76%, $\chi^2 = 15.6$, $P < 0.0001$). Not surprisingly, FIM measured at the time of the initial scan (~ 8 weeks post-injury) also had a high predictive accuracy (90%, $\chi^2 = 19.6$, $P < 0.00001$). However, adding FA in CP to a model containing FIM yielded a significantly improved predictive accuracy (increment $\chi^2 = 20.5$, $P < 0.00001$), which in this sample reached 100%. In comparison, conventional MRI variables (e.g. DAI grade) did not improve the predictive accuracy of FIM in a logistic regression model. Neither did FA in white matter ROIs other than CP.

Figure 4 displays the results analogous to Fig. 2 for the follow-up DTI ~ 12 months post-trauma. In the favourable

Table 6 Significance of demographic, clinical and conventional imaging variables relative to ~1 year outcome

	~1 year outcome (dichotomized GOS)		P
	Favourable (n = 16)	Unfavourable (n = 14)	
Age, years (mean ± SD)	34.9 ± 13.1	33.1 ± 15.9	0.73 ^a
Sex (no. males)	14	9	0.20 ^b
Education, years (mean ± SD)	13.9 ± 3.3	12.8 ± 2.8	0.33 ^a
Cause of trauma (no. MVA)	11	8	0.42 ^b
Post-resuscitation GCS (median, range)	4.5 (3–7)	3 (3–6)	0.036^c
Neurosurgery	5	4	1.0 ^b
ISS (no. with ISS > 25)	11	9	0.80 ^b
Occurrence of secondary insults	5	12	0.004^b
Days to GCS > 8 (median, range) ^d	7 (1–24)	16.5 (9–365)	0.002^c
Duration of PTA, days (median, range) ^d	61.5 (23–171)	327 (39–365)	0.0001^c
FIM at scan I (median, range)	96.5 (18–122)	20.5 (18–79)	0.00001^c
DAI grade III on conventional MRI	2	7	0.046^b
Contusion on conventional MRI	7	8	0.72 ^b

^aIndependent-samples t-test; ^bFisher's exact test; ^cMann–Whitney U-test ^dIf exceeds ~1 year follow-up, set to 365 days.

Unfavourable outcome: GOS = 1–3; favourable outcome: GOS = 4–5. For significant test results (uncorrected), P-values are marked in bold. GOS = Glasgow outcome scale; MVA = motor vehicle accident; GCS = Glasgow coma scale; ISS = injury severity score; PTA = post-traumatic amnesia; FIM = functional independence measure; Scan I = initial MRI; DAI = diffuse axonal injury.

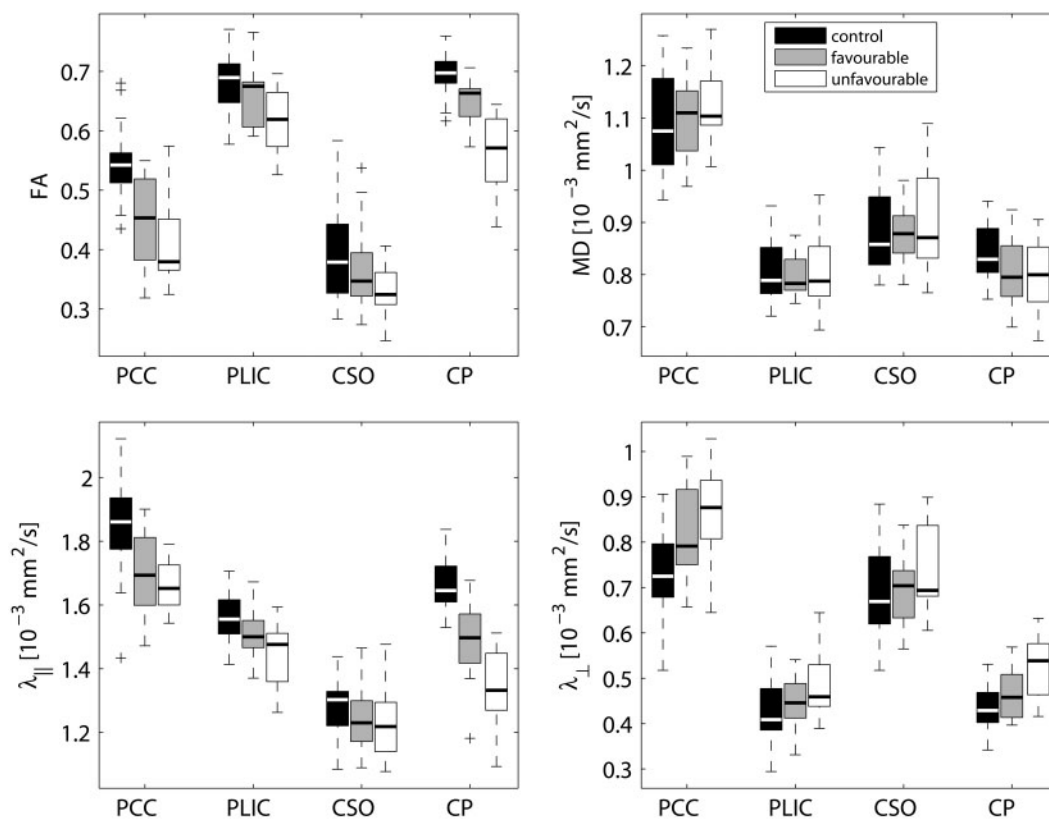


Fig. 2 Initial (~8 weeks post-injury) DTI parameters in the four white matter ROIs, grouped according to outcome at ~1 year post-injury [dichotomized GOS, unfavourable outcome: GOS = 1–3 (n = 14); favourable outcome: GOS = 4–5 (n = 15)]. Control values are shown for comparison (n = 30). Boxes represent lower, median (line) and upper quartiles; whiskers show the range of the data excluding outliers (+). PCC = posterior aspect of corpus callosum; PLIC = posterior limb of internal capsule; CSO = centrum semiovale; CP = cerebral peduncle.

outcome group, FA had returned to normal levels in PLIC and CSO, due to the selective interval increase of λ_{||} which in PLIC reached even supra-normal levels at follow-up (P < 0.01). Further analysis revealed a positive correlation

between individual λ_{||} in PLIC and GOS (r = 0.47, P = 0.03, Spearman's correlation). In PCC and CP, FA remained depressed in both outcome groups, but significantly more so in patients with unfavourable outcome (P < 0.05 and

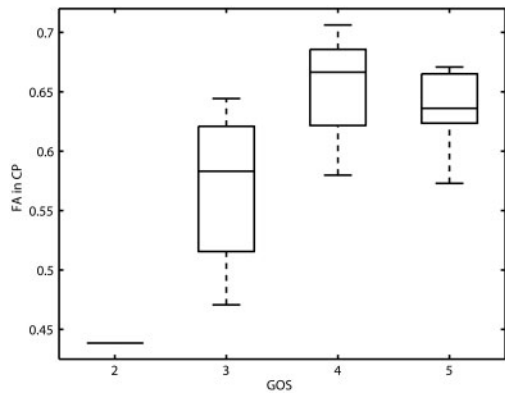


Fig. 3 Relationship between FA in the cerebral peduncle at the initial scan (~8 weeks post-injury) and 1-year outcome. Boxes represent lower, median (line) and upper quartiles; whiskers show the range of the data. Higher FA was related to better outcome ($r = 0.60$, $P < 0.001$, Spearman's correlation). GOS = Glasgow outcome scale: 1 = dead ($n = 0$), 2 = vegetative state ($n = 1$), 3 = severe disability ($n = 13$), 4 = moderate disability ($n = 9$), 5 = good recovery ($n = 6$); CP = cerebral peduncle; FA = fractional anisotropy.

$P = 0.01$, respectively). Finally, Fig. 5 displays the changes over time in favourable and unfavourable outcome patients as well as in controls.

Discussion

Using DTI, we prospectively and longitudinally examined white matter microstructure in individuals with severe TBI in the late subacute and chronic stages, and investigated the correlation to 1-year clinical outcome. In the late subacute stage (~8 weeks post-injury) we found FA to be decreased in all investigated white matter regions, due to decreased λ_{\parallel} and increased λ_{\perp} . Patients with unfavourable 1-year outcome, according to dichotomized GOS, tended to deviate more from control DTI values than patients with favourable outcome. FA in CP at the initial scan added predictive accuracy to concomitant clinical evaluation by FIM. At follow-up DTI ~12 months post-injury, FA had normalized in PLIC and CSO, primarily in patients with favourable outcome, caused by the increase of λ_{\parallel} to normal or supranormal levels with unchanged λ_{\perp} . In PCC and CP, λ_{\parallel} and λ_{\perp} both increased during the scan interval and, particularly in patients with unfavourable outcome, FA remained depressed.

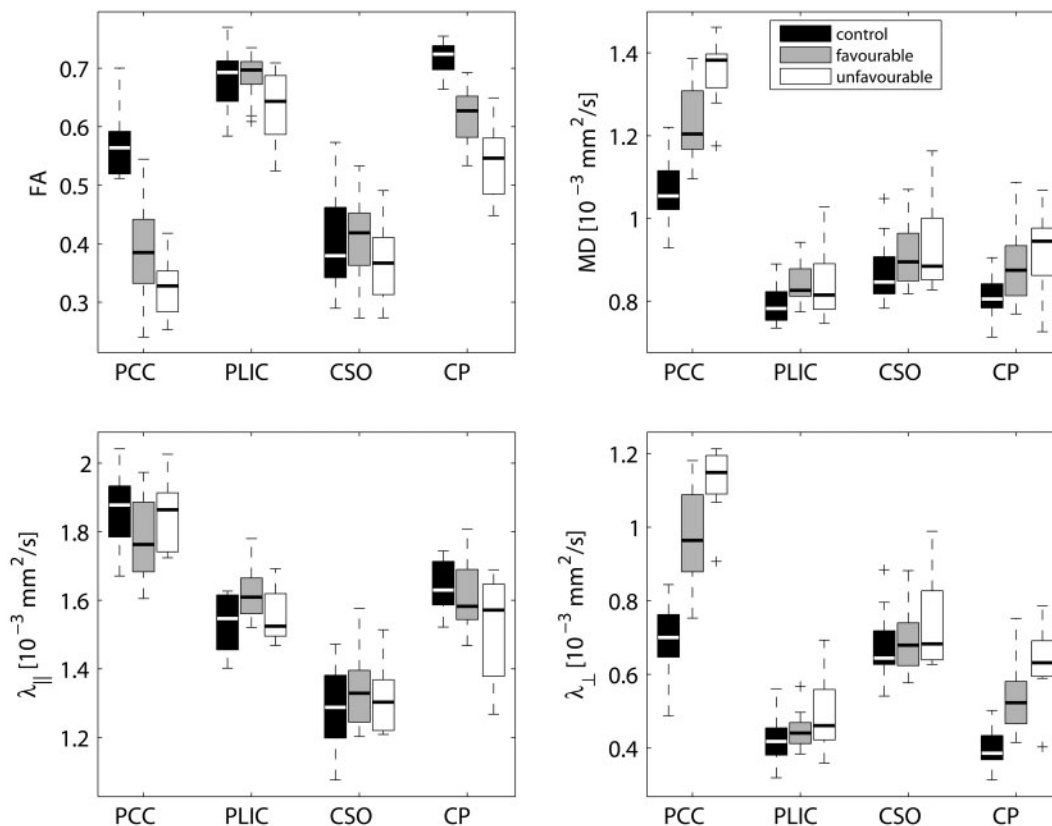


Fig. 4 Follow-up (~12 months post-injury) DTI parameters in the four white matter ROIs, grouped according to outcome at 1 year post-injury [dichotomized GOS, unfavourable outcome: GOS = 1–3 ($n = 8$); favourable outcome: GOS = 4–5 ($n = 14$)]. Control values are shown for comparison (follow-up scan, $n = 14$). Boxes represent lower, median (line) and upper quartiles; whiskers show the range of the data excluding outliers (+). PCC = posterior aspect of corpus callosum; PLIC = posterior limb of internal capsule; CSO = centrum semiovale; CP = cerebral peduncle.

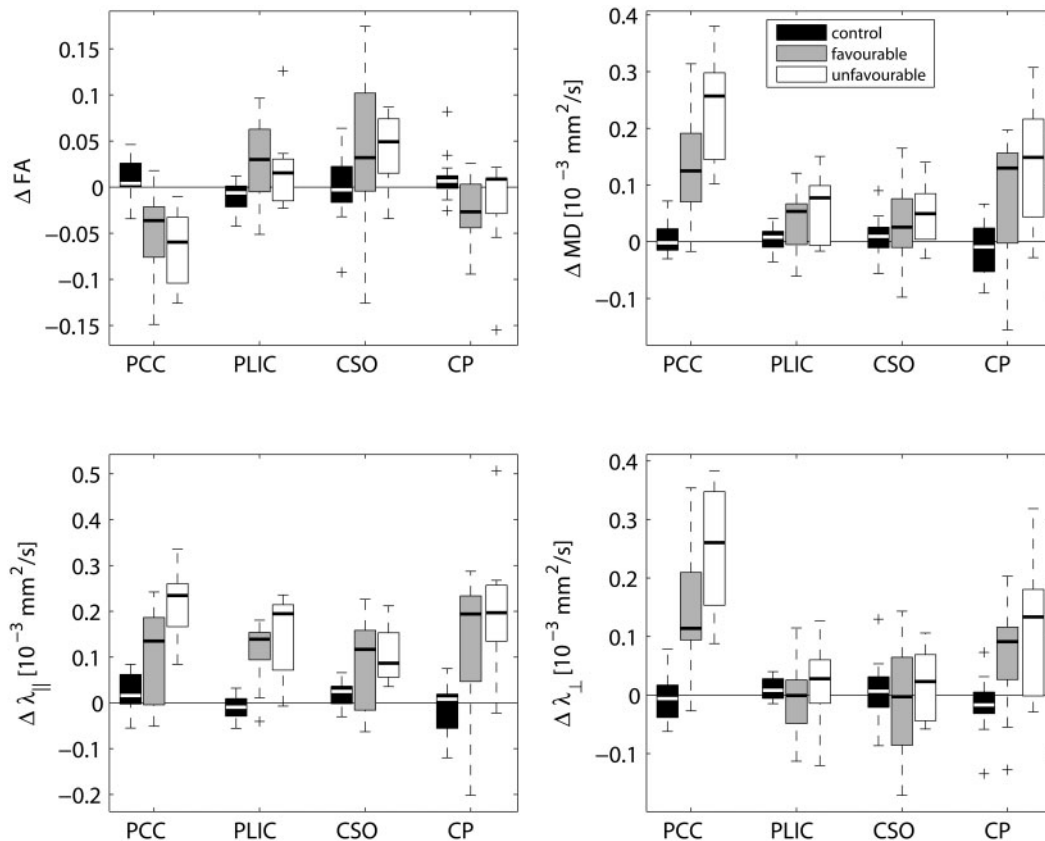


Fig. 5 Longitudinal changes ($\Delta = \text{scan 2} - \text{scan 1}$) of DTI parameters in the four white matter ROIs, grouped according to outcome at 1-year post-injury [dichotomized GOS, unfavourable outcome: GOS = 1–3 ($n = 8$); favourable outcome: GOS = 4–5 ($n = 14$)]. Control values are shown for comparison (follow-up scan, $n = 14$). Boxes represent lower, median (line) and upper quartiles; whiskers show the range of the data excluding outliers (+). PCC = posterior aspect of corpus callosum; PLIC = posterior limb of internal capsule; CSO = centrum semiovale; CP = cerebral peduncle.

Study design

The prospective longitudinal design of this study has several advantages, most importantly enabling the investigation of long-term dynamic evolution of diffusion changes, and the correlation to late clinical outcome. Serial DTI on one or two patients has previously been reported (Arfanakis *et al.*, 2002; Naganawa *et al.*, 2004; Le *et al.*, 2005; Voss *et al.*, 2006), but to our knowledge the present study is the first prospective longitudinal DTI study performed on a group of TBI patients. The study design enabled us to obtain reasonably uniform time intervals between injury-scan, scan-rescan and injury-outcome evaluation. All scans were acquired on the same scanner, and patients received a uniform intensity of rehabilitation following departmental guidelines. Furthermore, to reduce the heterogeneity inherent to clinical TBI studies, we only studied patients with severe TBI. As our patient population represented the most severely injured survivors of TBI (Engberg *et al.*, 2006), our results are however not directly comparable to those of other studies in which patients had milder or mixed injury severity. Importantly, in the present study a large proportion of the patients had sustained secondary insults.

Initial DTI and association with outcome

In the late subacute stage our findings of decreased λ_{\parallel} and increased λ_{\perp} in several white matter ROIs are in line with previous findings (Arfanakis *et al.*, 2002; Le *et al.*, 2005). Recently, animal models of axonal injury versus demyelination have indicated that axonal injury selectively decreases λ_{\parallel} , while demyelination increases λ_{\perp} (Song *et al.*, 2002; Sun *et al.*, 2006). Accordingly, our results could reflect the combination of axonal injury and demyelination, but could also be the result of increased content of isotropic tissue, notably gliosis (Pierpaoli *et al.*, 2001). Regardless of the exact proportionate contribution of these pathological processes, the observed DTI pattern is consistent with Wallerian or Wallerian-like degeneration (Pierpaoli *et al.*, 2001; Thomalla *et al.*, 2004), most likely reflecting consequences of DAI and/or secondary hypoxic–ischaemic injury.

The clinical significance of the measured DTI metrics is highlighted by the correlations between these quantities and long-term functional outcome. At the initial scan, DTI parameters for patients with unfavourable outcome tended to deviate more from control values than for patients with favourable outcome. The strongest correlation with 1 year

GOS was found for FA in CP, which predicted dichotomized 1-year GOS with 76% accuracy and even added predictive accuracy to FIM evaluated at the time of the initial scan. In comparison, conventional MRI variables (e.g. DAI grade) did not add predictive information to FIM, although in this group of severely injured patients we did find a just significant association between DAI grade III and unfavourable outcome. Other studies of patients with even mild TBI have found DTI abnormalities undetected by conventional MRI (Arfanakis *et al.*, 2002; Inglese *et al.*, 2005), clearly indicating that DTI is more sensitive to traumatic white matter injury than conventional imaging. These and the present study did not, however, apply susceptibility-weighted imaging, another MRI sequence which has proven more sensitive to haemorrhagic DAI than standard T2*-weighted sequences (Tong *et al.*, 2003). To determine the prognostic value of DTI, useful in clinical practice, larger studies are clearly needed.

Longitudinal findings—microstructural reorganization?

The 1-year follow-up DTI of 22 of the patients and 14 of the controls revealed interesting changes in the patients during a period of time when the vast majority of them improved considerably in function (median FIM increased from 48 to 113 during the scan interval). If we assume that the observed increase of λ_{\parallel} in various white matter regions does reflect true alterations of tissue microstructure over time, which processes might underlie these late DTI changes? In PCC and CP, the increase of all eigenvalues over time most likely represents accumulation of extracellular fluid as a consequence of progressive structural degradation. In PCC, DAI-related lesions were visible on conventional MRI in the majority of patients, and it may be that with time the filling of cystic spaces by CSF contributes to these alterations. In PLIC and CSO, however, the observed interval increase of λ_{\parallel} was not accompanied by an increase of λ_{\perp} , and so is unlikely to represent a change in extracellular fluid content. In the vast majority of patients the tissue comprised by these ROIs was normal-appearing on conventional MRI.

The changes in CSO should be interpreted with caution because of the limitations of the tensor model in this complex region (see next section). However, the fact that a similar pattern of DTI changes over time was found in the highly homogeneous PLIC argues in favour of true microstructural alterations. One possible interpretation of this interesting finding is that, despite progressive general atrophy, some reorganization of tissue microstructure has taken place during the scan interval. Specifically, late axonal recovery or even axonal regrowth (without concomitant remyelination) could account for the selective increase of λ_{\parallel} and the resulting FA increase. In a recent report including data on one patient who emerged from a minimally conscious state as late as 19 years post-trauma, the authors

found what was interpreted as a transient increase of FA in the cuneus–precuneus area, followed by an FA increase in the cerebellar vermis (Voss *et al.*, 2006). Our findings point towards an inference similar to that suggested by Voss and coauthors, namely that the observed FA increase over time may represent axonal regrowth at late stages following severe TBI. An increasing body of evidence points towards the role of neuroplastic changes as underlying late recovery following TBI (for a review, see Levin, 2003), and our study supports the notion that DTI may serve to probe white matter regeneration *in vivo*. To map the exact brain areas involved in white matter reorganization, future voxel-based analyses of longitudinal DTI data are needed. Using a voxel-based approach one could also investigate whether some relationship exists between DTI changes and brain volume changes over time. However, a major challenge to voxel-based analysis of DTI data is the registration of fibre tracts between mutually heterogeneous brains.

Limitations and possible pitfalls

Brains that structurally change over time pose certain challenges to the interpretation of longitudinal DTI findings. The tensor model is unable to model multiple fibre populations within each voxel, and specifically in complex regions of crossing fibre populations this is an important limitation. For instance, the perpendicular crossing within one voxel of two highly anisotropic fibre populations will lead to a low FA measured in that voxel. If one of these fibre populations degenerates over time, the orientational coherence within the voxel, and hence FA, increases. This major limitation of the tensor model demands cautious interpretation of longitudinal DTI findings in complex regions where fibres intersect, such as the CSO. In this study FA maps did reveal clear inhomogeneities within the CSO that appeared homogeneous on conventional MRI. Therefore we cannot exclude the possibility that the observed increase of FA over time in CSO could be caused by degeneration of one fibre population e.g. of fibres stemming from the corpus callosum. In contrast, the other white matter ROIs, PCC, PLIC and CP are thought to consist of well-defined coherently oriented fibre bundles. This was also suggested by the high control FA values in these ROIs (Table 3) and homogeneous appearance on FA maps. For these reasons we consider it unlikely that this limitation of the tensor model would account for our findings in these regions. Future studies, using more advanced diffusion imaging techniques such as q-ball imaging (Tuch, 2004), may allow modelling of different fibre populations within each voxel.

One important issue, which has already been dealt with, is that of systematic differences in partial voluming. Corpus callosum is particularly prone to partial voluming from neighbouring CSF, and even more so when DTI voxels are larger in the z-direction. As a consequence of progressive callosal thinning following DAI one could anticipate

increased partial voluming in patients, particularly at follow-up. Our results following successive erosion of the PCC could indicate partial voluming of the original ROI. However, differences between patients and controls as well as longitudinal changes remained significant following extensive erosion. As opposed to PCC, which was defined (except anteriorly) by its anatomical borders, the other ROIs were kept distant from neighbouring tissue. Although partial voluming cannot be avoided completely, the anatomical orientation of these ROIs relative to the *z*-direction makes them less susceptible to major influence by partial volume effects.

Systematic group or time differences in data acquisition need to be considered. In the present study, patients and controls were scanned interleaved, and with a similar scan-rescan interval. As we found no trends towards any time effects in the control group, any major influence of scanner drift on our results is considered highly unlikely.

Most patients ($n=25$) needed sedation for the initial scan, while only a few ($n=4$) were sedated for the follow-up scan. The potential influence of propofol sedation on parameters measured by DTI has not been systematically investigated. While any direct effect on tissue microstructure seems theoretically implausible, an indirect effect e.g. through change of body temperature could influence all diffusivities in the same direction. However, a temperature change of more than 8°C would be required to account for the observed changes of up to 20% in the eigenvalues [the diffusion coefficient varies $\sim 2.4\%/^{\circ}\text{C}$ in the physiological temperature range (Le Bihan, 1995)], and obviously, this cannot have occurred. Furthermore, systematic differences between sedated versus non-sedated individuals regarding noise due to motion might cause differential introduction of errors in the tensor computation (Chang *et al.*, 2005). However, we found no tendency towards systematic differences in the DTI parameters measured in sedated versus non-sedated patients. Moreover, diffusivities measured in CSF did not tend to differ between patients and controls or between initial and follow-up scans. This argues against any major confounding of our results by factors related to sedation.

One final limitation of our study relates to the clinical scales used. It would have been desirable to compare individual DTI changes and degree of functional improvement during the scan interval. However, as the distribution of FIM values at follow-up suffered from ceiling effects, this scale did not allow for adequate investigation of such a possible relationship. The Disability Rating Scale (Rappaport *et al.*, 1982) (range 0–29) may have offered less susceptibility to ceiling effects, however this would have been at the expense of reduced sensitivity to the subtle, yet sometimes significant, changes in function within a limited window of recovery. Monitoring clinical progress and outcome in TBI patients is a general and complex problem with a difficult choice between using a set of detailed scales that are consecutively applied as recovery proceeds,

and a single, yet less detailed scale that covers all phases of recovery.

Conclusions

This prospective longitudinal study of severe TBI provides new insight into the evolution of DTI parameters during rehabilitation, and suggests clinical relevance of these quantities to long-term clinical outcome. Our findings indicate microstructural alterations during the chronic stage of severe TBI, which may represent structural reorganization relevant to clinical recovery. DTI non-invasively provides quantitative pathophysiological information *in vivo*, and the prospect of tracking white matter microstructural changes over time holds the promise of measuring neuroplasticity and repair following TBI, which eventually may offer a way of monitoring therapeutic response. Future longitudinal studies are warranted that combine DTI with volumetric measurements and with other MRI modalities, such as spectroscopy, ideally with multiple data acquisitions at shorter time intervals. The potential of DTI as a prognostic marker needs further investigation in larger studies.

Acknowledgements

The authors would like to thank the participants of this study, Henrik K. Mathiesen and Sussi Larsen for skilled MRI acquisition, Hanns Reich for expert anaesthesiological assistance, Klaus Larsen and Kristoffer H. Madsen for statistical help, Arnold Skimminge and Tim Dyrby for advice on data analysis, and the staff at the Brain Injury Unit for experienced clinical rating. This study was supported by a generous grant from the Elsass Foundation.

References

- Arfanakis K, Haughton VM, Carew JD, Rogers BP, Dempsey RJ, Meyerand ME. Diffusion tensor MR imaging in diffuse axonal injury. *Am J Neuroradiol* 2002; 23: 794–802.
- Basser PJ, Mattiello J, Le Bihan D. MR diffusion tensor spectroscopy and imaging. *Biophys J* 1994; 66: 259–67.
- Chan JH, Tsui EY, Peh WC, Fong D, Fok KF, Leung KM, et al. Diffuse axonal injury: detection of changes in anisotropy of water diffusion by diffusion-weighted imaging. *Neuroradiology* 2003; 45: 34–8.
- Chang LC, Jones DK, Pierpaoli C. RESTORE: robust estimation of tensors by outlier rejection. *Magn Reson Med* 2005; 53: 1088–95.
- Chesnut RM, Marshall LF, Klauber MR, Blunt BA, Baldwin N, Eisenberg HM, et al. The role of secondary brain injury in determining outcome from severe head injury. *J Trauma* 1993; 34: 216–22.
- Choi SC, Clifton GL, Marmarou A, Miller ER. Misclassification and treatment effect on primary outcome measures in clinical trials of severe neurotrauma. *J Neurotrauma* 2002; 19: 17–22.
- Engberg AW, Liebach A, Nordenbo A. Centralized rehabilitation after severe traumatic brain injury – a population-based study. *Acta Neurol Scand* 2006; 113: 178–84.
- Gentry LR. Head trauma. In: Atlas SW, editor. *Magnetic resonance imaging of the brain and spine*. 3rd edn., Philadelphia: Lippincott Williams & Wilkins; 2002. p. 1059–98.
- Graham DI, Gennarelli TA. Trauma. In: Graham DI, Lantos PL, editors. *Greenfield's neuropathology*. 6th edn., London: Arnold; 1997. p. 197–262.

- Granger CV, Hamilton BB, Keith RA, Zielesny M, Sherwin FS. Advances in functional assessment for medical rehabilitation. *Top Geriatr Rehabil* 1986; 1: 59–74.
- Greenspan L, McLellan BA, Greig H. Abbreviated Injury Scale and Injury Severity Score: a scoring chart. *J Trauma* 1985; 25: 60–4.
- Huisman TA, Schwamm LH, Schaefer PW, Koroshetz WJ, Shetty-Alva N, Ozsunar Y, et al. Diffusion tensor imaging as potential biomarker of white matter injury in diffuse axonal injury. *Am J Neuroradiol* 2004; 25: 370–6.
- Inglese M, Makani S, Johnson G, Cohen BA, Silver JA, Gonen O, et al. Diffuse axonal injury in mild traumatic brain injury: a diffusion tensor imaging study. *J Neurosurg* 2005; 103: 298–303.
- Jennett B, Bond M. Assessment of outcome after severe brain damage. *Lancet* 1975; 1: 480–4.
- Jones PA, Andrews PJ, Midgley S, Anderson SI, Piper IR, Tocher JL, et al. Measuring the burden of secondary insults in head-injured patients during intensive care. *J Neurosurg Anesthesiol* 1994; 6: 4–14.
- Le Bihan D. Temperature imaging by NMR. In: Le Bihan D, editor. Diffusion and perfusion magnetic resonance imaging. Applications to functional MRI. New York: Raven Press; 1995. p. 181–7.
- Le TH, Mukherjee P, Henry RG, Berman JI, Ware M, Manley GT. Diffusion tensor imaging with three-dimensional fiber tractography of traumatic axonal shearing injury: an imaging correlate for the posterior callosal “disconnection” syndrome: case report. *Neurosurgery* 2005; 56: 189.
- Levin HS. Neuroplasticity following non-penetrating traumatic brain injury. *Brain Inj* 2003; 17: 665–74.
- Levin HS, O’Donnell VM, Grossman RG. The Galveston Orientation and Amnesia Test. A practical scale to assess cognition after head injury. *J Nerv Ment Dis* 1979; 167: 675–84.
- Mac Donald CL, Dikranian K, Song SK, Bayly PV, Holtzman DM, Brody DL. Detection of traumatic axonal injury with diffusion tensor imaging in a mouse model of traumatic brain injury. *Exp Neurol* 2007; 205: 116–31.
- MacKenzie EJ. Epidemiology of injuries: current trends and future challenges. *Epidemiol Rev* 2000; 22: 112–9.
- Marenco S, Rawlings R, Rohde GK, Barnett AS, Honea RA, Pierpaoli C, et al. Regional distribution of measurement error in diffusion tensor imaging. *Psychiatry Res* 2006; 147: 69–78.
- Naganawa S, Sato C, Ishihara S, Kumada H, Ishigaki T, Miura S, et al. Serial evaluation of diffusion tensor brain fiber tracking in a patient with severe diffuse axonal injury. *Am J Neuroradiol* 2004; 25: 1553–6.
- Nakayama N, Okumura A, Shinoda J, Yasokawa YT, Miwa K, Yoshimura SI, et al. Evidence for white matter disruption in traumatic brain injury without macroscopic lesions. *J Neurol Neurosurg Psychiatry* 2006; 77: 850–5.
- Pierpaoli C, Basser PJ. Toward a quantitative assessment of diffusion anisotropy. *Magn Reson Med* 1996; 36: 893–906.
- Pierpaoli C, Jezzard P, Basser PJ, Barnett A, Di Chiro G. Diffusion tensor MR imaging of the human brain. *Radiology* 1996; 201: 637–48.
- Pierpaoli C, Barnett A, Pajevic S, Chen R, Penix L, Varta A, et al. Water diffusion changes in Wallerian degeneration and their dependence on white matter architecture. *Neuroimage* 2001; 13: 1174–85.
- Ptak T, Sheridan RL, Rhea JT, Gervasini AA, Yun JH, Curran MA, et al. Cerebral fractional anisotropy score in trauma patients: a new indicator of white matter injury after trauma. *Am J Radiol* 2003; 181: 1401–7.
- Rappaport M, Hall KM, Hopkins K, Belleza T, Cope DN. Disability rating scale for severe head trauma: coma to community. *Arch Phys Med Rehabil* 1982; 63: 118–23.
- Rugg-Gunn FJ, Symms MR, Barker GJ, Greenwood R, Duncan JS. Diffusion imaging shows abnormalities after blunt head trauma when conventional magnetic resonance imaging is normal. *J Neurol Neurosurg Psychiatry* 2001; 70: 530–3.
- Salmond CH, Menon DK, Chatfield DA, Williams GB, Pena A, Sahakian BJ, et al. Diffusion tensor imaging in chronic head injury survivors: correlations with learning and memory indices. *Neuroimage* 2006; 29: 117–24.
- Schiff ND. Multimodal neuroimaging approaches to disorders of consciousness. *J Head Trauma Rehabil* 2006; 21: 388–97.
- Song SK, Sun SW, Ramsbottom MJ, Change C, Russell J, Cross AH. Demyelination revealed through MRI as increased radial (but unchanged axial) diffusion of water. *Neuroimage* 2002; 17: 1429–36.
- Sun SW, Liang HF, Trinkaus K, Cross AH, Armstrong RC, Song SK. Noninvasive detection of cuprizone induced axonal damage and demyelination in the mouse corpus callosum. *Magn Reson Med* 2006; 55: 302–8.
- Teasdale G, Jennett B. Assessment of coma and impaired consciousness. A practical scale. *Lancet* 1974; 2: 81–4.
- Thomalla G, Glauche V, Koch MA, Beaulieu C, Weiller C, Rother J. Diffusion tensor imaging detects early Wallerian degeneration of the pyramidal tract after ischemic stroke. *Neuroimage* 2004; 22: 1767–74.
- Tong KA, Ashwal S, Holshouser BA, Shutter LA, Herigault G, Haacke EM, et al. Hemorrhagic shearing lesions in children and adolescents with posttraumatic diffuse axonal injury: improved detection and initial results. *Radiology* 2003; 227: 332–9.
- Tuch DS. Q-ball imaging. *Magn Reson Med* 2004; 52: 1358–72.
- Voss HU, Uluc AM, Dyke JP, Watts R, Kobylarz EJ, McCandliss BD, et al. Possible axonal regrowth in late recovery from the minimally conscious state. *J Clin Invest* 2006; 116: 2005–11.

Appendix 2

PAPER II



Long-term global and regional brain volume changes following severe traumatic brain injury: A longitudinal study with clinical correlates

Annette Sidaros^{a,b,c,*}, Arnold Skimminge^{a,d}, Matthew G. Liptrot^a, Karam Sidaros^a, Aase W. Engberg^b, Margrethe Herning^a, Olaf B. Paulson^{a,c,e}, Terry L. Jernigan^{a,c,f}, Egill Rostrup^{a,c,g}

^a Danish Research Centre for Magnetic Resonance, Copenhagen University Hospital, Hvidovre, Denmark

^b Brain Injury Unit, Department of Neurorehabilitation, Copenhagen University Hospital, Hvidovre, Denmark

^c Faculty of Health Sciences, University of Copenhagen, Denmark

^d Department of Informatics and Mathematical Modelling, Technical University of Denmark, Lyngby, Denmark

^e Neurobiology Research Unit, Copenhagen University Hospital, Rigshospitalet, Denmark

^f Laboratory of Cognitive Imaging, Department of Psychiatry, University of California, San Diego, CA, USA

^g Department of Clinical Physiology, Copenhagen University Hospital, Glostrup, Denmark

ARTICLE INFO

Article history:

Received 27 June 2008

Revised 15 August 2008

Accepted 18 August 2008

Available online 4 September 2008

Keywords:

Traumatic brain injury (TBI)

Tensor-based morphometry (TBM)

SIENA

Magnetic resonance imaging (MRI)

Atrophy

ABSTRACT

Traumatic brain injury (TBI) results in neurodegenerative changes that progress for months, perhaps even years post-injury. However, there is little information on the spatial distribution and the clinical significance of this late atrophy. In 24 patients who had sustained severe TBI we acquired 3D T1-weighted MRIs about 8 weeks and 12 months post-injury. For comparison, 14 healthy controls with similar distribution of age, gender and education were scanned with a similar time interval. For each subject, longitudinal atrophy was estimated using SIENA, and atrophy occurring before the first scan time point using SIENAX. Regional distribution of atrophy was evaluated using tensor-based morphometry (TBM). At the first scan time point, brain parenchymal volume was reduced by mean 8.4% in patients as compared to controls. During the scan interval, patients exhibited continued atrophy with percent brain volume change (%BVC) ranging between −0.6% and −9.4% (mean −4.0%). %BVC correlated significantly with injury severity, functional status at both scans, and with 1-year outcome. Moreover, %BVC improved prediction of long-term functional status over and above what could be predicted using functional status at ~8 weeks. In patients as compared to controls, TBM (permutation test, FDR 0.05) revealed a large coherent cluster of significant atrophy in the brain stem and cerebellar peduncles extending bilaterally through the thalamus, internal and external capsules, putamen, inferior and superior longitudinal fasciculus, corpus callosum and corona radiata. This indicates that the long-term atrophy is attributable to consequences of traumatic axonal injury. Despite progressive atrophy, remarkable clinical improvement occurred in most patients.

© 2008 Elsevier Inc. All rights reserved.

Introduction

Traumatic brain injury (TBI) affects about 235 per 100,000 individuals each year in Europe (Tagliaferri et al., 2006) and is a major cause of death and severe morbidity worldwide. In survivors of severe TBI, long-term impairment of consciousness is usually attributable to traumatic axonal injury (TAI, also known as diffuse axonal injury). TAI results from rotational acceleration-deceleration causing shear strain deformation and subsequent disconnection of axons. It is characterized by microscopic lesions scattered throughout

the white matter in particular, with certain regions being characteristically involved, namely the dorsolateral rostral brain stem, the corpus callosum and the subcortical parasagittal white matter. Other regions susceptible to TAI are the internal and external capsules, the deep grey matter, the cerebellum, various tracts in the brain stem and the cerebellar peduncles (Graham et al., 2002). It has been repeatedly observed in animals (Smith et al., 1997; Bramlett and Dietrich, 2002; Rodriguez-Paez et al., 2005) and in humans (Graham et al., 2002) that TBI results in widespread brain atrophy that progresses over several months and perhaps even years post-injury. While it is remarkable that atrophy continues in the chronic phase of TBI, concurrently with clinical recovery, the clinical significance of this late atrophy remains unclear. The progressive degeneration is thought to involve Wallerian degeneration of the white matter tracts disrupted by TAI, but other mechanisms such as apoptosis, inflammation, excitotoxicity, and prolonged hypoperfusion may also play a role (Bramlett and Dietrich,

* Corresponding author. Danish Research Centre for Magnetic Resonance, Copenhagen University Hospital, Hvidovre, Department 340, 2650 Hvidovre, Denmark. Fax: +45 36470302.

E-mail address: annettes@drcmr.dk (A. Sidaros).

2002; Rodriguez-Paez et al., 2005). Characterising the spatial distribution of late atrophy might contribute to the understanding of its pathogenesis.

Few longitudinal MRI studies have quantitatively examined progressive atrophy following TBI and the correlation to clinical parameters. In seven patients with mild to moderate TBI, scanned twice at least 3 months (up to 2.5 years) apart, MacKenzie et al. reported a longitudinal change in brain parenchymal volume of on average -4.16% (relative to -1.49% in healthy controls) and found greater volume loss in patients with initial loss of consciousness than in those without loss of consciousness (MacKenzie et al., 2002). However, in this study early and late atrophy were conflated since the time from injury to the first scan varied between 7 and 430 days. Recently, Trivedi et al. (2007) published a study applying SIENA (Smith et al., 2002) to evaluate global brain volume change between approximately 79 and 409 days post-TBI in 37 patients with TBI ranging from mild to severe. The authors found a change in brain volume of mean -1.43% (relative to $+0.1\%$ in healthy controls), with greater decline in brain volume being associated with longer duration of post-injury coma. However, relation to outcome was not reported.

Characterising quantitatively the regional distribution of late atrophy following TBI is challenging, especially because focal lesions often coexist with diffuse lesions, causing regional distortions in brain shape and intensity inhomogeneities which complicate procedures such as registration and tissue segmentation. Until recently, previous studies on TBI have been based on regions-of-interest (for a review, see Bigler, 2001) or on voxel-based morphometry (Gale et al., 2005; Tomaiuolo et al., 2005; Salmond et al., 2005; Bendlin et al., in press). However, recent advances in computational techniques for nonlinear image registration have allowed for an unbiased and more precise registration that does not necessarily rely on tissue segmentation, thus overcoming some of the major limitations of traditional volumetric approaches. One such approach is tensor-based morphometry (TBM), which determines the deformation field required to warp the early image to match the late image within subject (or in cross-sectional studies, the deformation field required to warp the image to a study-specific template). Regional volume change is quantified by taking the Jacobian determinant at each voxel (Ashburner et al., 2000). One cross-sectional TBM study on TBI was very recently published (Kim et al., 2008). The population consisted of 29 patients with moderate to severe TBI, scanned once at least 3 months (ranging between 4 months and 27.5 years) following injury. The authors found localized volume loss most prominently in the thalamus, the midbrain, the corpus callosum, the cingulate cortex, and the caudate. Significant volume increase was found mainly in the ventricles. However, as this study was not based on serial scans, and as the time from injury to MRI varied considerably between patients, no conclusions could be drawn about the time course of the structural changes.

In the present prospective longitudinal study, we examined the morphological changes occurring between two time points, approximately 8 weeks and 12 months post-injury, in 24 patients with severe TBI, comparing them to 14 healthy matched controls scanned with a similar time interval. We used SIENA to provide an estimate of global atrophy between scans, and TBM to investigate the regional distribution of late volume change. Additionally we used SIENAX (Smith et al., 2002) to estimate global atrophy occurring before the first scan time point, in order to compare this with the late atrophy. We hypothesized that the most pronounced late volume change would be found within regions susceptible to TAI (listed at the beginning of this introduction) as well as along the affected white matter tracts (as a consequence of secondary Wallerian degeneration). Further, we expected that the extent of global brain volume change from first to second scan would be larger in patients with longer duration of coma/post-traumatic amnesia and with poorer functional status and outcome.

Materials and methods

Subjects

Twenty-six adult patients with severe TBI were evaluated for this study. As two patients were subsequently excluded because of motion artefacts in the MR images, the final TBI group comprised 24 patients. Fourteen healthy control subjects were selected to match the patient group with respect to age, sex and education. Both patients and controls had two MR scans with an interval of 345 ± 42 days (mean \pm SD). Group comparisons of age, sex, education and scan interval are listed in Table 1.

Patients were recruited from the Brain Injury Unit at Copenhagen University Hospital, Hvidovre, Denmark, to which they were admitted for subacute rehabilitation. Patients were referred from neuro-intensive units, and admitted for rehabilitation only if Glasgow Coma Scale score (GCS; Teasdale and Jennett, 1974) was still subnormal after cessation of sedation. Severe TBI was defined as a post-resuscitation GCS < 8 measured within 24 h post-injury and prior to the initiation of paralytics or sedatives. Patients were excluded from the present study if they had any previous history of TBI or other neurological disorder, if contraindications to MRI or to sedation during MRI were present, or if the first MRI could not be performed within 12 weeks post-trauma for safety or practical reasons. Controls had no history of significant TBI or other neurological disorder.

The study was approved by the local Scientific Ethics Committee (KF 01-038/03), meeting criteria of the Helsinki Declaration. Informed consent was obtained from the participants or, for patients with impaired consciousness, from next of kin.

Clinical assessments

For all patients, clinical data were documented in medical files, and ratings were performed by trained staff, neurologists, and neuropsychologists. Cause of trauma was either motor vehicle accident ($n=16$), fall ($n=7$) or assault ($n=1$). Accidents with any direct involvement of a motor vehicle (including pedestrian or bicyclist hit by car) were classified as motor vehicle accident. Neurosurgery was defined as surgery that involved craniotomy, excluding insertion of ICP monitoring devices. The number of days from TBI until GCS > 8 was registered as a measure of coma duration, and the Galveston Orientation and Amnesia Test (Levin et al., 1979) was repeatedly applied to establish duration of post-traumatic amnesia (PTA). Both were regarded as measures of injury severity. The Functional Independence Measure (FIM; Granger et al., 1986) was documented regularly, including at both scan time points (sum score ranging from 18 indicating "total assist", to 126 indicating "complete independence"). Functional outcome at ~ 12 months post-TBI was evaluated using the 8-point Glasgow Outcome Scale Extended (GOS-E; Wilson et al., 1998), ranging from 1=dead to 8=good recovery (upper). For dichotomized outcome, the commonly used division into unfavourable outcome (GOS-E=1–4) and favourable outcome (GOS-E=5–8) was applied, distinguishing whether or not patients were able to live independently.

Image acquisition

All patients and controls were scanned on the same 1.5 T MRI scanner (Magnetom Vision; Siemens Medical Solutions, Erlangen, Germany) using a standard circular-polarized head coil. During the study period, MRI sessions for patients and controls were interleaved in time, and no major upgrades were carried out on the scanner during the study.

A 3D sagittal T1-weighted sequence (MPRAGE, TR/TE/TI=13.5/7/100 ms, flip angle 15° , isotropic 1 mm resolution) was acquired in all

Table 1
Group comparisons of demographics and scan interval

	Patients (n=24)	Controls (n=14)	Group differences
Age, at scan 1 (years) [mean (SD)]	33.2 (13.5)	31.2 (8.1)	$P > 0.5^a$
Sex: M/F	18/6	9/5	$P > 0.7^b$
Education (years) [mean (SD)]	13.3 (3.1)	13.7 (2.7)	$P > 0.6^a$
Scan interval (days) [mean (SD)]	343 (47)	348 (30)	$P > 0.6^b$

^a Independent-samples *t*-test.^b Fishers Exact test.

subjects at both scan time points. For patients, additional conventional sequences included: axial T2-weighted images (spin-echo, TR/TE=5400/99 ms, 27 contiguous, 5 mm thick slices, 0.5×0.5 mm in-plane resolution), coronal T2*-weighted gradient-echo images (TR/TE=544/15 ms, 34 contiguous, 5 mm thick slices, 0.9×0.9 mm in-plane resolution), axial and sagittal FLAIR (TR/TE/TI=9000/110/2500 ms, 34 contiguous, 5 mm thick slices, 0.9×0.9 mm in-plane resolution). All the structural images were evaluated by a neuroradiologist (M.H.) for identification and classification of lesions.

All patients were referred for the first MRI for clinical purposes. The majority of patients ($n=19$) were sedated for this scan, since they were unable to cooperate due to decreased level of consciousness or cognitive impairment. Intravenously administered propofol was used for sedation, and patients were monitored by anaesthesiology staff. Oxygen supply and mechanical ventilation were provided when necessary.

For the follow-up scan, subjects were repositioned as close as possible to their position in the previous scan. For ethical reasons patients were sedated only if a follow-up MRI was requested for clinical purposes and patients were unable to cooperate for MRI. While 4 patients were sedated for the follow-up MRI, 20 were fully cooperative without sedation. Two additional non-sedated patients were excluded from this study due to motion artefacts in the follow-up images. All the remaining images were judged of good quality.

Table 2
Clinical characteristics and global brain volume results for the 24 patients

Patient no.	Age at scan1 (years)	Sex	Cause of trauma	Neurosurgery	Duration of coma (days)	Duration of PTA (days)	TBI to scan1 (days)	TAI grade ^a	Focal lesions ^b	FIM at scan1	FIM at scan2	GOS-E at ~1 year	BPV at scan1	%BVC
1	23	F	Fall	-	>FU	>FU	58	2	-	18	18	2	1406	-9.42
2	21	F	MVA	+	12	39	64	2	+	79	117	4	1536	-5.29
3	34	M	MVA	-	126	>FU	81	3	-	18	30	3	1471	-8.80
4	40	F	Fall	+	9	>FU	64	2	+	18	20	3	1263	-7.02
5	40	M	Assault	-	4	88	50	0	-	87	122	6	1405	-1.16
6	60	M	Fall	+	21	>FU	46	2	+	34	35	3	1543	-7.21
7	28	M	MVA	-	24	66	69	3	-	122	125	8	1595	-4.08
8	54	M	Fall	-	14	119	45	2	+	60	125	5	1429	-1.80
9	23	M	MVA	+	18	47	81	2	+	117	124	6	1584	-2.56
10	24	M	MVA	-	1	39	36	1	-	93	125	5	1549	-0.62
11	65	M	Fall	-	3	39	42	1	+	116	120	6	1449	-2.60
12	31	M	MVA	+	7	48	40	2	+	38	102	5	1609	-6.28
13	37	M	MVA	+	14	40	69	1	+	117	122	7	1535	-2.74
14	22	M	MVA	-	7	31	55	2	-	120	125	7	1587	-1.78
15	19	M	MVA	-	2	23	37	1	-	113	124	7	1673	-1.28
16	41	F	MVA	+	10	65	41	2	+	55	113	5	1537	-3.73
17	26	M	MVA	-	22	65	77	1	+	106	124	6	1500	-1.87
18	22	M	MVA	-	9	178	79	2	-	18	103	4	1543	-2.45
19	23	M	MVA	-	11	107	55	3	+	23	111	4	1515	-5.58
20	18	F	MVA	-	15	66	62	3	+	24	105	4	1443	-2.69
21	40	M	Fall	+	10	84	48	2	+	100	117	5	1484	-1.63
22	53	M	Fall	+	5	171	39	3	+	18	111	5	1443	-6.80
23	27	M	MVA	-	10	77	47	2	-	49	113	5	1498	-2.98
24	26	F	MVA	-	4	58	29	2	-	59	126	8	1557	-4.75

MVA = motor vehicle accident; >FU = exceeds ~1 year follow-up; PTA = post-traumatic amnesia; FIM = functional independence measure; GOS-E = Glasgow outcome scale, extended; BPV = brain parenchymal volume; %BVC = percent brain volume change. See text for details.

^a According to location of microhaemorrhages on T2*-W images (0 = none, 1 = subcortical only, 2 = callosal, 3 = brainstem).^b Parenchymal lesions excluding TAI (mainly contusions).

Image processing

Preprocessing: global volume changes

The 3D T1-weighted images were first reoriented manually to the anterior–posterior commissure (AC–PC) orientation, and resliced to 1 mm³ voxels. Intensity normalisation within and between scans was performed using N3 and MRI Normalise from the MNI toolbox (www.bic.mni.mcgill.ca).

We used SIENA, available in the FSL 3.3 toolbox (www.fmrib.ox.ac.uk/fsl), to evaluate global brain volume change between the two scan time points for each subject. Additionally we applied SIENAX (also within FSL) for an estimation of brain parenchymal volume, normalized for head size, at the first scan time point. These methods have been described in detail elsewhere (Smith et al., 2001; Smith et al., 2002). In brief, SIENA starts by extracting brain and skull images from the two-timepoint whole-head input data. The two brain images are then aligned to each other (using the skull images to constrain the registration scaling); both brain images are resampled into the space halfway between the two. (This intermediate result was later entered into the TBM analysis, see below). Then segmentation is carried out in order to find brain/non-brain edge points. Perpendicular edge displacement, between the two time points, is estimated at these edge points, and the mean edge displacement is converted into a global estimate of percentage brain volume change (%BVC) from first to second scan. Measurement error of %BVC is reported to be approximately ±0.20% (Smith et al., 2002).

In SIENAX, brain and skull images are extracted, and the brain image is affine-registered to an MNI standard template (using the skull image to determine registration scaling, to be used as a normalisation for head size). Next, segmentation with partial volume estimation is carried out in order to calculate the total volume of brain tissue: normalised brain parenchymal volume (BPV).

Preprocessing: regional volume changes

We used TBM to evaluate the regional distribution of brain volume change between the two scan time points. Following the intensity

normalisation and initial registration steps from SIENA, described above, we then applied the high dimensional warping available in the SPM2 'Deformation toolbox' (www.fil.ion.ucl.ac.uk/spm) to these images. This TBM analysis estimates the deformation field that would warp the early T1 image to match the late T1 image within each subject (Ashburner et al., 2000). From this deformation field the amount of regional expansion or contraction is extracted by taking the Jacobian determinant at each point, thus generating a Jacobian determinant map in alignment with the late image. Following logarithmic transformation of the Jacobian determinant values (Leow et al., 2007) regional contraction corresponded to positive values and regional expansion to negative values. The non-skull-stripped follow-up T1 images were then normalized in SPM2 to the MNI standard space, and this transformation was applied to the log-transformed Jacobian determinant maps. Finally, these images were smoothed with an 8 mm Gaussian kernel.

Statistical analysis: global volume changes

The outputs from SIENA and SIENAX, %BVC and BPV respectively, were analysed group-wise using the non-parametric Mann Whitney *U*-test. Correlation analyses with clinical and conventional imaging variables were performed using the Spearman's rho. Prediction of

functional status at follow-up by BPV and FIM at the first scan and % BVC was assessed using linear regression.

Statistical analysis: regional volume changes

For statistical analysis of TBM results, we used a permutation test (Randomise, available in FSL). Unlike the general linear model, permutation tests do not rely on the assumption that data are normally distributed (Nichols and Holmes, 2001). To compare patients and controls, a design matrix was constructed that included the nuisance variables age, sex, education and scan interval. Calculations were performed voxel-wise with 10,000 permutations, and a whole-brain correction for multiple comparisons was applied using a false discovery rate (FDR) of 0.05. Clusters with a radius of <2 mm (volume <33.5 mm³) were rejected for display purposes. Anatomy atlas tools available in FSL were used to help identify anatomical regions.

Results

Global volume changes

Already at the first scan time point ~8 weeks post-trauma, normalized BPV, derived from SIENAX, was 8.4% lower in patients

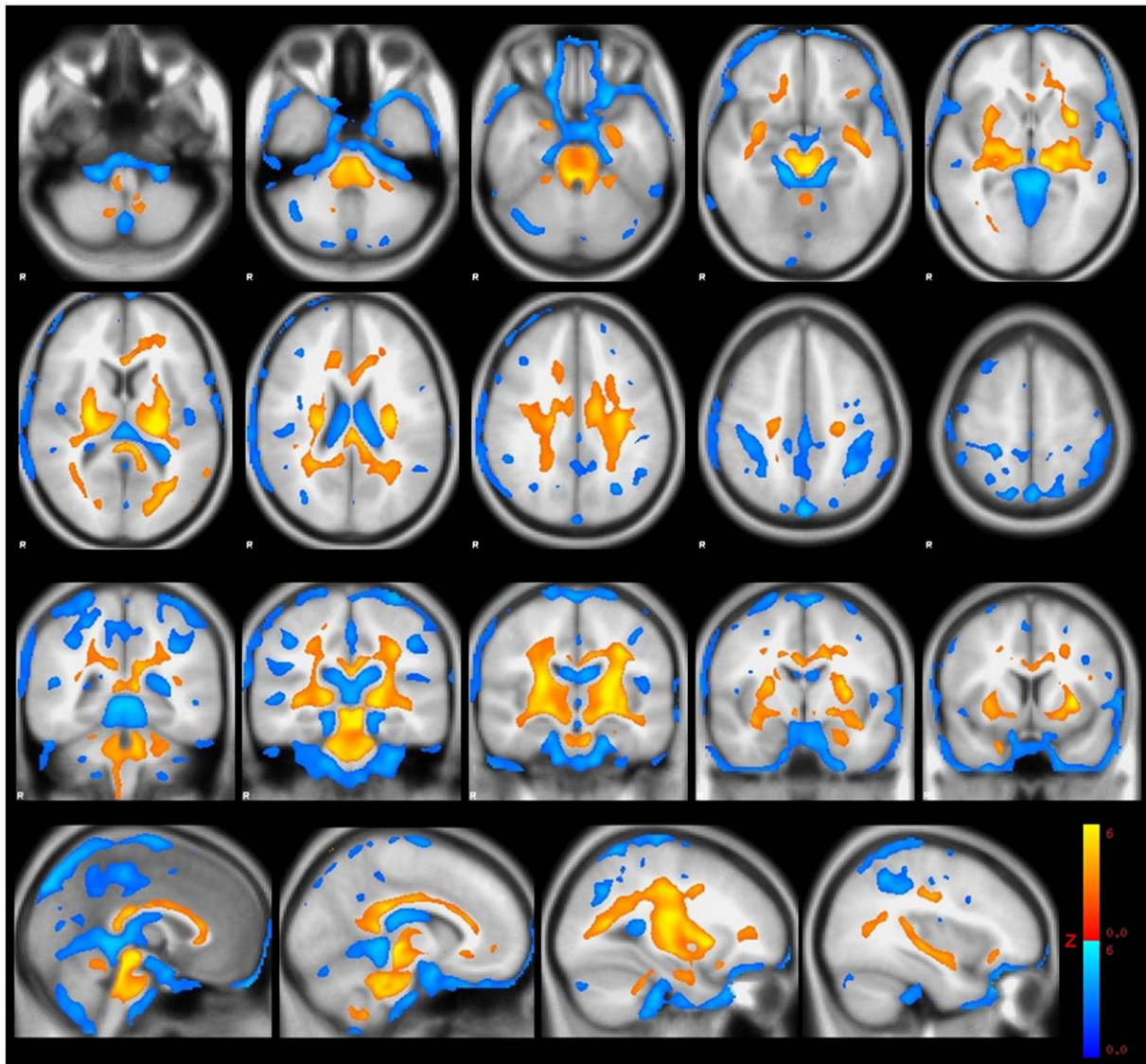


Fig. 1. Regions of significant volume changes in TBI patients between ~8 weeks and ~12 months post-injury, as compared to controls, thresholded at false discovery rate (FDR) 0.05 (clusters of <33.5 voxels rejected). Longitudinal volume reduction is coded red/yellow, volume expansion is coded blue. Results are overlaid onto the MNI standard template.

than controls (mean±SD: 1506 ml±85 ml vs. 1645 ml±85 ml, $P<0.0001$, Mann–Whitney U -test).

During the ~11 months scan interval %BVC, derived from SIENA, ranged between -0.6% and -9.4% (mean -4.0%, median -2.9%) in patients, compared to between -0.9% and +0.3% (mean -0.18%, median -0.13%) in controls (patients vs. controls: $P<0.000001$, Mann–Whitney U -test).

For each patient, Table 2 lists BPV and %BVC together with selected demographic, clinical and conventional imaging variables. There was a significant correlation between BPV and %BVC when all subjects were considered ($r=0.57$, $P<0.001$, Spearman's rho); however this correlation was not significant for either patients or controls separately. No significant correlations were found between %BVC and scan interval, age or gender. All but one patient had microhaemorrhages on T2*-weighted images, indicating TAI. Graded according to location (Graham et al., 2002), TAI grade correlated with %BVC ($r=-0.59$, $P<0.01$, Spearman's rho), but not with BPV.

To check for the robustness of SIENAX for these traumatized brains, we also applied SIENAX on the follow-up scans, again comparing to controls, and calculated the differences (in %) between BPV at the first and second scan (data not shown). These values were roughly comparable to the %BVC derived from SIENA, indicating that the estimates from SIENAX were reliable, at least as rough estimates of BPV.

Regional volume changes

TBM, with whole-brain correction for multiple comparisons, identified regions with significant volume loss or volume expansion over time in patients as compared to controls. Fig. 1 shows the differences between patients and controls using an FDR of 0.05. At this threshold, a large coherent cluster of volume loss extended from the brain stem and cerebellar peduncles and bilaterally through the thalamus, internal capsule, external capsule, putamen, inferior and superior longitudinal fasciculus, corpus callosum (genu, body and splenium) and corona radiata. Small clusters of significant volume loss were also found, mainly in the cerebellum and in the frontal lobes. Significant longitudinal volume expansion in patients compared to controls was found in the ventricles and scattered in the subarachnoidal space (with a large cluster at the fundus of the intraparietal sulcus). In general the pattern of volume loss as well as volume expansion was relatively symmetric. The statistical strength of volume loss, reaching its maximum in the tectum mesencephali ($Z=6.86$), exceeded that of volume expansion (maximum $Z=5.07$). Details of significant volume loss are found in Table 3.

Table 3

Clusters of significant volume loss in patients compared to controls at false discovery rate (FDR) 0.05

	Anatomical region	Tissue type	Side	MNI coordinates of voxel of maximum significance			PeakZ	Cluster size (voxels)
				x	y	z		
1	Large coherent cluster in the brain stem and cerebellar peduncles, extending bilaterally through internal capsule, thalamus, putamen, external capsule, inferior and superior longitudinal fasciculus, corpus callosum, corona radiata	WM+GM	L/R	-1	-31	-16	6.86	129013
2	Cerebellum	GM	L	-8	-50	-54	4.06	963
3	Frontal orbital cortex	GM	L	-29	18	-18	3.54	736
4	Cerebellum	GM	R	10	-62	-52	3.74	508
5	Frontal orbital cortex	GM	R	9	20	-21	3.04	301
6	Cerebellum	GM	R	25	-53	-23	3.05	212
7	Frontal lobe, subcortical WM	WM	L	-43	10	18	3.13	178
8	Frontal lobe, cortex/subcortical WM	WM+GM	L	-42	29	2	3.77	148
9	Middle temporal gyrus	GM	L	-60	-56	10	3.40	122
10	Superior corona radiata	WM	R	23	8	38	2.72	110
11	Lateral occipital cortex	GM	L	-50	-77	13	3.06	61

Coordinates of each cluster maximum are reported. Cluster maximum for cluster 1 corresponds to tectum mesencephali. GM = grey matter; WM = white matter; L = left; R = right.

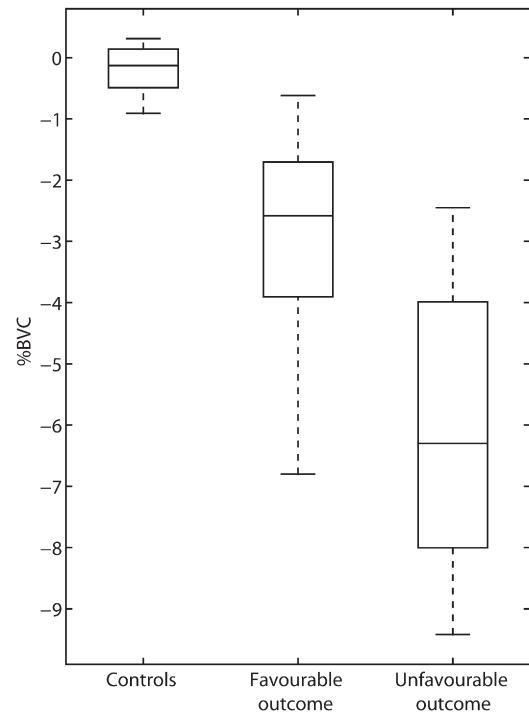


Fig. 2. Box and whiskers plot of %BVC in patients with favourable ($n=16$) and unfavourable ($n=8$) outcome ($P<0.01$, Mann–Whitney U -test). Control values ($n=14$) are displayed for comparison. %BVC = percent brain volume change.

Correlation with clinical variables

Injury severity

BPV at the first scan correlated significantly with duration of PTA ($r=-0.59$, $P<0.01$, Spearman's rho), however not with duration of coma. Both duration of coma and PTA correlated significantly with %BVC between the two scan time points ($r=-0.45$, $P<0.05$ and $r=-0.53$, $P<0.01$, respectively, Spearman's rho).

Functional status and outcome

BPV at the first scan correlated significantly with concomitantly evaluated FIM ($r=0.46$, $P<0.05$, Spearman's rho). Also %BVC between the two scan time points was significantly correlated with FIM evaluated both at the first and at the second scan time point ($r=0.62$, $P=0.001$ and $r=0.68$, $P<0.001$ respectively, Spearman's rho).

With respect to 1-year outcome, BPV at the first scan did not differ significantly between favourable and unfavourable outcome groups (Mann–Whitney *U*-test). However, BPV correlated significantly with the full scale GOS-E ($r=0.48$, $P<0.05$). Late volume change (%BVC between the two scan time points) was significantly different between outcome groups (Fig. 2; $P<0.01$, Mann–Whitney *U*-test) and also correlated significantly with the full scale GOS-E ($r=0.55$, $P<0.01$).

In a linear regression model with FIM at the follow-up scan as the dependent variable, FIM at the initial scan significantly predicted late FIM, as one would expect ($P<0.001$). Adding BPV at the first scan did not improve the model. However, adding %BVC to the model improved prediction of late FIM (increment $F=4.7$ and parameter estimate $P<0.001$ for %BVC), with pronounced late atrophy predicting lower FIM at follow-up, and vice versa.

Discussion

We studied late atrophy occurring between ~8 weeks and ~12 months following severe TBI, using TBM to evaluate the regional distribution of volume change and SIENA to estimate individual global atrophy. Additionally, SIENAX was used to estimate global atrophy occurring prior to the first time point. In patients, as compared to controls, significant atrophy during the scan interval was found in: a large coherent cluster in the brain stem and cerebellar peduncles extending bilaterally through the thalamus, internal capsule, external capsule, putamen, inferior and superior longitudinal fasciculus, corpus callosum and corona radiata; and in smaller clusters mainly in the cerebellum and the frontal lobe. At ~8 weeks post-injury brain volume was already reduced by mean 8.4% in patients as compared to controls, but an additional mean 4.0% (median 2.9%) volume loss occurred in patients during the scan interval. The magnitude of this late volume loss was significantly correlated with injury severity (duration of coma and PTA), with FIM at both scan time points, and with 1-year GOS-E.

Global volume changes

We found a highly significant decline in brain volume during the late subacute and chronic phases of TBI. This is in agreement with the recent study by Trivedi et al. also using SIENA (Trivedi et al., 2007). While our patient population represented very severely injured survivors of TBI (Engberg et al., 2006), Trivedi studied a population of mixed injury severity ranging from mild to severe TBI. This probably explains why we found a greater decline in brain volume (mean -4.0%, median -2.9%) compared to their study (mean -1.43%). However, part of this difference may also be due to the fact that the time from TBI to the first scan was slightly shorter in our study (55 days, range=29–81 days compared to 79 days, range=39–109 days).

All but one patient in the present study had microhaemorrhages on conventional T2*-weighted images, indicating the presence of TAI. In accordance with the view that general atrophy post-TBI is mainly caused by TAI, we found that TAI grade, as evaluated on T2*-weighted images, correlated with %BVC. However, a similar correlation could not be found for initial atrophy estimated by BPV.

To relate longitudinal decline in brain volume to the early atrophy occurring between the time of injury and the first scan time point (the first ~8 weeks post-injury), we used SIENAX, comparing brain volume in patients at the first scan time point to that of the controls. With SIENAX we found that BPV in patients at the first scan time point was on average 8.4% smaller than BPV in controls. While this should be regarded as a fairly rough estimate (see subsection Limitations), it clearly indicates that the rate of decline in brain volume is much higher in the acute/early subacute phase post-trauma than at later stages. Obviously our study does not allow further conclusions to be made about the time course of atrophy following TBI, as we cannot know whether the late atrophy occurred gradually during the whole scan interval, or whether the degenerative process ended already after

a few months. However, animal studies suggest a gradual volume decrease up to at least 1 year post-trauma (Rodriguez-Paez et al., 2005). Future human studies with multiple scan time points should be conducted to better characterize the time course of the progressive atrophy following TBI.

Regional volume changes

The pattern of late atrophy observed in patients as compared to controls corresponds well to those regions known from neuropathological and biomechanical studies to be susceptible to TAI or to consequences of TAI (Graham et al., 2002; Maxwell et al., 1997). The continuous involvement of the corticospinal tract from the corona radiata through the posterior limb of the internal capsule, crus cerebri and pons is likely to represent Wallerian degeneration secondary to TAI. These results suggest that the progressive atrophic process following TBI is a direct consequence of TAI. The highest level of significance was found for the tectum mesencephali, which is one area particularly susceptible to TAI.

The results of the present study are mainly in agreement with the findings of the single available TBM study on TBI (Kim et al., 2008). When comparing these two studies, one should bear in mind that while we investigated the regional distribution of late atrophy only, the study by Kim et al. was not longitudinal and therefore did not distinguish between early and late atrophy. In both studies, the statistical strength of volume loss was generally higher than that of volume expansion. As concluded by Kim et al. this suggests that using ventricular enlargement to indirectly measure atrophy is not the most sensitive measure. Like in the study by Kim et al. we found significant volume loss (at FDR 0.05) in the brainstem, thalamus, corpus callosum, putamen and cerebellum. However, the volume loss was more widespread in our study and included the entire corticospinal tract from corona radiata to pons as one coherent cluster. Additionally we found significant volume loss in the external capsule, inferior and superior longitudinal fasciculus and in the cerebellar peduncles. Unlike Kim et al. we did not find volume loss in the caudate. While in both studies significant volume expansion was found in CSF, Kim et al. also found apparent volume expansion in some white matter areas including the internal capsule, which they interpreted as secondary to heavy atrophy of surrounding areas.

Some of the discrepancies between the present study and the study by Kim et al. are likely to be due to differences in injury severity, as Kim et al. included patients with both moderate and severe TBI. It is possible that there are also some differences in the regional distribution of the atrophy occurring in the acute/early subacute phase compared to the late atrophy in the late subacute/chronic phase. One should also bear in mind the somewhat random nature of the injuries in the individual TBI patients, which inadvertently is another source of variability between studies. Finally, discrepancies may also be related to methodological differences in the two studies. Importantly, in the cross-sectional study by Kim et al., every brain was warped to a population-specific template based on both controls and patients, while in our longitudinal study warping was performed within subject.

In a very recent longitudinal study, Bendlin and co-workers (Bendlin et al., *in press*) measured regional volume changes in patients with moderate TBI using voxel-based morphometry (VBM). Their study design is somewhat similar to ours, but differs in some key elements. Firstly, there is a difference in injury severity of the TBI patients. Secondly, as opposed to VBM, TBM is based on intra-subject volume change. Thirdly, VBM relies on segmented white matter and grey matter maps, whereas our TBM analysis has the advantage of not relying on tissue segmentation (in our dataset tissue segmentation tended to misclassify focal lesions, see subsection Limitations). Despite these differences, our results are largely in agreement with the findings of Bendlin et al. who reported longitudinal volume losses

in corona radiata, corpus callosum, internal and external capsules, superior and inferior longitudinal fasciculus, cingulum, inferior fronto-occipital fasciculus, corticospinal tract, cerebellar peduncles, thalamus, and pallidum, as well as small areas with volume loss in the cerebellar white matter, right post-central and precentral gyri, supplementary motor area, and putamen.

Clinical significance of progressive atrophy

One of the advantages of the prospective longitudinal design used in this study is that it allowed us not only to scan the patients with a uniform time interval, but also to collect clinical data at predefined time points, including outcome evaluation about 1 year post-injury. We found several correlations between clinical variables and the degree of late global atrophy. In agreement with the study by Trivedi et al., we found a significant correlation between duration of coma and %BVC, although duration of coma was defined slightly differently in the two studies. Another indicator of injury severity, duration of PTA, also correlated significantly with %BVC in our study. These findings are not surprising given that the extent of TAI is likely to be a major determinant of %BVC as well as of the severity of impairment of consciousness reflected by duration of coma or PTA.

Furthermore, we found significant correlations between %BVC and functional status (as evaluated by FIM) at both scan time points, and between %BVC and 1-year GOS-E. These findings, however, do not necessarily imply that late volume loss *per se* is a determinant of functional status and outcome. It might be that the extent of TAI is the major determinant of both %BVC and clinical function including long-term clinical outcome. The consequences of TAI may involve cellular processes other than atrophy, which also might account for some of the clinical consequences following TAI.

Using linear regression, we determined which parameters predicted functional status at the follow-up scan. We found that inclusion of %BVC dramatically improved upon the predictive performance offered by the ~8 week FIM values alone. Thus, a higher rate of volume loss during the scan interval was associated with poorer functional status at follow-up, controlling for the degree of functional impairment present at the first scan time point. It should be noted, however, that the four most severely injured patients (patient no. 1, 3, 4 and 6 in Table 2, who all had PTA > 1 year) stood out from the rest, causing the correlation between %BVC and FIM at ~12 months to be driven mainly by these subjects. Larger studies are clearly needed to confirm the observed relationship between atrophy and functional impairment.

For the majority of patients, decline in brain volume occurred concurrently with remarkable clinical improvement, as for example reflected in the median FIM-value which increased from 60 (18–122) at the time of the first scan to 117 (18–126) at the second scan. This apparent paradox indicates that some regenerative processes must occur despite the macroscopic degeneration. From animal studies evidence is accumulating that neuroplastic changes, such as axonal sprouting and synaptic reorganization, accompany functional recovery following TBI (reviewed e.g. by Levin 2003; Albenis and Janigro 2003, Dancause 2006) and may even be enhanced by pharmacological procedures (see e.g. Priestley 2007). In humans, using diffusion tensor imaging, we recently found that diffusion abnormalities following severe TBI, supposedly reflecting disruption of axonal micro-architecture, partly normalise during clinical recovery, particularly in patients with good outcome (Sidaros et al., 2008). Metabolite abnormalities, as measured by MR proton spectroscopy, also have been found to recover over time to near normal levels in good outcome patients (Holshouser et al., 2006; Signoretti et al., 2008).

Limitations

The use of SIENAX is based on the assumption that brain volume of the patients prior to injury was comparable to that of the controls.

Since the groups were matched with respect to age, sex and education, this may be a reasonable approximation. Even if it had been feasible to acquire another MRI in the very acute phase following trauma, oedema would have greatly confounded longitudinal volume comparisons.

In principle, clearing of brain oedema between scans could be responsible for an apparent loss of brain volume over time. However, we found no radiological evidence of oedema at the first MRI (evaluated on T2-weighted and FLAIR images), consistent with the experience that oedema resolution usually occurs within the first four weeks post-injury, i.e. before the first scan time point of this study. Furthermore, the fact that BPV was found to be substantially lower in patients than controls at the first scan time point, strongly argues that oedema had resolved at that point and thus did not mediate the observed longitudinal decline in brain volume.

Grey matter/white matter segmentation tended to misclassify focal lesions as grey matter, regardless of original tissue type. This prevented us from studying grey and white matter atrophy separately. However, lesioned tissue was never misclassified as CSF, and the sum of grey matter and white matter volume estimates, derived from SIENAX, were therefore regarded as valid estimates of BPV.

One limitation related to voxel-wise morphometric approaches such as TBM is that the sensitivity to areas with high anatomical variability between subjects, such as cortical gyri and sulci, is less than to areas exhibiting little inter-subject variability. In a TBI population, the correct warping of cortical areas is even further complicated by the occurrence of focal lesions, which are often cortical in location. Therefore, we cannot exclude the possibility that the observed relative sparing of cortical areas, in terms of late atrophy, could be a false-negative result. On the other hand, we did not expect cortical atrophy to be a prominent feature in comparison with white matter atrophy, because local cortical atrophy due to focal lesions would vary in location between patients and thus be unlikely to emerge as significant in a voxel-wise group analysis. The possibility of more widespread cortical thinning, e.g. secondary to TAI with retrograde degeneration, would probably be below the limit of detection by TBM. Future studies, using for example cortical thickness mapping, might elucidate a possible cortical involvement in the degenerative process following TBI.

Finally, another limitation of our study is that we did not acquire MRI at more than two time points. Future studies using multiple data acquisitions at shorter time intervals would allow for a more detailed description of the time course of atrophy following TBI.

Conclusions

In this prospective longitudinal study of late volume changes following severe TBI we have demonstrated that the most pronounced atrophy is found in regions susceptible to TAI or to consequences of TAI, suggesting that TAI is a major factor responsible for late degeneration. We have further shown associations between the extent of global atrophy and clinical parameters, including duration of coma and PTA, functional status and 1-year outcome. Interestingly, in most patients these long-term degenerative changes occurred concurrently with functional improvement, suggesting that macroscopic tissue loss is less important than supposedly microscopic neuroplastic processes in determining clinical function.

Acknowledgments

We wish to thank the participants of this study and the staff at the Brain Injury Unit for experienced clinical rating. We are grateful to Henrik K. Mathiesen and Sussi Larsen for skilled MRI acquisition, Hanns Reich for expert anaesthesiological assistance, William Baaré for advice on data analysis, and Kristoffer H. Madsen for statistical help. This study was supported by a generous grant from the Elsass Foundation.

References

- Albensi, B.C., Janigro, D., 2003. Traumatic brain injury and its effects on synaptic plasticity. *Brain Inj.* 17 (8), 653–663.
- Ashburner, J., Andersson, J.L., Friston, K.J., 2000. Image registration using a symmetric prior – in three dimensions. *Hum. Brain Mapp.* 9 (4), 212–225.
- Bendlin, B.B., Ries, M.L., Lazar, M., Alexander, A.L., Dempsey, R.J., Rowley, H.A., et al., in press. Longitudinal changes in patients with traumatic brain injury assessed with diffusion-tensor and volumetric imaging. *Neuroimage*. doi:10.1016/j.neuroimage.2008.04.254.
- Bigler, E.D., 2001. Quantitative magnetic resonance imaging in traumatic brain injury. *J. Head Trauma Rehabil.* 16 (2), 117–134.
- Bramlett, H.M., Dietrich, W.D., 2002. Quantitative structural changes in white and gray matter 1 year following traumatic brain injury in rats. *Acta Neuropathol.* 103 (6), 607–614.
- Dancause, N., 2006. Neurophysiological and anatomical plasticity in the adult sensorimotor cortex. *Rev. Neurosci.* 17 (6), 561–580.
- Engberg, A.W., Liebach, A., Nordenbo, A., 2006. Centralized rehabilitation after severe traumatic brain injury – a population-based study. *Acta Neurol. Scand.* 113 (3), 178–184.
- Gale, S.D., Baxter, L., Roundy, N., Johnson, S.C., 2005. Traumatic brain injury and grey matter concentration: a preliminary voxel based morphometry study. *J. Neurol. Neurosurg. Psychiatry* 76 (7), 984–988.
- Graham, D.I., Gennarelli, T.A., McIntosh, T.K., 2002. Trauma. In: Lantos, G.A.P.L. (Ed.), *Greenfield's Neuropathology*, seventh ed., vol. 1. Arnold Publishers, London, pp. 823–898.
- Granger, C.V., Hamilton, B.B., Keith, R.A., Zielesny, M., Sherwin, F.S., 1986. Advances in functional assessment for medical rehabilitation. *Top. Geriatr. Rehabil.* 1, 59–74.
- Holshouser, B.A., Tong, K.A., Ashwal, S., Oyoyo, U., Ghamsary, M., Saunders, D., et al., 2006. Prospective longitudinal proton magnetic resonance spectroscopic imaging in adult traumatic brain injury. *J. Magn. Reson. Imaging* 24 (1), 33–40.
- Kim, J., Avants, B., Patel, S., Whyte, J., Coslett, B.H., Pluta, J., et al., 2008. Structural consequences of diffuse traumatic brain injury: a large deformation tensor-based morphometry study. *Neuroimage* 39 (3), 1014–1026.
- Leow, A.D., Yanovsky, I., Chiang, M.C., Lee, A.D., Klunder, A.D., Lu, A., et al., 2007. Statistical properties of Jacobian maps and the realization of unbiased large-deformation nonlinear image registration. *IEEE Trans. Med. Imaging* 26 (6), 822–832.
- Levin, H.S., 2003. Neuroplasticity following non-penetrating traumatic brain injury. *Brain Inj.* 17 (8), 665–674.
- Levin, H.S., O'Donnell, V.M., Grossman, R.G., 1979. The Galveston Orientation and Amnesia Test. A practical scale to assess cognition after head injury. *J. Nerv. Ment. Dis.* 167 (11), 675–684.
- MacKenzie, J.D., Siddiqi, F., Babb, J.S., Bagley, L.J., Mannon, L.J., Sinson, G.P., et al., 2002. Brain atrophy in mild or moderate traumatic brain injury: a longitudinal quantitative analysis. *AJNR Am. J. Neuroradiol.* 23 (9), 1509–1515.
- Maxwell, W.L., Povlishock, J.T., Graham, D.L., 1997. A mechanistic analysis of nondisruptive axonal injury: a review. *J. Neurotrauma* 14 (7), 419–440.
- Nichols, T.E., Holmes, A.P., 2001. Nonparametric permutation tests for functional neuroimaging: a primer with examples. *Hum. Brain Mapp.* 15 (1), 1–25.
- Priestley, J.V., 2007. Promoting anatomical plasticity and recovery of function after traumatic injury to the central or peripheral nervous system. *Brain* 130 (Pt. 4), 895–897.
- Rodriguez-Paez, A.C., Brunschwig, J.P., Bramlett, H.M., 2005. Light and electron microscopic assessment of progressive atrophy following moderate traumatic brain injury in the rat. *Acta Neuropathol.* 109 (6), 603–616.
- Salmund, C.H., Chatfield, D.A., Menon, D.K., Pickard, J.D., Sahakian, B.J., 2005. Cognitive sequelae of head injury: involvement of basal forebrain and associated structures. *Brain* 128 (Pt. 1), 189–200.
- Sidaros, A., Engberg, A.W., Sidaros, K., Liptrot, M.G., Herning, M., Petersen, P., et al., 2008. Diffusion tensor imaging during recovery from severe traumatic brain injury and relation to clinical outcome: a longitudinal study. *Brain* 131 (Pt. 2), 559–572.
- Signoretti, S., Marmarou, A., Aygok, G.A., Fatouros, P.P., Portella, G., Bullock, R.M., 2008. Assessment of mitochondrial impairment in traumatic brain injury using high-resolution proton magnetic resonance spectroscopy. *J. Neurosurg.* 108 (1), 42–52.
- Smith, D.H., Chen, X.H., Pierce, J.E., Wolf, J.A., Trojanowski, J.Q., Graham, D.I., et al., 1997. Progressive atrophy and neuron death for one year following brain trauma in the rat. *J. Neurotrauma* 14 (10), 715–727.
- Smith, S.M., De Stefano, N., Jenkinson, M., Matthews, P.M., 2001. Normalised accurate measurement of longitudinal brain change. *J. Comput. Assist. Tomogr.* 25 (3), 466–475.
- Smith, S.M., Zhang, Y., Jenkinson, M., Chen, J., Matthews, P.M., Federico, A., et al., 2002. Accurate, robust and automated longitudinal and cross-sectional brain change analysis. *Neuroimage* 17 (1), 479–489.
- Tagliaferri, F., Compagnone, C., Korsic, M., Servadei, F., Kraus, J., 2006. A systematic review of brain injury epidemiology in Europe. *Acta Neurochir. (Wien)* 148 (3), 255–268.
- Teasdale, G., Jennett, B., 1974. Assessment of coma and impaired consciousness. A practical scale. *Lancet* 2 (7872), 81–84.
- Tomaiuolo, F., Worsley, K.J., Lerch, J., Di Paola, M., Carlesimo, G.A., Bonanni, R., et al., 2005. Changes in white matter in long-term survivors of severe non-missile traumatic brain injury: a computational analysis of magnetic resonance images. *J. Neurotrauma* 22 (1), 76–82.
- Trivedi, M.A., Ward, M.A., Hess, T.M., Gale, S.D., Dempsey, R.J., Rowley, H.A., et al., 2007. Longitudinal changes in global brain volume between 79 and 409 days after traumatic brain injury: relationship with duration of coma. *J. Neurotrauma* 24 (5), 766–771.
- Wilson, J.T., Pettigrew, L.E., Teasdale, G.M., 1998. Structured interviews for the Glasgow Outcome Scale and the Extended Glasgow Outcome Scale: guidelines for their use. *J. Neurotrauma* 15 (8), 573–585.

Appendix 3

Supplemental short review in Danish
(summary in English)

[Magnetic resonance imaging in severe traumatic brain injury]

Sidaros A, Herning M.

Ugeskr Laeger 2007; 169 (3): 214-6. Danish

English summary:

Modern neuroimaging techniques are continuously improving the diagnostic and prognostic assessment of patients with traumatic brain injury. The rapid developments within the field of magnetic resonance imaging (MRI) in particular provide several complementary tools for evaluating structural and functional changes in the injured brain. This article summarizes the current clinical use and future potential of the main structural and functional MRI techniques in the evaluation of severe non-missile head injury in the subacute phase.

Magnetisk resonans-skanning ved svær traumatisk hjerneskade

Klinisk assistent Annette Sidaros & overlæge Margrethe Herning

Hvidovre Hospital, MR-afdelingen

Til primær billeddiagnostik i akutfasen ved svære kranietraumer anbefales internationalt computertomografi (CT), da intrakraniale læsioner, som kræver akut kirurgisk intervention, diagnosticeres hurtigt og præcist herved. Nøjere diagnostik af primære og eventuelle sekundære læsioner, grundlaget for den resulterende »hjerneskade«, er imidlertid kun i begrænset omfang mulig med CT. Navnlig diffus aksonal skade (DAI), der er en karakteristisk og klinisk vigtig læsionstype ved højenergitraumer, ses sjældent eller slet ikke ved CT.

Magnetisk resonans (MR)-skanning giver langt mere detaljerede oplysninger om de parenkymatøse hjernelæsioner og bliver i tiltagende omfang anvendt hos denne patientkategori efter den akutte fase, eller når patientens tilstand tillader det. MR som billeddiagnostisk princip dækker over en række modaliteter til belysning af såvel hjernens struktur som dens funktion.

Indledningsvis praktiske betragtninger følges i nærværende statusartikel af en kortfattet omtale af eksisterende MR-modaliteter af relevans for traumatisk hjerneskade. For en oversigt over traumatiske læsionstyper henvises til [1].

Magnetisk resonans-skanning af kranietraumepatienten

Der er ingen kendte helbredsmæssige effekter af MR ved feltstyrker, der anvendes klinisk, men en række kontraindikationer og sikkerhedsforanstaltninger skal overholdes ved ophold i et magnetfelt [2]. Mest omstændeligt i praksis er, at såvel patienter som personale skal kontrolleres for planterede eller løstsiddende magnetiske metaldele før adgang til et MR-rum. Desuden skal alt udstyr i MR-rummet være umagnetisk.

Den samlede skanningstid med nuværende MR-teknikker er sjældent under 30 minutter. Til sammenligning kan CT af cerebrum med spiral-CT-skanner udføres på få minutter f.eks. som led i traume-CT af flere regioner. Den ekstra information, der opnås ved MR i forhold til CT har ikke direkte og akut neurokirurgisk konsekvens. Endelig er MR særdeles følsom for patientbevægelser, og da patienter med traumatisk hjerneskade ofte er motorisk urolige trods bevidsthedssvækkelse, er universel anæstesi typisk nødvendig, for at man kan opnå tilstrækkelig billedkvalitet. Af disse grunde foretages der generelt ikke akut MR ved svære kranietraumer.

Efter almen stabilisering, dage til uger efter et kranietraume, opstår der som regel et behov fra såvel behandlere

som pårørende for en nærmere kortlægning af den egentlige hjerneskades art og omfang, navnlig med henblik på prognostisk vurdering. Planlagt MR, oftest i anæstesi, kan med fordel gennemføres i denne fase. Specielt er MR indiceret ved uoverensstemmelse mellem kliniske fund og CT-fund, f.eks. ved manglende forventet opvågning hvor CT-fund ikke forklarer tilstanden.

Konventionel strukturel magnetisk resonans

Siden introduktion af de første MR-skannere til klinisk brug omkring 1980 er der sket en rivende videreudvikling af MR, hovedsagelig i form af teknisk optimering. De klassiske vægtninger efter relaksationstiderne T_1 og T_2 er fortsat det grundlæggende princip ved strukturel MR, men justering af skanneparametre giver mulighed for en række forskellige måleserier (sekvenser), som kan kombineres successivt. Her skal blot fremhæves enkelte sekvenser, som er særlig værdifulde til visualisering af traumatiske hjernelæsioner.

Såkalde T_2^* -vægtede sekvenser har høj sensitivitet for hæmoglobinderivater og er derfor specielt egnede til detektion af blødninger. Petekkiale blødninger ledsagende DAI bliver herved synlige [3] (Figur 1). Alligevel tillader T_2^* -vægtning kun visualisering af et mindretal af DAI-læsioner, idet man fra autopsistudier ved at mere end 80% af DAI-læsioner er nonhæmoragiske. Antallet af synlige DAI-læsioner på T_2^* -vægtede billeder er da heller ikke nogen god prognostisk markør. Punktformede hypointensiteter ved prædilektionssteder for DAI, dvs. subkortikal hvid substans, corpus callosum og dorsolaterale mesencefalon er ikke desto mindre indikativt for tilstedeværelse af en svær primær diffus hjerneskade.

Fluid-attenuated inversion recovery (FLAIR) er en anden værdifuld MR-sekvens, som specielt muliggør visualisering af læsioner nær cerebrospinalvæsken, hvilket ellers er vanskeliggjort af det kraftige signal herfra [3]. Nonhæmoragiske DAI-læsioner kan sommetider synliggøres med denne sekvens. FLAIR er desuden velegnet til visualisering af andre traumatiske læsionstyper eksempelvis kontusioner [3] (Figur 2).

T_1 -vægtet højopløselig MR er den foretrukne sekvens til vurdering af substansstab. Denne sekvens giver desuden mulighed for kvantitative volumenmålinger.

Mikrostrukturelle og funktionelle magnetisk resonans-teknikker

Nonkonventionelle MR-modaliteter omfatter nyere avancerede teknikker til bestemmelse af mikrostrukturelle eller funktionelle parametre, og de vigtigste af disse skal omtales i det følgende. Kun de færreste af disse modaliteter anvendes på

VIDENSKAB OG PRAKSIS | STATUSARTIKEL

nuværende tidspunkt som klinisk rutine. De enkelte sekvenser kan udføres som ekstra måleserier i forbindelse med konventionelle MR-optagelser.

Diffusionsmålinger med magnetisk resonans

Ved diffusionsvægtet MR afbildes den regionale vanddiffusion i hjernevævet. Diffusiviteten kan udtrykkes kvantitativt som den tilsyneladende diffusionskoefficient, der er øget ved vasogent ødem og reduceret ved cytotoxisk ødem. Ved en videreudvikling af diffusionsvægtet MR, benævnt diffusions-tensor-billeddannelse, kan man kvantificere vævets retnings-specifikke vanddiffusion, der udtrykkes ved den fraktionelle anisotropi. Idet vand i højere grad diffunderer langs med aksonernes fiberretning end på tværs af denne, vil der hos raske findes høje værdier for fraktionel anisotropi i hvid substans-strukturer med overvejende parallelle fiberbunder, som f.eks. den midtsagittale del af corpus callosum. Ved DAI forstyrres netop den aksonale mikroarkitektur, og den fraktionelle anisotropi reduceres følgelig [4, 5] (Figur 3). Som ovenfor nævnt underestimeres omfanget af DAI ved konventionel MR, fordi læsionerne er mikroskopiske og derfor kun synlige ved større samlede læsioner eller ved ledsagende hæmorage. Foreløbige resultater tyder på, at den fraktionelle anisotropi eksempelvis i corpus callosum kan anvendes som et kvantitativt estimat af det reelle omfang af DAI [4, 5]. Hvorvidt denne parameter kan anvendes som markør for prognosen på længere sigt, afventer nærmere undersøgelser.

Perfusionsmålinger med magnetisk resonans

Ved perfusionsvægtet MR afbildes den regionale blodgennemstrømning i hjernevævet, og kvantitative perfusionsmål kan beregnes. Forskellige teknikker eksisterer til MR-perfusionsmåling, hvoraf nogle er baseret på passage af gadoliniumholdigt kontraststof, mens andre er noninvasive, såkaldt arteriel spinmærkning. Begge typer metoder er forholdsvis nye, og der foreligger kun få studier af kranietraumepatienter [6]. Kvantificering af den cerebrale perfusion hos denne patientkategori har potentielt stor klinisk værdi, da hypoperfusion pga. hypotension og/eller intrakraniell trykforhøjelse kan medføre sekundære iskæmiske hjerneskader med markant negativ indflydelse på prognosen [7].

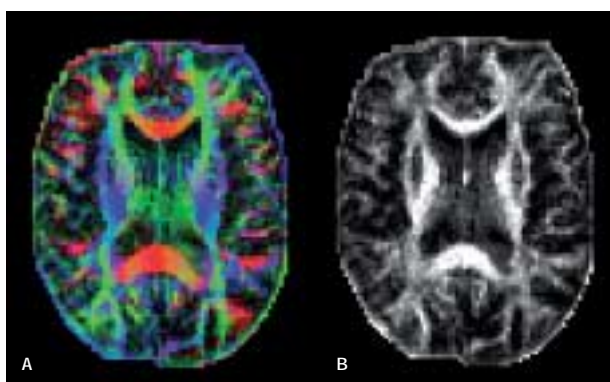
Magnetisk resonans-spektroskopi

Ved MR spektroskopi (MRS) fremstilles kemiske forhold i vævet, og undersøgelsesresultatet angives som et spektrum med toppe, der afspejler den enkelte metabolit og mængden af denne i vævet. Mest almindeligt er proton-MRS, hvor der måles på brintkernernes spektre; herved fås kvantitative oplysninger om metabolitterne N-acetylaspartat, kolin, kreatin, laktat og evt. myoinositol og glutamin/glutamat. MRS kan udføres enten fra et udvalgt volumen hjernevæv (*single voxel MRS*) eller som billeddannende MRS, der dækker det meste af storhjerne (*chemical shift imaging*).

Figur 1. Magnetisk resonans, koronal T₂*-vægtet sekvens, hos 18-årig mand otte uger efter svært kranietraume. Mest udtalt i venstre frontallap ses multiple små hypointensiteter subkortikalt (pile). Disse repræsenterer småblødninger associeret med diffus aksonal skade. CT viste ingen forandringer.



Figur 2. Magnetisk resonans, aksial fluid-attenuated inversion recovery-sekvens, hos 26-årig mand 11 uger efter svært kranietraume. Der er svære kontusionsfølgere i begge temporallapper med udtalt gliose (pile).



Figur 3. Magnetisk resonans, diffusionstensor-billeddannelse. A. Farvekodet billede, der angiver den dominerende diffusionsretning i tre på hinanden vinkelrette retninger: rød = højre-venstre, grøn = anterior-posterior, blå = superior-inferior. B. Beregnede værdier for fraktionel anisotropi er her vist i gråtone-skala, hvor tiltagende intensitet angiver stigende anisotropi mellem nul (isotrop dvs. retningsuspecifik diffusion) og en (maksimal retnings-specifik diffusion). De viste billeder er fra en raske person.

I en række studier med kranietraumepatienter udført med *single voxel* MRS i hjerneområder uden fokale skader har man bl.a. fundet reduktion af N-acetylaspartat og forhøjelse af kolin, hvilket menes at være udtryk for henholdsvis neuron-skade og membrannedbrydning eller gliose [8]. Hos komatøse

Billeddiagnostik ved svær traumatisk hjerneskade

Computertomografi (CT) anbefales som akut billeddiagnostisk undersøgelse med henblik på diagnostik af akutte kirurgikrævende intrakranielle læsioner, men normal CT udelukker ikke diffuse parenkymatøse læsioner såsom diffus aksonal skade

Magnetisk resonans (MR) er langt mere sensitiv end CT for specielt diffuse skadetyper, og MR anbefales i stabil fase i tilfælde af diskrepans mellem CT-fund og kliniske fund

Avancerede MR-teknikker som spektroskopi og diffusions-tensor-billeddannelse forventes i tiltagende omfang at blive anvendt til karakterisering og kvantificering af diffuse skadetyper og som led i prognostisk og terapeutisk evaluering

Resultaterne af aktiveringsundersøgelser med funktionel MR ventes at bidrage yderligere til den videnskabelige indsigt i regenerative processer under neurorehabilitering og klinisk til vurdering af langvarigt bevidsthedssvækkede patienter.

traumepatienter har *Danielsen* [8, 9] fundet, at metaboliske forandringer overvejende i hvid substans indikerer DAI, mens påvirkning af grå substansspektre kan være udtryk for hypoksisk vævsskade. Mulighed for differentiering mellem primær DAI og sekundær hypoksisk og/eller iskæmisk skade har afgørende prognostisk værdi, idet det i større kliniske opgørelser ses, at en sekundær skadekomponent forringer prognosen efter kranietraume med op til en faktor ti [7]. MRS er implementeret til klinisk brug enkelte steder i landet.

Neuronal aktivering med magnetisk resonans

Endelig skal nævnes funktionelle MR-teknikker, som anvendes til måling af aktiviteten i specifikke hjerneområder som respons på et kontrolleret stimulus. Den mest udbredte metode er baseret på de ændringer i forholdet mellem oxy- og deoxyhæmoglobin, som sker ved neuronal aktivitet. Funktionel MR (fMRI) anvendes endnu overvejende i forskningen, men rummer væsentlige kliniske perspektiver. For patienter med traumatisk hjerneskade forventes metoden f.eks. anvendt til undersøgelse af stimuleret hjerneaktivitet ved længerevarende bevidsthedspåvirkning. Funktionel MR kan endvidere anvendes til studier af den funktionelle kobling mellem hjerneområder af betydning for regenerative processer under neurorehabilitering [10].

Konklusion

Metoder til bedømmelse af den individuelle prognose efter svær traumatisk hjerneskade savnes. Der er stærk klinisk evidens for, at sekundære hypoksisk-iskæmiske skader har

markant prognostisk indflydelse, og kortlægning af primære og sekundære skadeelementer er derfor væsentlig ved bedømmelse af den individuelle prognose. MR-skanning efter svært kranietraume, med fordel foretaget i den subakutte fase, muliggør langt mere nøjagtig læsionsdiagnostik end CT. Supplerende kvantitative MR-metoder som spektroskopi og diffusionstensor-billeddannelse rummer potentielt prognostisk information, og disse metoder forventes i tiltagende grad implementeret fremover. Aktiveringsundersøgelser med funktionel MR har særlige perspektiver for bedømmelse af langvarigt bevidsthedssvækkede patienter. Endelig er det sandsynligt, at flere af disse MR-metoder kan anvendes som led i evaluering af farmakologiske og nonfarmakologiske behandlingstiltag.

Korrespondance: *Annette Sidaros*, MR-afdelingen 340, Hvidovre Hospital, DK-2650 Hvidovre. E-mail: *annettes@dadlnet.dk*

Antaget: 30. januar 2006

Interessekonflikter: Ingen angivet

Litteratur

1. Eskesen V. Traumatisk hjerneskade – patofysiologi og klinik set fra et neurokirurgisk synspunkt. *Ugeskr Læger* 2007;169:208-10.
2. Shellock FG, Crues JV. MR procedures: biologic effects, safety, and patient care. *Radiology* 2004;232:635-52.
3. Parizel PM, van Goethem JW, Ozsarlak O et al. New developments in the neuroradiological diagnosis of craniocerebral trauma. *Eur Radiol* 2005;15:569-81.
4. Huisman TA, Schwamm LH, Schaefer PW et al. Diffusion tensor imaging as potential biomarker of white matter injury in diffuse axonal injury. *Am J Neuroradiol* 2004;25:370-6.
5. Chan JH, Tsui EY, Peh WC et al. Diffuse axonal injury: detection of changes in anisotropy of water diffusion by diffusion-weighted imaging. *Neuroradiology* 2003;45:34-8.
6. Garnett MR, Blamire AM, Corkill RG et al. Abnormal cerebral blood volume in regions of contused and normal appearing brain following traumatic brain injury using perfusion magnetic resonance imaging. *J Neurotrauma* 2001;18:585-93.
7. Chesnut RM, Marshall LF, Klauber MR et al. The role of secondary brain injury in determining outcome from severe head injury. *J Trauma* 1993;34:216-22.
8. Danielsen ER, Ross B. *Magnetic resonance spectroscopy diagnosis of neurological diseases*. New York: Marcel Dekker, 1999:327 pp.
9. Danielsen ER, Thomsen C. Proton MRS: et prognostisk og diagnostisk redskab ved diffuse hjernelidelser. *Ugeskr Læger* 2001;163:4358-64.
10. Strangman G, O'Neil-Pirozzi TM, Burke D et al. Functional neuroimaging and cognitive rehabilitation for people with traumatic brain injury. *Am J Phys Med Rehabil* 2005;84:62-75.

Appendix 4

Clinical rating scales

Glasgow Coma Scale (GCS)

Eye Opening

- 4 - Spontaneous eye opening
- 3 - Eyes open to speech
- 2 - Eyes open to pain
- 1 - No eye opening

Verbal Response

- 5 - Alert and oriented
- 4 - Confused, yet coherent, speech
- 3 - Inappropriate words and jumbled phrases consisting of words
- 2 - Incomprehensible sounds
- 1 - No sounds

Motor Response

- 6 - Obeys commands fully
- 5 - Localizes to noxious stimuli
- 4 - Withdraws from noxious stimuli
- 3 - Abnormal flexion, i.e. decorticate posturing
- 2 - Extensor response, i.e. decerebrate posturing
- 1 - No response

The final score is determined by adding the values of I+II+III.

Modified from Teasdale & Jennett, 1974

Rancho Los Amigos Scale (RLAS)

I. No Response

A person at this level will:

- not respond to sounds, sights, touch or movement.

II. Generalized Response

A person at this level will:

- begin to respond to sounds, sights, touch or movement;
- respond slowly, inconsistently, or after a delay;
- responds in the same way to what he hears, sees or feels. Responses may include chewing, sweating, breathing faster, moaning, moving and/or increasing blood pressure.

III. Localized Response

A person at this level will:

- be awake on and off during the day;
- make more movements than before;
- react more specifically to what he sees, hears or feels. For example, he may turn towards a sound, withdraw from pain, and attempt to watch a person move around the room;
- react slowly and inconsistently;
- begin to recognize family and friends;
- follow some simple directions such as "Look at me" or "squeeze my hand";
- begin to respond inconsistently to simple questions with "yes" or "no" head nods.

IV. Confused-Agitated

A person at this level will:

- be very confused and frightened;
- not understand what he feels, or what is happening around him;
- overreact to what he sees, hears or feels by hitting, screaming, using abusive language, or thrashing about. This is because of the confusion;
- be restrained so he doesn't hurt himself;
- be highly focused on his basic needs; ie., eating, relieving pain, going back to bed, going to the bathroom, or going home;
- may not understand that people are trying to help him;
- not pay attention or be able to concentrate for a few seconds;
- have difficulty following directions;
- recognize family/friends some of the time;
- with help, be able to do simple routine activities such as feeding himself, dressing or talking.

V. Confused-Inappropriate, Non-Agitated

A person at this level will:

- be able to pay attention for only a few minutes;
- be confused and have difficulty making sense of things outside himself;
- not know the date, where he is or why he is in the hospital;
- not be able to start or complete everyday activities, such as brushing his teeth, even when physically able. He may need step-by-step instructions;
- become overloaded and restless when tired or when there are too many people around; have a very poor memory, he will remember past events from before the accident better than his daily routine or information he has been told since the injury;
- try to fill in gaps in memory by making things up; (confabulation)
- may get stuck on an idea or activity (perseveration) and need help switching to the next part of the activity;

- focus on basic needs such as eating, relieving pain, going back to bed, going to the bathroom, or going home.

VI. Confused-Appropriate

A person at this level will:

- be somewhat confused because of memory and thinking problems, he will remember the main points from a conversation, but forget and confuse the details. For example, he may remember he had visitors in the morning, but forget what they talked about;
- follow a schedule with some assistance, but becomes confused by changes in the routine;
- know the month and year, unless there is a serious memory problem;
- pay attention for about 30 minutes, but has trouble concentrating when it is noisy or when the activity involves many steps. For example, at an intersection, he may be unable to step off the curb, watch for cars, watch the traffic light, walk, and talk at the same time;
- brush his teeth, get dressed, feed himself etc., with help;
- know when he needs to use the bathroom;
- do or say things too fast, without thinking first;
- know that he is hospitalized because of an injury, but will not understand all the problems he is having;
- be more aware of physical problems than thinking problems;
- associate his problems with being in the hospital and think he will be fine as soon as he goes home.

VII. Automatic-Appropriate

A person at this level will:

- follow a set schedule
- be able to do routine self care without help, if physically able. For example, he can dress or feed himself independently; have problems in new situations and may become frustrated or act without thinking first;
- have problems planning, starting, and following through with activities;
- have trouble paying attention in distracting or stressful situations. For example, family gatherings, work, school, church, or sports events;
- not realize how his thinking and memory problems may affect future plans and goals. Therefore, he may expect to return to his previous lifestyle or work;
- continue to need supervision because of decreased safety awareness and judgement. He still does not fully understand the impact of his physical or thinking problems;
- think slower in stressful situations;
- be inflexible or rigid, and he may be stubborn. However, his behaviors are related to his brain injury;
- be able to talk about doing something, but will have problems actually doing it.

VIII. Purposeful-Appropriate

A person at this level will:

- realize that he has a problem in his thinking and memory;
- begin to compensate for his problems;
- be more flexible and less rigid in his thinking. For example, he may be able to come up with several solutions to a problem;
- be ready for driving or job training evaluation;
- be able to learn new things at a slower rate;
- still become overloaded with difficult, stressful or emergency situations;
- show poor judgement in new situations and may require assistance;
- need some guidance making decisions;
- have thinking problems that may not be noticeable to people who did not know the person before the injury.

Los Amigos Research and Educational Institute (LAREI), 1990

(Modified from Hagen, 1984)

The Galveston Orientation and Amnesia Test

Instructions: Can be administered daily. Score of 78 or more on three consecutive occasions is considered to indicate that patient is out of post-traumatic amnesia (PTA).

Question	Error Score	Notes
What is your name?	-2 _____	Must give both first name and surname.
When were you born?	-4 _____	Must give day, month, and year.
Where do you live?	-4 _____	Town is sufficient.
Where are you now:		
(a) City	-5 _____	Must give actual town.
(b) Building	-5 _____	Usually in hospital or rehab center. Actual name necessary.
When were you admitted to this hospital?	-5 _____	Date.
How did you get here?	-5 _____	Mode of transport.
What is the first event you can remember after the injury?	-5 _____	Any plausible event is sufficient (record answer)
Can you give some detail?	-5 _____	Must give relevant detail.
Can you describe the last event you can recall before the accident?	-5 _____	Any plausible event is sufficient (record answer)
What time is it now?	-5 _____	-1 for each half-hour error.
What day of the week is it?	-3 _____	-1 for each day error.
What day of the month is it? (i.e. the date)	-5 _____	-1 for each day error.
What is the month?	-15 _____	-5 for each month error.
What is the year?	-30 _____	-10 for each year error.
Total Error:		
Total Actual Score = (100 - total error) = 100 - _____ =		Can be a negative number.
76-100 = Normal / 66-75 = Borderline / <66 = Impaired		

Reference: Levin et al, 1979

Functional Independence Measure (FIM)

	ADMISSION	DISCHARGE	FOLLOW-UP
Self-Care			
A. Eating			
B. Grooming			
C. Bathing			
D. Dressing - Upper Body			
E. Dressing - Lower Body			
F. Toileting			
Sphincter Control			
G. Bladder Management			
H. Bowel Management			
Transfers			
I. Bed, Chair, Wheelchair			
J. Toilet			
K. Tub, Shower			
Locomotion			
L. Walk/Wheelchair			
M. Stairs			
<i>Motor Subtotal Score</i>			
Communication			
N. Comprehension			
O. Expression			
Social Cognition			
P. Social Interaction			
Q. Problem Solving			
R. Memory			
<i>Cognitive Subtotal Score</i>			
TOTAL FIM Score			

L E V E L S	Independent 7 Complete Independence (Timely, Safely) 6 Modified Independence (Device)	NO HELPER
	Modified Dependence 5 Supervision (Subject = 100%+) 4 Minimal Assist (Subject = 75%+) 3 Moderate Assist (Subject = 50%+)	HELPER
	Complete Dependence 2 Maximal Assist (Subject = 25%+) 1 Total Assist (Subject = less than 25%)	

Glasgow Outcome Scale (GOS) and Extended Glasgow Outcome Scale (GOS-E)

GOS-E	GOS	Corresponding term	Description
1	1	Dead	Dead
2	2	Vegetative state	Unresponsive
3	3	Severe disability (lower)	Able to follow commands; unable to live independently Cannot be left alone for 8 hours
4	3	Severe disability (upper)	Able to follow commands; unable to live independently But can be without assistance for 8 hours
5	4	Moderate disability (lower)	Able to live independently; unable to return to work or school Might be able to work in a protected environment
6	4	Moderate disability (upper)	Able to live independently; unable to return to work or school. Able to return to certain kinds of work/school if it does not involve a high level of performance
7	5	Good recovery (lower)	Able to return to work or school However, do have some problems in everyday life due to the trauma
8	5	Good recovery (upper)	Able to return to work or school No limitations of activities (either mental or physical), no problems in everyday life due to the trauma

References: Jennett et al, 1981; Wilson et al, 1998.

